FIELD PATTERNS FOR A PLASMA FILLED WAVEGUIDE

MASSACHUSETTS INSTITUTE OF TECHNOLOGY

MAY, 1964

ROY WILBURN DODY

COURSE XIII A

FIELD PATTERNS FOR A PLASMA FILLED WAVEGUIDE

by

ROY WILBURN DODY

S. B., KANSAS STATE UNIVERSITY
(1958)

SUBMITTED IN PARTIAL FULFILLMENT OF THE
REQUIREMENTS FOR THE DEGREES OF

MASTER OF SCIENCE IN ELECTRICAL ENGINEERING
AND NAVAL ENGINEER

at the

MASSACHUSETTS INSTITUTE OF TECHNOLOGY
May, 1964

Signature of Author _____
Department of Electrical Engineering, May 22, 1964

Certified by _____
Thesis Supervisor

Accepted by _____
Chairman, Departmental Committee on Graduate Students

FIELD PATTERNS FOR A PLASMA FILLED WAVEGUIDE

by

ROY WILBURN DODY

Submitted to the Department of Electrical Engineering on May 22, 1964 in partial fulfillment of the requirements for the degrees of Master of Science in Electrical Engineering and Naval Engineer.

ABSTRACT

Field patterns are drawn for a plasma filled waveguide of circular cross section immersed in an axial magnetic field. The plasma is assumed to be cold and collisionless, and linearized field equations are used.

Besides the exact analysis the MHD approximation (low frequency) and the quasi-static approximation (slow wave) are used. Comparisons are made among field patterns determined by the various methods of analysis. Among the field patterns at different frequencies and wave numbers certain features are pointed out and comparisons are made. These field patterns include particle charge density and current density, total charge density and current density, the electric field and magnetic field.

Thesis Supervisor: Abraham Bers
Title: Associate Professor of Electrical Communications

TABLE OF CONTENTS

I.	INTRODUCTION	5
II.	EQUATIONS GOVERNING FIELDS	6
	2.1 Preliminary Assumptions	6
	2.2 Determination of the Dielectric Tensor	8
	2.3 Determination of the Fields	10
	2.4 Determinantal Equation for Cylindrical Coordinates	13
	2.5 Cutoff Fields ($\Gamma=0$)	16
	2.5.1 H-Cutoff ($m = 1$)	18
	2.6 Low Frequency, MHD Regime	20
	2.7 Modified Quasi-Statics Approximation	22
	2.7.1 Derivation of Field Equations	23
III.	FIELD PLOTS	27
	3.1 Equations and Conventions Used	27
	3.2 Low Frequency, MHD Regime	31
	3.3 Electron Cyclotron Resonance	32
	3.4 Plasma Resonance	33
	3.5 Cutoff Fields ($\Gamma = 0$)	34
	3.5.1 $\underset{\sim}{E}$ - Waves	34
	3.5.2 $\underset{\sim}{H}$ - Waves	35
	3.6 Patterns Between Cutoff and Resonance	37
IV.	FIGURES	38
	4.1 ($\beta-\omega$) Diagram for Exact Analysis ($m = 0$)	38
	4.2 Plot of Equation (96.) for Low Frequencies	39
	4.3 Plot of Equation (96.) for High Frequencies	40
	4.4 Plot of Equation (95.) for Low Frequencies	41
	4.5 Plot of Equation (95.) for High Frequencies	42
	4.6 ($\beta-\omega$) Diagram for Low Frequencies, MHD and Quasi-Static Approximations	43
	4.7 Normalized ($\beta-\omega$) Diagram for Quasi-Static Analysis	44
V.	FIELD PATTERNS	45
	5.1 Low Frequency, MHD Regime	45
	5.2 Electron Cyclotron Resonance	61
	5.3 Plasma Resonance	76
	5.4 Cutoff Fields ($\Gamma = 0$)	96
	5.5 Patterns Between Cutoff and Resonance	132
BIBLIOGRAPHY		144

ACKNOWLEDGEMENTS

The author is grateful to Professor A. Bers for his guidance and many helpful suggestions throughout the course of this thesis.

The author would like to thank Professor M. Vlaardingerbroek for his assistance in trying to find solution points on the $(\beta\text{-}\omega)$ Diagram.

The author would like to thank Miss Martha Pennell of the Joint Computing Group for the programming of numerical computations and the determining accurate values for the $\underset{\sim}{H}$- Cutoffs.

The author acknowledges the work of Messrs. P. Serafim and P. Chorney on the $(\beta\text{-}\omega)$ diagram on which this thesis depends.

The author is greatly indebted to his beloved wife for performing the time consumming task of plotting points from computer runs and the drawing of some of the field patterns for $m \neq 0$.

FIELD PATTERNS FOR A PLASMA FILLED WAVEGUIDE

I. INTRODUCTION

The objective of this thesis has been to draw field patterns for a specific plasma filled waveguide in order that field patterns of plasma filled waveguides in general may better be visualized. At the beginning of Chapter I several assumptions are set forth. From these assumptions the necessary equations for the fields are derived. In Chapter II, the equations are organized in a manner used in arriving at the field patterns and then specific regions of the ($\beta - \omega$) diagram are discussed. The ($\beta - \omega$) diagram is divided into the magnetohydrodynamic (MHD) region, the cyclotron resonance region, the plasma resonance region, the region of cutoff fields (propagation constant equals zero), and a region with the propagation constant intermediate between cutoff and resonance.

II. EQUATIONS GOVERNING FIELDS

In this chapter the equations of the fields are derived. Eight preliminary assumptions are made concerning the plasma model and the type of geometry. The first derivation is the dielectric tensor which comes from applying conservation of momentum principles to the particles. Under the heading of the determination of the fields the transverse fields are found in terms of the axial fields and the dispersion relation is derived. Under the heading for the determinantal equation boundary conditions are matched for fields having no variation in the angular direction. For this case the fields are written out in explicit form. Under the heading of cutoff fields a method of solution is given for finding the cutoff frequencies. A discussion of the MHD-regime is then made and finally the theory of the modified quasi-statics approximation is developed.

2.1 Preliminary Assumptions

The field plots of this thesis are for a very restricted situation; therefore the development of the equations will be restricted from the beginning and further restricted as the development of the equations progresses. A more general development which this thesis parallels closely is given in (1.) Waves in Anisotropic Plasmas, PP. (18-24), CH. 9, and CH. 10. The preliminary assumptions and restrictions are:

(1) A linearized macroscopic description has been chosen for the analysis. This means that every time dependent field quantity that is determined is a small perturbation from an unperturbed state.

(2.) The system, waveguide and plasma is homogeneous in time and space. Fields of the form $e^{j\omega t}$ will be assumed and the plasma characteristics do no change with position.

(3.) The geometry will be restricted to cylindrical coordinates with the radius of the waveguide a= .05m.

(4.) The conducting surfaces of the waveguide are assumed to be perfect electric conductors, i.e., $\underset{\sim}{n} \times \underset{\sim}{E} = 0$ at r = a.

(5.) The plasma description is further simplified by assuming that no collisions occur and that the plasma is temperate. A temperate plasma is one which satisfies the inequalities that the particle induced velocity be much less than the random thermal velocity* which must be much less than the phase velocity of the wave. The lowest phase velocity which is considered is in the magnetohydrodynamic region where the phase velocity is as low as 1.75×10^{-2} times the velocity of light. For the electrons to have a thermal velocity less than one-tenth the phase velocity of the wave in the MHD region the temperature of the plasma must be less than 10^4 ^{o}K or in terms of electron volts the plasma must be less than a 1 ev. plasma. All the rest of the patterns have a phase velocity greater than one-tenth the phase velocity of light.

*For a Maxwell velocity distribution the most probable velocity of a particle is given by $u_T = \sqrt{\frac{2kT}{m}}$ where k is Boltzman's constant, m is mass, and T is temperature. It is by definition the thermal velocity.

(6.) The axial unperturbed magnetic field has a strength of .1023 webers / m^2. *

(7.) The plasma is made up of electrons and ions, i.e., protons which have a mass of 1.836×10^3 times the mass of an electron.

(8.) The unperturbed density of each type of particles is 1.808×10^{17} particles/m^3. *

*The values of the quantities in assumptions (6.) and (8.) were chosen as such for two reasons. The first is that a normalization of quantities which is used in the derivation of equations gives convenient numbers to work with. Secondly, the order of magnitude was chosen because they are thought to represent typical values for a plasma filled waveguide.

2.2 Determination of Dielectric Tensor

The equations governing the fields are Maxwell's equations and a conservation of momentum equation for each type of particles.

$$\nabla \times \underset{\sim}{E} = -j\omega\mu_o \underset{\sim}{H} \qquad (1.)$$

$$\nabla \times \underset{\sim}{H} = j\omega\epsilon_o \underset{\sim}{E} + \underset{\sim}{J} \qquad (2.)$$

$$j\omega m_k \underset{\sim}{v}_k = e_k (\underset{\sim}{E} + \underset{\sim}{v}_k \times \underset{\sim}{B}_o) \qquad (3.)$$

where the k subscript stands for the type of particle.

Since there is uniformity in the z direction, the fields will be broken into their transverse (T) and axial (z) components with $\underset{\sim}{B}_o = B_o \bar{i}_z$. Solving equation (3.) for $\underset{\sim}{v}$ gives

$$\underset{\sim}{v}_{kT} = \left[\frac{j\omega - \frac{e_k B_o}{m_k} \bar{i}_z \times}{-\omega^2 + \left(\frac{e_k B_o}{m_k}\right)^2}\right] \frac{e_k}{m_k} \underset{\sim}{E}_T \qquad (4.)$$

$$v_{kz} = \frac{e_k}{j\omega m_k} E_z \qquad (5.)$$

In order to have the units stand out some normalization constants will be introduced and some quantities will be defined.

$$\omega_n = \frac{c}{a} \qquad (6.)$$

$$u_{ck} = \frac{e_k B_o}{m_k \omega_n} \qquad (7.)$$

$$u_{pk} = \sqrt{\frac{N_o e^2_k}{\epsilon_o m_k \omega_n^2}} \qquad (8.)$$

$$u = \frac{\omega}{\omega_n} \qquad (9.)$$

$$u^2_p = u^2_{pe} + u^2_{pi} \qquad (10.)$$

where c is the velocity of light in free space and a is the radius of the waveguide. u_{ck} is the normalized cyclotron frequency, u_{pk} is the normalized plasma frequency, u_p is the effective normalized plasma frequency, and u is the normalized frequency. Assumptions (6.), (7.), and (8.) gives $u_{ce} = -3$ and $u_p = 4$.

Substituting the normalization constants into equations (4.) and (5.) and then writing the velocity in matrix form gives

$$\underset{\sim}{v}_k = \frac{e_k}{m_k \omega_n} \left[\begin{array}{c|c|c} \dfrac{-ju}{u^2 - u^2_{ck}} & \dfrac{-u_{ck}}{u^2 - u^2_{ck}} & 0 \\ \hline \dfrac{u_{ck}}{u^2 - u^2_{ck}} & \dfrac{-ju}{u^2 - u^2_{ck}} & 0 \\ \hline 0 & 0 & \dfrac{-j}{u} \end{array}\right] \cdot \underset{\sim}{E} \qquad (11.)$$

In order to determine $\underset{\sim}{J}$ in terms of $\underset{\sim}{E}$ some definitions are introduced.

$$\underset{\sim}{J}_k = N_o \, e_k \, \underset{\sim}{v}_k \qquad (12.)$$

$$\underset{\sim}{J} = \underset{\sim}{J}_e + \underset{\sim}{J}_i \qquad (13.)$$

$$\underset{\sim}{J} = \underset{\approx}{\sigma} \cdot \underset{\sim}{E} \qquad (14.)$$

$$\underset{\approx}{K} = \underset{\approx}{I} + \frac{\underset{\approx}{\sigma}}{j \omega \epsilon_o} \qquad (15.)$$

$\underset{\approx}{\sigma}$ is determined from equations (11.), (12.), (13.) and (14.). From equations (12.), (13.), and (14.)

$$\underset{\approx}{\sigma} \cdot \underset{\sim}{E} = N_o \left(e_e \underset{\sim}{v}_e + e_i \underset{\sim}{v}_i\right) \qquad (16.)$$

Substituting equation (11.) into equation (16.) determines $\underset{\approx}{\sigma}$. The $\underset{\approx}{\sigma}$ thus found substituted into equation (15.) determines $\underset{\approx}{K}$ the dielectric tensor. Carrying out the above operations give

$$\underset{\approx}{K} = \left[\begin{array}{c|c|c} K_\perp & -K_x & 0 \\ \hline K_x & K_\perp & 0 \\ \hline 0 & 0 & K_{||} \end{array}\right] \tag{17.}$$

where

$$K_\perp = 1 - \frac{u^2_p \left(u^2 + u_{ce}\, u_{ci}\right)}{\left(u^2 - u^2_{ce}\right)\left(u^2 - u^2_{ci}\right)} \tag{18.}$$

$$K_x = \frac{-j\, u\, u^2_p \left(u_{ce} + u_{ci}\right)}{\left(u^2 - u^2_{ce}\right)\left(u^2 - u^2_{ci}\right)} \tag{19.}$$

$$K = 1 - \left(\frac{u_p}{u}\right)^2 \tag{20.}$$

Waves in Anisotropic Plasmas has the equations of this section on pages 18 - 23. Equation (11.) is equation (2.8) on page 19, equation (17.) is equation (2.11) on page 20, and equations (18. - 20.) are equations (2.21) on page 23.

2.3 Determination of the Fields

Substitution of equations (14.) and (15.) into equation (2.) leaves two vector equations with two vector unknowns. Equations (1.) and (2.) are rewritten along with two auxillary equations found by taking the divergence of the two curl equations. These auxillary equations are not independent of the first two, but nevertheless, are useful relations.

$$\nabla \times \underset{\sim}{E} = -j\omega \mu_o \underset{\sim}{H} \tag{21.}$$

$$\nabla \times \underset{\sim}{H} = j\omega \epsilon_o \underset{\approx}{K} \cdot \underset{\sim}{E} \tag{22.}$$

$$\nabla \cdot \underset{\approx}{K} \cdot \underset{\sim}{E} = 0 \tag{23.}$$

$$\nabla \cdot \underset{\sim}{H} = 0 \tag{24.}$$

Again the procedure is to split the fields into transverse and axial components. Since uniformity exists in the z-direction, the axial dependence of the fields can be taken as $\bar{e}^{\gamma z}$. The operators become

$$\nabla = \nabla_T - \gamma \hat{i}_z \tag{25.}$$

$$\underset{\approx}{K} \cdot \underset{\sim}{E} = K_\perp \underset{\sim}{E_T} + K_x \hat{i}_z \times E_T + K_{||} E_z \hat{i}_z \tag{26.}$$

After splitting the fields into their components, the transversely directed part of equations (21.) and (22.) can be solved for the transverse fields in terms of the axial fields. This is matrix (27.). Using this matrix and the remaining parts of equations (18 - 24) two coupled equations between E_z and H_z can be found in a straight forward manner. These are equations (36.) and (37.). The above procedure is carried out in more detail in Waves in Anisotropic Plasmas, pages 134 - 138. Matrix (27.) is the same as matrix (9.21) on page 135, and equations (36.) and (37.) are the same as equations (9.30) and (9.31) repsectively on page 136.

$$\begin{bmatrix} \underset{\sim}{E_T} \\ \underset{\sim}{H_T} \\ \hat{i}_z \times \underset{\sim}{E_T} \\ \hat{i}_z \times \underset{\sim}{H_T} \end{bmatrix} = \left[\begin{array}{c|c|c|c} P & R & Q & S \\ \hline T & P & U & Q \\ \hline -Q & -S & P & R \\ \hline -U & -Q & T & P \end{array}\right] \cdot \begin{bmatrix} \nabla_T E_z \\ \nabla_T H_z \\ \hat{i}_z \times \nabla_T E_z \\ \hat{i}_z \times \nabla_T H_z \end{bmatrix} \tag{27.}$$

where

$$D = \frac{(\Gamma^2 + u^2 K_\perp)^2 + (u^2 K_x)^2}{a} \tag{28.}$$

$$\Gamma = a\gamma \tag{29.}$$

$$P = \frac{-\Gamma(\Gamma^2 + u^2 K_\perp)}{D} \tag{30.}$$

$$R = \frac{j u^3 K_x}{D} \sqrt{\frac{\mu_o}{\epsilon_o}} \tag{31.}$$

$$Q = \frac{\Gamma u^2 K_x}{D} \tag{32.}$$

$$S = \frac{ju(\Gamma^2 + u^2 K_\perp)}{D} \sqrt{\frac{\mu_o}{\epsilon_o}} \tag{33.}$$

$$T = \frac{j\Gamma^2 u K_x}{D} \sqrt{\frac{\epsilon_o}{\mu_o}} \tag{34.}$$

$$U = \frac{-j u K_\perp}{D}\left(\Gamma^2 + u^2 K_\perp + \frac{u^2 K_x^2}{K_\perp}\right)\sqrt{\frac{\epsilon_o}{\mu_o}} \tag{35.}$$

The two coupled equations are

$$\nabla_T^2 \; E_z + c \; E_z = d \; H_z \qquad (36.)$$

$$\nabla_T^2 \; H_z + f \; H_z = g \; E_z \qquad (37.)$$

where

$$c = \left(\Gamma^2 + u^2 K_\perp \right) \frac{K_\parallel}{a^2 K_\perp} \qquad (38.)$$

$$d = \frac{j \, u \, \Gamma \, K_x}{a^2 K_\perp} \sqrt{\frac{\mu_o}{\epsilon_o}} \qquad (39.)$$

$$f = \left(\Gamma^2 + u^2 K_\perp + \frac{u^2 K_x^2}{K_\perp} \right) \frac{1}{a^2} \qquad (40.)$$

$$g = \frac{-j \, u \, \Gamma \, K_x \, K_\parallel}{a^2 K_\perp} \sqrt{\frac{\epsilon_o}{\mu_o}} \qquad (41.)$$

Equations (36.) and (37.) can be combined to give two uncoupled fourth order equations. The equation for E_z is

$$\left[\nabla_T^4 + (c + f) \nabla_T^2 + (cf - dg) \right] E_z = 0 \qquad (42.)$$

Plane wave solutions of the form $\exp(-j\underset{\sim}{p} \cdot \underset{\sim}{r}_T)$ satisfy equations (36.), (37.) and (42.) where $\underset{\sim}{p}$ is a complex function of frequency only. The application of the identity (43.) to equation (42.) gives the dispersion relation for the medium equation (44.).

$$\nabla_T \; e^{-j \, \underset{\sim}{p} \cdot \underset{\sim}{r}_T} = -j \, \underset{\sim}{p} \, e^{-j \, \underset{\sim}{p} \cdot \underset{\sim}{r}_T} \qquad (43.)$$

$$p^4 - (c + f) \, p^2 + (cf - dg) = 0 \qquad (44.)$$

In order to satisfy the boundary conditions at the waveguide wall two two dimensional Helmholtz equations will be solved using equation (42.) to give the relation between the two p valves.

$$\left(\nabla_T^2 + p_i^2\right) E_{zi} = 0 \qquad (45.)$$

$$E_z = E_{z1} + E_{z2} \qquad (46.)$$

$$H_z = h_1 E_{z1} + h_2 E_{z2} \qquad (47.)$$

where h_i is determined from equation (36.)

$$h_i = \frac{c - p_i^2}{d} \qquad (48.)$$

The above equations can be found on pages (154.) and (155.) in Waves in Anistropic Plasmas.

2.4 Determinantal Equation for Cylindrical Coordinates

For cylindrical coordinates equation (45.) is

$$\frac{\partial^2 E_{zi}}{\partial r^2} + \frac{1}{r}\frac{\partial E_{zi}}{\partial r} + \frac{1}{r^2}\frac{\partial^2 E_{zi}}{\partial \phi^2} + p_i^2 E_{zi} = 0 \qquad (49.)$$

Applying a separation of variables, equation (50.), to equation (49.) gives equations (51.) and (52.). m_i is the separation constant and is not to be confused with the m used for mass earlier. The m for mass will not be used in any of the following discussions.

$$E_{zi} = A_i R(r) \Phi(\phi) \qquad (50.)$$

$$\frac{d^2\Phi}{d\phi^2} + m_i \Phi = 0 \qquad (51.)$$

$$(p_i r)^2 \frac{d^2R(r)}{d(p_i r)^2} + p_i r \frac{dR(r)}{d(p_i r)} + \left[(p_i r)^2 - m_i^2\right] = 0 \qquad (52.)$$

In order to have the boundary conditions satisfied for all ϕ $m_i = m$, and for the fields to be periodic with ϕ m must be an integer. Finally, $R(r) = J_m(p_i r)$ since there is no need for singular solutions in the waveguide. Therefore, the solution

sought is

$$E_{zi} = A_i J_m (P_i r) e^{jm\phi} \qquad (53.)$$

For the rest of this section it is assumed that $m = 0$. For $m \neq 0$ see page 226. in Waves in Anisotropic Plasmas. The boundary condition $E_z = 0$ at $r = a$ gives

$$A_2 J_o(X_2) = -A_1 J_o(X_1) \qquad (54.)$$

where

$$X_i = p_i a \qquad (55.)$$

The boundary condition that $E_\phi = 0$ at $r = a$ gives the determinantal equation. E_ϕ is determined from matrix (27.) and equations (46.), (47.) and (53.). The determinantal equation is

$$\frac{X_1}{b_1} \frac{J_1(X_1)}{J_o(X_1)} = \frac{X_2}{b_2} \frac{J_1(X_2)}{J_o(X_2)} \qquad (56.)$$

where

$$b_i = 1 - \left(\frac{\Gamma^2 + u^2 K_\perp}{a D} \right) X^2_i \qquad (57.)$$

Rewriting equation (44.) in its explicit form gives

$$\begin{bmatrix} p_1^2 \\ p_2^2 \end{bmatrix} = \frac{1}{2} \left[(c + f) \overset{+}{-} \sqrt{(c - f)^2 + 4dg} \right] \qquad \begin{matrix} (58.) \\ (59.) \end{matrix}$$

The simultaneous solution of equations (56.), (58.) and (59.), for varying values of u determines the $(\beta\text{-}\omega)$ diagram. Fig. (1.) is the part of the diagram that is complete for $m = 0$. This diagram results from the work of Messrs. P. Serafim and P. Chorney.

Using the following four definitions, the complex functions for the $\underset{\sim}{E}$ and $\underset{\sim}{H}$ fields for $m = 0$ are given by equations (64.) through (69.).

$$F_1 = A_1 J_o \left(X_1 \frac{r}{a}\right) e^{ju(\omega_n t)} \; e^{-\{\Gamma(\frac{z}{a})\}} \tag{60.}$$

$$F_2 = -A_1 \left(\frac{J_o(X_1)}{J_o(X_2)}\right) J_o\left(X_2 \frac{r}{a}\right) e^{ju(\omega_n t)} \; e^{-\{\Gamma(\frac{z}{a})\}} \tag{61.}$$

$$G_1 = a \frac{\partial F_1}{\partial r} \tag{62.}$$

$$G_2 = a \frac{\partial F_2}{\partial r} \tag{63.}$$

$$E_r = \sum_{i=1}^{2} G_i \left[\frac{(\Gamma - u^2 K_{||})(\Gamma^2 + u^2 K_\perp) + u^2 K_\perp X_i^2}{-\Gamma(\Gamma^2 + u^2 K_\perp)^2 + (u^2 K_x)^2}\right] \tag{64.}$$

$$E_\phi = \sum_{i=1}^{2} G_i \left[\frac{(\Gamma u K_x)^2 + (\Gamma^2 + u^2 K_\perp)^2 K_{||} - K_\perp(\Gamma^2 + u^2 K_\perp) X_i^2}{\Gamma K_x \left[(\Gamma^2 + u^2 K_\perp)^2 + (u^2 K_x)^2\right]}\right] \tag{65.}$$

$$E_z = F_1 + F_2 \tag{66.}$$

$$H_r = \sqrt{\frac{\epsilon_o}{\mu_o}} \sum_{i=1}^{2} G_i \left[\frac{(\Gamma u K_x)^2 + (\Gamma^2 + u^2 K_\perp)^2 K_{||} - K_\perp(\Gamma^2 + u^2 K_\perp) Xi^2}{-juK_x \left[(\Gamma^2 + u^2 K_\perp)^2 + (u^2 K_x)^2\right]}\right] \tag{67.}$$

$$H_\phi = \sqrt{\frac{\epsilon_o}{\mu_o}} \sum_{i=1}^{2} G_i \left[\frac{-ju\left[(K_\perp + K_{||})(\Gamma^2 + u^2 K_\perp) + u^2 K_x^2 - K_\perp X_i^2\right]}{(\Gamma^2 + u^2 K_\perp)^2 + (u^2 K_x)^2}\right] \tag{68.}$$

$$H_z = \sqrt{\frac{\epsilon_o}{\mu_o}} \sum_{i=1}^{2} F_i \left[\frac{(\Gamma^2 + u^2 K_\perp) K_{||} - K_\perp X_i^2}{ju \Gamma K_x}\right] \tag{69.}$$

By inspection of equations (65.) and (66.) give

$$H_r = \sqrt{\frac{\epsilon_o}{\mu_o}} \left(\frac{j\Gamma}{u}\right) E_\phi \tag{70.}$$

A more general statement of equation (70.) can be found from matrix (27.). It applies to field patterns for which $\nabla_T E_{z_1}$ is parallel to $\nabla_T E_{z_2}$. By definition

$$\vec{i}_a \times \vec{i}_b = \vec{i}_z \tag{71.}$$

$$\nabla_T E_{zi} = F_i \left(E_{zi}\right) \vec{i}_a \tag{72.}$$

Matrix (27.) then gives

$$\vec{i}_b \cdot \underset{\sim}{E_T} = \vec{i}_b \cdot \vec{i}_z \times \sum_{i=1}^{2} \left(Q \nabla_T E_{zi} + S \nabla_T H_{zi}\right) \tag{73.}$$

$$\vec{i}_a \cdot \underset{\sim}{H_T} = \vec{i}_a \cdot \sum_{i=1}^{2} \left(T \nabla_T E_{zi} + P \nabla_T H_{zi}\right) \tag{74.}$$

Therefore $$H_a = \sqrt{\frac{\epsilon_o}{\mu_o}} \left(\frac{j \Gamma}{u}\right) E_b \tag{75.}$$

2.5 Cutoff Fields ($\Gamma = 0$)

By definition a cutoff wave is one whose propagation constant equals zero. When cutoff occurs the coefficients P, Q, T, d, and g become zero and equations (36.) and (37.) become uncoupled.

Therefore

$$\left(\nabla_T^2 + p_e^2\right) E_z = 0 \tag{76.}$$

$$X_e^2 = \left(p_e a\right)^2 = u^2 K_{\|} \tag{77.}$$

$$\left(\nabla_T^2 + p_h^2\right) H_z = 0 \tag{78.}$$

$$X_h^2 = \left(p_h a\right)^2 = u^2 \frac{\left(K_x^2 + K_\perp^2\right)}{K_\perp} \tag{79.}$$

$\underset{\sim}{E}$ - Waves:

$$E_z = A_e J_m \left(X_e \frac{r}{a}\right) e^{jm\phi} e^{ju(\omega_n t)} \tag{80.}$$

$$H_z = 0 \tag{81.}$$

$$\underset{\sim}{E_T} = 0 \tag{82.}$$

$$\underset{\sim}{H_T} = \frac{-ja}{u} \sqrt{\frac{\epsilon_o}{\mu_o}} \vec{i}_z \times \nabla_T E_z \tag{83.}$$

The boundary condition that $E_z = 0$ at $r = a$ requires X_e to be a root of the $J_m(X_e)$ Bessel function. The cutoff frequencies are given by

$$u^2_{co} = X^2_e + u^2_p \tag{84.}$$

$\underset{\sim}{H}$ - Waves:

$$H_z = A_h J_m \left(X_h \frac{r}{a}\right) e^{jm\phi} e^{ju(\omega_n t)} \tag{85.}$$

$$E_z = 0 \tag{86.}$$

$$\underset{\sim}{H_T} = 0 \tag{87.}$$

$$\underset{\sim}{E_T} = \sqrt{\frac{\mu_o}{\epsilon_o}} \frac{jua}{X^2_h} \left[\frac{K_x}{K_\perp} \nabla_T H_z + \vec{i}_z \times \nabla_T H_z\right] \tag{88.}$$

For the $\underset{\sim}{H}$-cutoffs the boundary conditions become more difficult; therefore $m = 0$ and $m = 1$ will be considered separately. For $m = 0$ $\nabla_T H_z$ is in the $\vec{i}_r$ direction. The boundary condition $E_\phi = 0$ at $r = a$ requires

$$\vec{i}_z \times \nabla_T H_z = 0 \tag{89.}$$

Again the boundary condition requires X_h to be a root of the $J_1(X_h)$ Bessel functions. The cutoff frequencies are given by equation (79.) which expands into equation (90.). Figures (2.) and (3.) are plots of equation (79.) and nine of the solution points are indicated.

$$u_{co}^6 + a_1 u_{co}^4 + a_2 u_{co}^2 + a_3 = 0 \qquad (90.)$$

where $$a_1 = u_{ce}^2 + u_{ci}^2 + 2u_p^2 + X_h^2 \qquad (91.)$$

$$a_2 = \left(u_p^2 - u_{ce}\, u_{ci}\right)^2 + X_h^2\left(u_{ce}^2 + u_{ci}^2 + u_p^2\right) \qquad (92.)$$

$$a_3 = X_h^2\, u_{ce}\, u_{ci}\left(u_{ce}\, u_{ci} - u_p^2\right) \qquad (93.)$$

2.51 $\underset{\sim}{H}$ - Cutoff (m = 1)

$$\nabla_T H_z = \frac{X_n A_h}{a} e^{j\Phi} e^{ju(\omega_n t)} \left[\left(J_o\left(X_h \frac{r}{a}\right) - \frac{J_1\left(X_h \frac{r}{a}\right)}{X_h \frac{r}{a}}\right)\vec{i}_r + j\,\frac{J_1\left(X_h \frac{r}{a}\right)}{X_h \frac{r}{a}}\,\vec{i}_\Phi\right] \qquad (94.)$$

The boundary condition that $E_\phi = 0$ at $r = a$ gives

$$X_h \frac{J_o(X_h)}{J(X_h)} - 1 = -j\,\frac{K_x}{K_\perp} \qquad (95.)$$

The simultaneous solution of equation (79.) which is repeated as equation (96.) with equation (95.) gives the cutoff frequencies for m = 1

$$X_h^2 = \frac{u^2\left(K_x^2 + K_\perp^2\right)}{K_\perp} \qquad (96.)$$

Figures (2.) and (4.) for low frequencies and figures (3.) and (5.) for high frequencies demonstrate one method for solving for the cutoff frequencies. Equation (95.) is plotted on figures (4.) and (5.). The left hand side of equation (95.) is plotted versus X_h.

The right hand side is plotted on the same axis to the same scale as the left hand side but versus u. From these figures a function of (X_h vs. u) is generated by selecting an ordinant on the graph and reading the corresponding X_h and u, then repeating with a new choice of ordinant. Equation (96.) has been plotted on figures (2.) and (3.). Also plotted on these two figures is the (X_h vs u) function generated from figures (4.) and (5.). The dashed curves are for imaginary values of X_h. Therefore, intersections of either solid lines or dashed lines simultaneous satisfy equations (95.) and (96.) and thus are solutions from the H-cutoffs from $m = 1$.

For finding field solutions in the cutoff region equations (83.) and (88.) are written in a more explicit form. Equation (83.) for $m = 0$ and $m = 1$ respectively is

$$A_e(X_e, u) = A_e \; e^{ju(\omega_n t)} \left(\frac{X_e}{u}\right)\sqrt{\frac{\epsilon_o}{\mu_o}} \qquad (97.)$$

$$\underset{\sim}{H_T} = j \; A_e (X_e, u) \; J_1\left(X_e \; \frac{r}{a}\right) \vec{i}_\phi \qquad (98.)$$

$$\underset{\sim}{H_T} = j \, A_e(X_e, u) \; e^{j\phi} \left[j \, \frac{J_1\left(X_e \; \frac{r}{a}\right)}{X_e \; \frac{r}{a}} \; \vec{i}_r - \left(J_o\left(X_e \; \frac{r}{a}\right) - \frac{J_1\left(X_e \; \frac{r}{a}\right)}{X_e \; \frac{r}{a}}\right) \vec{i}_\phi \right] \qquad (99.)$$

The explicit form of equation (88.) for $m = 0$ and $m = 1$ respectively is

$$A_h \; (X_h, u) = A_h \; e^{ju(\omega_n t)} \left(\frac{u}{X_h}\right)\sqrt{\frac{\mu_o}{\epsilon_o}} \qquad (100.)$$

$$\underset{\sim}{E_T} = A_h \; (X_h, u) \; J_1\left(X_h \; \frac{r}{a}\right)\left[\frac{-j \; K_x}{K_\perp} \; \vec{i}_r - j \; \vec{i}_\phi\right] \qquad (101.)$$

$$\underset{\sim}{E_T} = A_h(X_h, u)\, e^{j\phi}\left[-\left\{\frac{-jK_x}{K_\perp} J_o\left(X_h \frac{r}{a}\right) - \left(1 - \frac{jK_x}{K_\perp}\right) \frac{J_1\left(X_h \frac{r}{a}\right)}{X_h \frac{r}{a}}\right\}\vec{i}_r \right. \quad (102.)$$
$$\left. + j\left\{J_o\left(X_h \frac{r}{a}\right) - \left(1 - \frac{jK_x}{K_\perp}\right) \frac{J_1\left(X_h \frac{r}{a}\right)}{X_h \frac{r}{a}}\right\}\vec{i}_\phi\right]$$

where the characteristics of ($-j\ K_x\ /\ K_\perp$) is given in Figures (4.) and (5.).

Waves in Anisotropic Plasmas considers the cutoff fields on pages 158 - 162 and page 227.

2.6 Low Frequency, MHD Regime

By definition the MHD regime is the limit that occurs when the frequency is much less than both plasma frequency and the ion cyclotron frequency. In this limit

$$K_\perp \longrightarrow 1 - \frac{u_p^2}{u_{ce}\, u_{ci}} \quad (103.)$$

$$K_x \longrightarrow \frac{-ju\, u_p^2\, (u_{ce} + u_{ci})}{u_{ce}^2\, u_{ci}^2} \quad (104.)$$

$$K_{||} \longrightarrow -\left(\frac{u_p}{u}\right)^2 \quad (105.)$$

$$(c - f) \longrightarrow -\left(\frac{u_p^2}{a}\right)\left(1 + \frac{\Gamma^2}{u^2 K_\perp}\right) \quad (106.)$$

$$4\ d\ g \longrightarrow -\left(\frac{2\, u_p\, K_x\, \Gamma}{a\ K_\perp}\right) \quad (107.)$$

In the limit of zero frequency ($K_\perp \longrightarrow$ constant), ($K_x \longrightarrow 0$), and ($K_{||} \longrightarrow -\infty$). A comparison of equations (106.) and (107.) shows that $|(c-f)^2| >> |4\ \ dg|$; therefore from equations (58.) and (59.) $p_1 \approx c$ and $p_2 \approx f$. Only a slight coupling exists between equations (36.) and (37.). The MHD approximation considers the two equations to be uncoupled:

For the H-Wave, equation (37.) when ($g = 0$), the cutoff frequency is much greater than the ion cyclotron frequency, hence it is not in the MHD region.

$\underset{\sim}{E}$ - Wave:

$$\nabla_T^2 \; E_z + p_e^2 \; E_z = 0 \qquad (108.)$$

$$X_e^2 = (p_e a)^2 = \left(\Gamma^2 + u^2 \; K_\perp\right) \frac{K_{||}}{K_\perp} \qquad (109.)$$

Equation (109.), the dispersion relation, is plotted in figure (6.). In this figure, the slope (β_n/u) approximately equals 67, whereas a slope of 57.1 gives a phase velocity equal to the Alvén velocity. The definitions of phase velocity and Alvén velocity respectively are

$$v_p = \frac{u}{\beta_n} c \qquad (110.)$$

$$v_a = \sqrt{\frac{-u_{ce}\, u_{ci}}{u_p^2}}\, c \qquad (111.)$$

In the limit of zero frequency Q and T, equations (32.) and (34.), approach zero; and P and U, equations (30.) and (35.), are given by

$$P \longrightarrow \frac{-\Gamma a}{\Gamma^2 + u^2 K_\perp} \qquad (112.)$$

$$U \longrightarrow \frac{-j\, a\, u\, K_\perp}{\Gamma^2 + u^2\, K_\perp} \sqrt{\frac{\epsilon_o}{\mu_o}} \qquad (113.)$$

giving

$$\underset{\sim}{E_T} = \frac{-\Gamma\, a\; K_{||}}{X_e^2\, K_\perp} \nabla_T E_z \qquad (114.)$$

$$\underset{\sim}{H_T} = \frac{-j\, u\, a}{X_e^2} \sqrt{\frac{\epsilon_o}{\mu_o}}\; \vec{i}_z \times \nabla_T E_z \qquad (115.)$$

Equations (114.) and (115.) were used in arriving at the field plots for the MHD regime rather than using actual values for the coefficients. The results seem questionable and will be discussed in the following chapter.

2.7 Modified Quasi - Statics Approximation

Near the resonances it is possible to have waves with arbitrarily slow phase velocities in the assumed plasma model. By definition the phase velocity of a wave is its frequency divided by its propagation constant. Quasi-statics is an approximation that takes advantage of the slow phase velocities. In this approximation the velocity of light is assumed to be infinite as compared to the phase velocity. From this it follows that the $\underset{\sim}{E}$ field is approximately curl free. (This statement becomes more clear when one assumes plane wave solutions of the form $\exp.(-j\,\underset{\sim}{k}\cdot\underset{\sim}{r})$ for Maxwell's curl equation for $\underset{\sim}{E}$.

$$-j\,\underset{\sim}{k}\times\underset{\sim}{E} = j\omega\mu_0\,\underset{\sim}{H} \qquad (116.)$$

$$\frac{\underset{\sim}{k}}{k}\times\underset{\sim}{E} = \frac{v_p}{c}\sqrt{\frac{\mu_0}{\epsilon_0}}\;\underset{\sim}{H} \qquad (117.)$$

For finite $\underset{\sim}{H}$ the right hand side of equation (117.) approaches zero.) In Waves in Anisotropic Plasmas pages (162-169) Professor Bers studies these resonances by taking limits of the exact solution. At plasma resonance he shows that the $\underset{\sim}{H}$ field approaches zero. For this case quasi-statics is a very good approximation. At cyclotron resonance he shows that ($H_z \longrightarrow 0$) and $\underset{\sim}{H_T}$ remains finite. For this case the dispersion relations differ in the two approximations. The

limit of the exact solution gives for the normalized p-number

$$X_{ec}^2 = \frac{\Gamma^2 K_{\parallel}}{K_{\perp}} + 2 u^2 K_{\parallel} \qquad (118.)$$

while that found from quasi-statics is

$$X^2 = \Gamma^2 \frac{K_{\parallel}}{K_{\perp}} \qquad (119.)$$

Before proceeding with the derivation it should be noted that the field plots are for a modified quasi-statics. That is the $\underset{\sim}{E}$ field as determined by quasi-statics is used to determine an $\underset{\sim}{H}$ field, hence the name modified quasi-statics.

Waves in Anisotropic Plasmas has the derivation of the quasi-static field solutions on pages (240 - 248) and for the modified quasi-statics on pages (253-254). Also equation (118.) is the same as equation (9.219) page (164.) in the book.

2.7.1 Derivation of Field Equations

For the quasi-static approximation equations (120.) and (121.) are assumed to describe the fields.

$$\nabla \times \underset{\sim}{E} = 0 \qquad (120.)$$

$$\nabla \cdot \epsilon_0 \underset{\approx}{K} \cdot \underset{\sim}{E} = 0 \qquad (121.)$$

Since the field is cure free a potential can be defined

$$E = -\nabla \phi \qquad (122.)$$

Splitting the field into its components as previous proceedures followed give the following equations from equations (121.) and (122.)

$$\nabla_T^2 \phi + p^2 \phi = 0 \qquad (123.)$$

$$p^2 = \gamma^2 \frac{K_\parallel}{K_\perp} \qquad (124.)$$

$$\underset{\sim}{E}_T = -\nabla_T \phi \qquad (125.)$$

$$E_z = \gamma \phi \qquad (126.)$$

Figures (6.) and (7.) are a plot of equation (124.). The boundary condition that $E_z = 0$ at $r = a$ requires ($X = p\,a$) to be a root of the Bessel function.

The $\underset{\sim}{H}$— field is determined from the $\underset{\sim}{E}$ — field and Maxwell's equations.

$$\nabla \times \underset{\sim}{H} = j\omega \epsilon_o \underset{\approx}{K} \cdot \underset{\sim}{E} \qquad (127.)$$

$$\nabla \cdot \underset{\sim}{H} = 0 \qquad (128.)$$

For equation (127.) a particular solution can be found which satisfies the right hand side and a homogeneous solution can be found which will be added to the particular solution in order that boundary conditions can be satisfied.

Again the fields are split into their components and solutions of the form $\exp.(-j\underset{\sim}{p} \cdot \underset{\sim}{r}_T)$ are assumed. A few algebraic operations on equations (127.) and (128.) give

$$H_{pT} = Y_1 \underset{\sim}{E}_T + Y_2 \underset{\sim}{E}_T \qquad (129.)$$

$$H_{pz} = Y_3 E_z \qquad (130.)$$

where $$Y_1 = \frac{-ju}{\Gamma}\sqrt{\frac{\epsilon_o}{\mu_o}}\ \frac{K_x K_\perp}{K_\perp - K_{||}} \qquad (131.)$$

$$Y_2 = \frac{j u}{\Gamma}\sqrt{\frac{\epsilon_o}{\mu_o}}\ K_\perp \qquad (132.)$$

$$Y_3 = \frac{-j u}{\Gamma}\sqrt{\frac{\epsilon_o}{\mu_o}}\ \frac{K_x K_{||}}{K_\perp - K_{||}} \qquad (133.)$$

The homogeneous part is found from equations (134.) and (135.)

$$\nabla \times \underset{\sim}{H}_h = 0 \qquad (134.)$$

$$\nabla \cdot \underset{\sim}{H}_h = 0 \qquad (135.)$$

Therefore $$\underset{\sim}{H}_h = -\nabla \psi \qquad (136.)$$

$$\nabla_T^2 \psi + \gamma^2 \psi = 0 \qquad (137.)$$

and the total $\underset{\sim}{H}$ - field is

$$\underset{\sim}{H} = \underset{\sim}{H}_p + \underset{\sim}{H}_h \qquad (138.)$$

Equation (138.) is complete when boundary conditions are specified. Since the boundarys are perfect electric conductors, the arbitrary constant in the homogeneous part is found by lettering $H_r = 0$ at $r = a$.

After defining some symbols, the $\underset{\sim}{E}$ and $\underset{\sim}{H}$ fields are written in explicit form.

$$A(u,\beta_n,\phi,t) = \frac{\Gamma}{a}\, A_1 \cdot e^{j\left[u(\omega_n t) - \beta_n\left(\frac{z}{a}\right)\right]} \cdot e^{jm\phi} \tag{139.}$$

$$\beta_n = -j\Gamma = X\sqrt{\frac{-K_\perp}{K_{||}}} \tag{140.}$$

$$C_h = \frac{Y_1\, J_o(X)}{I_o(\beta_n) - \dfrac{I_1(\beta_n)}{\beta_n}} \tag{141.}$$

m = 0:

$$\underset{\sim}{E} = A(u,\beta_n,t)\left[\frac{-jX}{\beta_n}\, J_1\left(X\frac{r}{a}\right)\vec{i}_r + J_o\left(X\frac{r}{a}\right)\vec{i}_z\right] \tag{142.}$$

$$\underset{\sim}{H} = A(u,\beta_n,t)\left[\frac{jY_1X}{\beta_n}\left\{J_1\left(X\frac{r}{a}\right) - \frac{J_1(X)}{I_1(\beta_n)}\, I_1\left(\beta_n\frac{r}{a}\right)\right\}\vec{i}_r \right. \tag{143.}$$

$$+ \frac{jY_2X}{\beta_n}\, J_1\left(X\frac{r}{a}\right)\vec{i}_\phi$$

$$\left. + \left\{Y_3\, J_o\left(X\frac{r}{a}\right) - \frac{Y_1X}{\beta_n}\,\frac{J_1(X)}{I_1(\beta_n)}\, I_o\left(\beta_n\frac{r}{a}\right)\right\}\vec{i}_z\right]$$

m = 1:

$$\underset{\sim}{E} = A(u,\beta_n,\phi,t)\left[\frac{jX}{\beta_n}\left\{J_o\left(X\frac{r}{a}\right) - \frac{J_1\left(X\frac{r}{a}\right)}{X\frac{r}{a}}\right\}\vec{i}_r\right. \tag{144.}$$

$$\left. - \frac{X}{\beta_n}\,\frac{J_1\left(X\frac{r}{a}\right)}{X\frac{r}{a}}\,\vec{i}_\phi + J_1\left(X\frac{r}{a}\right)\vec{i}_z\right]$$

$$\underset{\sim}{H} = \frac{X}{\beta_n}\, A(u,\beta_n,\phi,t)\left[h_r\,\vec{i}_r + h_\phi\,\vec{i}_\phi + h_z\,\vec{i}_z\right] \tag{145.}$$

(146.)

where $$h_r = -j\left[Y_1\, J_o\left(X\frac{r}{a}\right) - (Y_1+jY_2)\,\frac{J_1\left(X\frac{r}{a}\right)}{X\frac{r}{a}} + C_h\left(\frac{I_1\left(\beta_n\frac{r}{a}\right)}{\beta_n\frac{r}{a}} - I_o\left(\beta_n\frac{r}{a}\right)\right)\right]$$

$$h_\phi = -\left[jY_2\, J_o\left(X\frac{r}{a}\right) - (Y_1+jY_2)\,\frac{J_1\left(X\frac{r}{a}\right)}{X\frac{r}{a}} + C_h\,\frac{I_1\left(\beta_n\frac{r}{a}\right)}{\beta_n\frac{r}{a}}\right] \tag{147.}$$

$$h_z = \left[\frac{\beta_n Y_3}{X}\, J_1\left(X\frac{r}{a}\right) + C_h\, I_1\left(\beta_n\frac{r}{a}\right)\right] \tag{148.}$$

III. FIELD PLOTS

The section describing the conventions has the equations which describe the particle motions listed and a discussion of the two conventions used in generating the field patterns. The two conventions are (1.) polarization ellipses at various locations to describe the field strength and a vector to describe its direction and (2.) spacing of lines to determine the strength of the field and direction of the lines to describe the direction of the field. All the rest of the sections consider the plots for various regions of the (β-ω) diagram. Comparisons are made between various plots and the interesting characteristics of certain field patterns are pointed out.

3.1 Equations and Conventions Used

The objective of this thesis has been to use those equations which were developed in Chapter I in order to arrive at patterns of the fields for selected points of the (β-ω) diagram. Figure (1.) has indicated on it those points for which field patterns have been drawn. In order to get the equations for the field patterns $\underset{\sim}{E}$ and $\underset{\sim}{H}$ were determined from those equations developed in chapter one in the various sections. The rest of the field patterns were calculated by using the following equations. From equations (14.) and (15.)

$$\underset{\sim}{J} = \frac{ju}{a}\sqrt{\frac{\epsilon_o}{\mu_o}}\left(\underset{\approx}{K} - \underset{\approx}{I}\right)\cdot \underset{\sim}{E} \qquad (149.)$$

Equations (8.), (11.), and (12.) give

$$\underset{\sim}{J}_k = \frac{u_{pk}^2}{a}\sqrt{\frac{\epsilon_o}{\mu_o}} \begin{bmatrix} \frac{-j\,u}{u^2-u_{ck}^2} & \frac{-u_{ck}}{u^2-u_{ck}^2} & 0 \\ \frac{-u_{ck}}{u^2-u_{ck}^2} & \frac{-j\,u}{u^2-u_{ck}^2} & 0 \\ 0 & 0 & \frac{-j}{u} \end{bmatrix} \cdot \underset{\sim}{E} \qquad (150.)$$

$$\underset{\sim}{J} = \underset{\sim}{J}_e + \underset{\sim}{J}_i \qquad (151.)$$

$$\rho_k = \frac{j}{u\omega_n} \quad \nabla \cdot \underset{\sim}{J}_k \qquad (152.)$$

$$\rho = \frac{j}{u\omega_n} \quad \nabla \cdot \underset{\sim}{J} \qquad (153.)$$

Taking the curl of equation (2.) and equation (153.) give

$$\rho = \nabla \cdot \epsilon_o E \qquad (154.)$$

The constants for the plasma are given by

$$u_{pe} = -4 \qquad u_{pi}^2 = \frac{16}{1836.1} \qquad u_p = 4 \qquad (155.)$$

$$u_{ce} = -3 \qquad u_{ci} = \frac{3}{1836.1} \qquad (156.)$$

Equations (151.) and (153.) were used to check the correctness of the answers. Equation (151.) was used to check that sum of the current densities as determined from equation (150.) actually equalled the current density as found from equation (149.). Equation (153.) was a second method for calculating the total charge density and was used to check the correctness of the answers as found by equation (154). This check is equivalent to equation (23.) $\nabla \cdot \underset{\approx}{K} \cdot \underset{\sim}{E} = 0$. Finally, since the computations were performed by slide rule, no more than three significant figures can be expected.

No patterns were drawn for the separate particles except for frequencies below ($u \doteq 1$). This is because nearly all the current is from movement of electrons at high frequencies. Therefore, the pattern for the electrons is the same as the total current. The pattern for the ions is nearly the same as that for the $\underset{\sim}{E}$ - field.

The justification of this statement comes from assuming $u^2 >> u^2_{ci}$ and looking at equation (150.).

$$\underset{\sim}{J}_i = \left(\frac{u_{pi}}{u}\right)^2 \frac{1}{a} \sqrt{\frac{\epsilon_o}{\mu_o}} \left[-j\, u\, \underset{\sim}{E} + u_{ci}\, \vec{i}_z \times \underset{\sim}{E}\right] \quad (157.)$$

The most noticable case for disagreement between the patterns for $\underset{\sim}{E}$ and $\underset{\sim}{J}_i$ would be for $\underset{\sim}{E}_T$ to be linearly polarized. This would produce elliptical polarization for $\underset{\sim}{J}_{iT}$ with the ratio of major to minor axis equal to 1.6×10^{-3}. Therefore, it is concluded that the term $(u_{ci}\, \vec{i}_z \times \underset{\sim}{E})$ has negligible affect on the field pattern and the current density pattern for the ions is approximately the same as that for the $\underset{\sim}{E}$ field.

For the field patterns two sets of conventions were used to give two sets of field patterns. The first convention has ellipses of polarization at various locations to show the relative strength of the fields. In each ellipse a line is drawn from the center to the outside which indicates the strength and direction of the field at time $t = o$ when the constant of amplitude for the fields is taken as a positive real number. As time increases the arrow indicates the direction in which the vector rotates.

The three components of any field are drawn to the same scale unless it is noted otherwise by (X Number) on the pattern. The particle current and the total current are drawn to the same scale. Finally, the scale of any particular ($\underset{\sim}{E}$, $\underset{\sim}{J}$, or $\underset{\sim}{H}$) was chosen to give convenient sized ellipses of polarization.

Only two of these views are necessary since the third can be drawn from the first two. The $(r - \phi)$ view is taken looking down the waveguide axis ($\perp$ z-direction) at $z = 0$; the $(r - z)$ view is taken looking across the waveguide into the minus ϕ-direction at $\phi = 0$. The $(\phi - z)$ view actually is generated from the preceeding views. It corresponds to looking into the minus r-direction at $\phi = 0$ and moving the polarization ellipse up or down a given distance r depending whether the ellipse is at plus r or minus r respectively when $\phi = 0$.

The second convention indicates the strength of the field by the spacing of lines. This convention has been applied to all of the transverse fields for $m = 1$ and to the radial fields for $m = 0$. The ϕ-directed component is divergence free for $m = 0$ and its fields are readily visualized from the patterns of the first convention. The z-dependence of the patterns was not accomplished due to lack of time but can be sketched easily from the patterns of the first convention. For an increase in z the vector rotates in the direction of the arrow. When $\frac{z}{a} = \frac{\pi}{2\beta_n}$ the vector has rotated by 90° in space.

The second convention illustrates two features. It clearly illustrates the divergence of the fields, especially at cutoff. Laying the pattern for the $\underset{\sim}{E}$-field or for the $\underset{\sim}{J}$-field rotated by 90° in space over the charge density contours shows that where the density is the greatest the number of lines starting or ending per unit area is also the greatest. The second feature is that the total transverse pattern rotates in the counterclockwise direction for $m = 1$.

Before proceeding with the discussions of the individual regions on the (β-ω) diagram, it should be noted that the assumed model of the plasma may break down at the boundary. Inherent in the model is the assumption of specular reflection. Specular reflection accounts for the fact that particles cannot flow through the walls of the waveguide as the field patterns indicate.

3.2 Low Frequency, MHD Regime

For this region, four sets of fields were calculated, two by the MHD approximation and two by the quasi-static approximation. Such good agreement occurred between the two approximations that only two sets of patterns were drawn, one for $m = 0$ and one for $m = 1$. The largest variation between the two approximations was a factor of two for $\underset{\sim}{E}_T$, $\underset{\sim}{J}_T$, and ρ.

For this region and exact analysis was not possible because of failure to find a solution point on the (β-ω) diagram. A comparison of the coefficients which were used with those from an exact analysis using the same frequency and propagation constant will indicate the degree of the error. For an assumed $u = 17 \times 10^{-5}$ and $\beta_n = 1.2 \times 10^{-2}$ one of the p numbers, equation (58.), is very close to c, equation (38.), but for the exact analysis it is not necessarily a root of the Bessel function since there are two p numbers. Coefficients which would have been used for the approximate analysis to find the transverse fields are

$$P = j\ 12.3 \qquad (158.)$$

$$Q = 0.0 \qquad (159.)$$

$$T = 0.0 \qquad (160.)$$

$$U = 1.53 \qquad (161.)$$

while the coefficients from an exact analysis are

$$P = j\,12.9 \qquad (162.)$$

$$Q = -2.6 \qquad (163.)$$

$$T = 0.5 \qquad (164.)$$

$$U = j1.63 \qquad (165.)$$

From a comparison of the coefficients and knowing that there are two p-numbers each of which are different from the approximations raises an element of doubt as to the value of the approximations.

Assuming the approximations are a valid representation of the fields, it can then be concluded that for both $m = 0$ and $m = 1$ the fields lie in the transverse plane except for $\underset{\sim}{J}$ and $\underset{\sim}{J}_e$. The strong axial electron current is a result of $(K_{11} \rightarrow -\infty)$ as $(\omega \rightarrow 0)$. Another interesting feature of this pattern is that the ions move in the transverse plane in such a fashion that the divergence of the total current is negligible compared to the divergence of either particle current, i.e., the particle charge density is approximately 3×10^3 times greater than the total charge density.

3.3 Electron Cyclotron Resonance

Three sets of field patterns, two for $m = 1$ and one for $m = 0$, were drawn for this region from the quasi-statics approximation. Here larger p-numbers than those used for other regions were assumed for two reasons. The first one was to develop some patterns with more variations in the radial direction. The second and most important reason is that the dispersion relation as determined by quasi-statics approaches the true dispersion relation only for large p numbers.

This can be seen by a comparison of equations (118.) and (119.). The model for the quasi-statics approximation assumed the velocity of light to be infinite compared to the phase velocity of the wave, in this case the phase velocity in the transverse direction, hence large p numbers.

Two points seem to be indicated from these patterns. The first is that some of the lines for $\underset{\sim}{J}_T$ and $\underset{\sim}{H}_T$ enclose upon themselves. The $\underset{\sim}{H}_T$ for other regions is completely encircling, cutoff and MHD, or no encircling lines as plasma resonance. The second point is that a comparison of the fields at electron cyclotron resonance with those at plasma resonance shows that the $\underset{\sim}{H}$-field for electron cyclotron resonance is about an order of magnitude greater than the $\underset{\sim}{H}$ - field at plasma resonance when the two fields have similar propagation constants and similar values for E_z.

3.4 Plasma Resonance

This is an interesting region because several comparisons can be made. As a first choice the exact analysis and the quasi-static analysis at $u = 4.08$ will be made. Here it can be seen that there is very good agreement between the two patterns and field solutions. The difference which occurs is that the $\underset{\sim}{E}$ - field becomes slightly elliptically polarized in the transverse plane for the exact analysis and the strength of the z-directed field as found by the exact method is about twice that from the quasi-static method.

The second interesting comparison is that at similar propagation constants the plasma resonance comes closer to being an $\underset{\sim}{E}$-wave than cyclotron resonance as was discussed in the preceeding section. Also E_z for plasma resonance is about twice E_z at cyclotron resonance when the two have similar magnitudes for $\underset{\sim}{E}_T$

The third interesting comparison is to compare the patterns of those fields which have solution points that lie on the curve on the $(\beta\text{-}\omega)$ diagram that originates at $u = 3.94$. See Figure (1.). As the propagation constant increases the z component of the $\underset{\sim}{E}$ and $\underset{\sim}{J}$ fields grow while the $\underset{\sim}{H}$ - field decreases. The transverse $\underset{\sim}{H}$ - field grows from nothing at cutoff to strong radial then to almost circular while the $\underset{\sim}{E}$ - field starts from almost circular and decreases to almost radial. The $\underset{\sim}{J}_T$ field is very similar to the $\underset{\sim}{H}_T$ field except that it has a strong radial field at cutoff.

The fourth interesting point is that $\underset{\sim}{J}$ and $\underset{\sim}{H}$ have a polarization in the transverse plane which is opposite to that of the $\underset{\sim}{E}$ - field. The $\underset{\sim}{E}$ vector rotates in the counterclockwise direction while $\underset{\sim}{J}$ and $\underset{\sim}{H}$ rotate in the clockwise direction.

3.5 Cutoff Fields ($\Gamma = 0$)

3.5.1 $\underset{\sim}{E}$ - Waves

All that seems apparent for these cutoffs is that the $\underset{\sim}{H}$ field is the only one with transverse components and the charge density is zero. They are similar to the cutoffs for $\underset{\sim}{E}$ - waves in an empty waveguide. They differ in that the cutoff frequency is higher than that for the empty waveguide and that the empty waveguide has no particles, hence no current density. For the empty waveguide ($u_{co} = X_e$) of equation (8.0) and is a root of the Bessel function.

3.5.2 $\underset{\sim}{H}$ - Waves

m = 0:

Three field patterns were drawn for m = 0. For the cutoff at u = .0430 the ion and electron charge density nearly cancel each other. From the patterns of $\underset{\sim}{J}_{eT}$ and $\underset{\sim}{J}_{iT}$ the particle paths can be drawn for low excitation, i.e., localized motion of particles.

(a.) The small ellipse is the path of the ion.

(b.) The large ellipse is the path of the electron.

For u = 3.94 the interesting feature is that a nearly circularly polarized $\underset{\sim}{E}_T$ - field produces a strong radially polarized $\underset{\sim}{J}$ - field. The reason for this is that $u_{ce}E_r$ approximately equals $u\,E_\phi$ in equation (150.) hence ($J_\phi \approx 0$).

The cutoff frequency u = 6.34 has nothing that particularly stands out. A comparison of the three patterns shows that as frequency is increased, the $\underset{\sim}{E}$-field goes from nearly radial, to almost circular with the stronger field being r-directed and then to almost circular with the strongest field being ϕ directed. For m = 0 the $\underset{\sim}{H}$ wave at cutoff in an empty waveguide has the $\underset{\sim}{E}$ field entirely in the ϕ direction; therefore none of the patterns are like those of the empty waveguide. The higher the frequency the more nearly the modes look like empty waveguide modes.

m = 1:

For m = 1 there are four sets of field patterns. A comparison of the patterns for $u = .04326$ and $m = 1$ with $u = .0430$ and $m = 0$ shows that for both sets the charge density of the electrons tends to cancel that of the ions, that is, $\rho_e = -3.75\rho$ and $\rho_i = 4.75\rho$. The particle paths for m = 1 look like

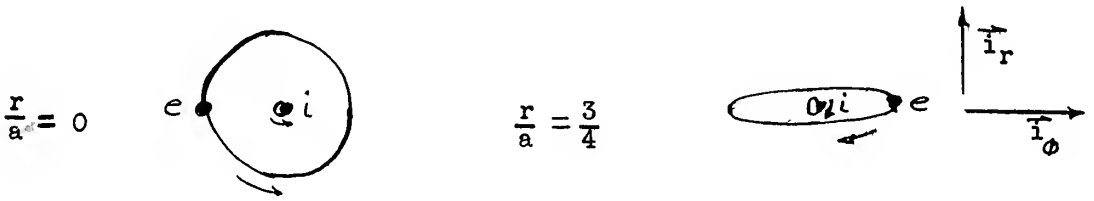

(a.) The smaller ellipse is the path of the ion.

(b.) The large ellipse is the path of the electron.

In order to visualize the way the electrons tend to cancel the charge density of the ions the second convention is the better.

A comparison of $u = 3.37$ for $m = 1$ with $u = 3.94$ for $m = 0$ shows that both have nearly circular polarization ellipses across the cross section of the waveguide, and both have the same direction of polarization.

The last two sets of patterns are for imaginary p numbers. The fields for $u = 5.07$ show how large imaginary p numbers produce very strong fields near r = a. This is because a modified Bessel function grows rapidly as its argument grows. The fields for $u = 5.77$ are for p numbers that are practically equal to zero.

3.6 Patterns Between Cutoff and Resonance

Two sets of patterns have been categorized under this heading, one for $u = 4.773$ and one for $u = 1.00$. For the patterns at $u = 4.773$ one of the normalized p-numbers is 8.65 and the other is 2.40. The large p-number causes three variations in the field pattern as r goes from zero to a. For this pattern it is necessary to use the patterns from the second convention because the large number of variations renders the first set of patterns practically useless.

The special feature the patterns at $u = 1$ have is that this is the only set which was drawn for complex p-numbers. For it a new complex constant of amplitude was chosen in order that the fields would be in either the (r or ϕ)-directions at time $t = 0$. Like the cutoff fields with imaginary p - numbers the fields are strongest near the outside of the waveguide.

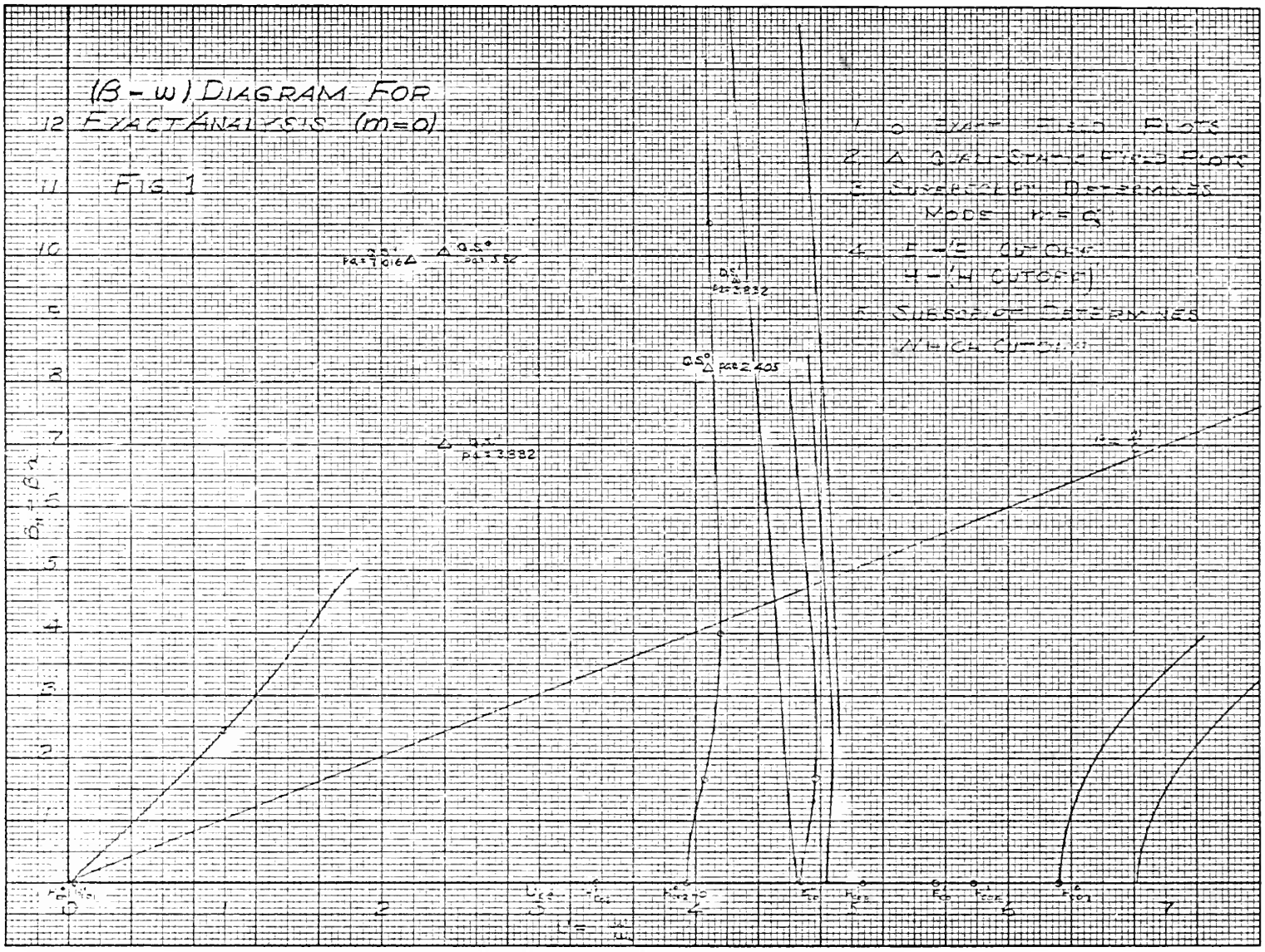
(B - W) DIAGRAM FOR
EXACT ANALYSIS (m=0)
FIG. 1

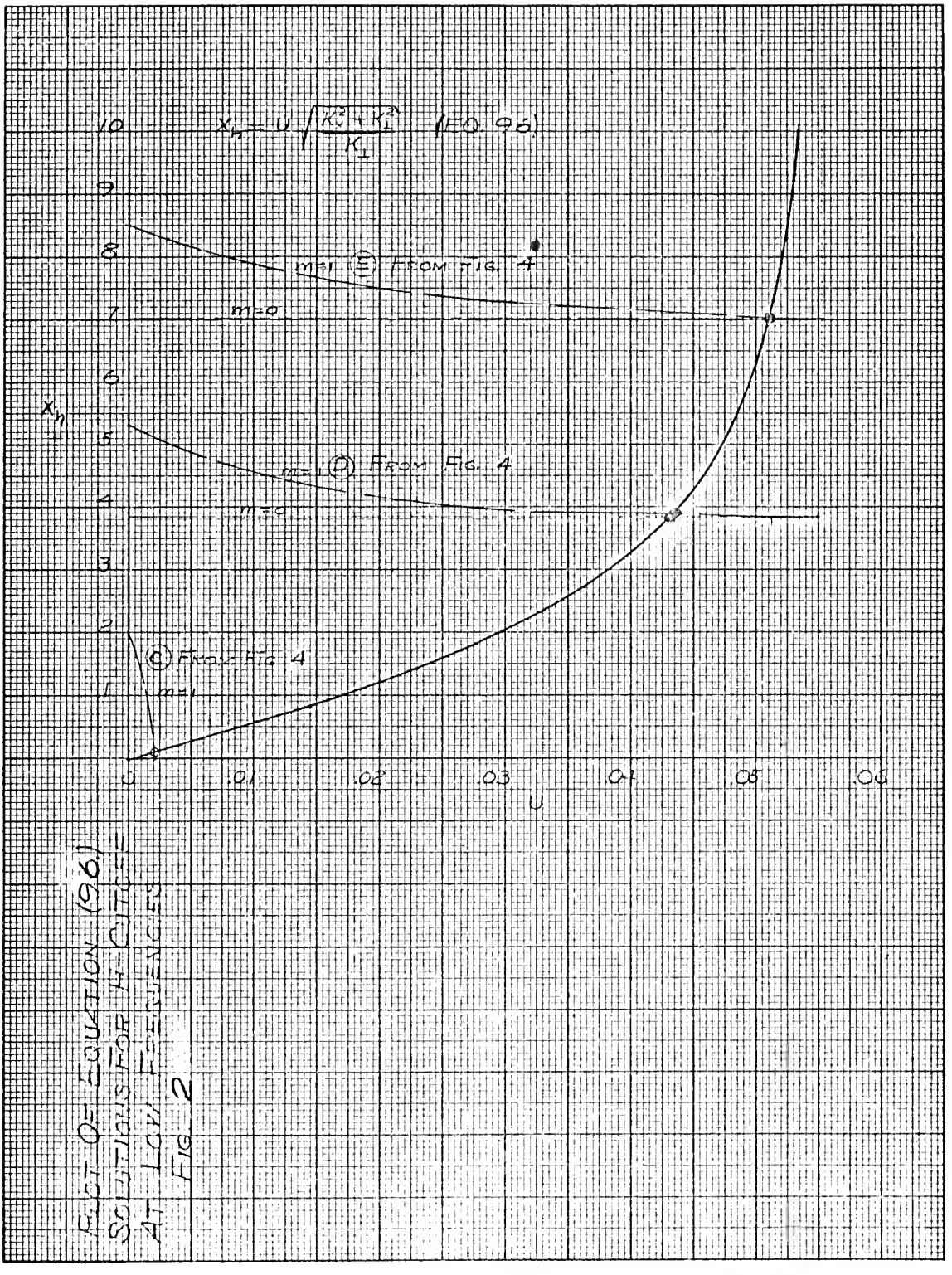

FIG. 2 — SOLUTIONS FOR $\mu = 0$ EQUATION (96) AT LOW FREQUENCIES

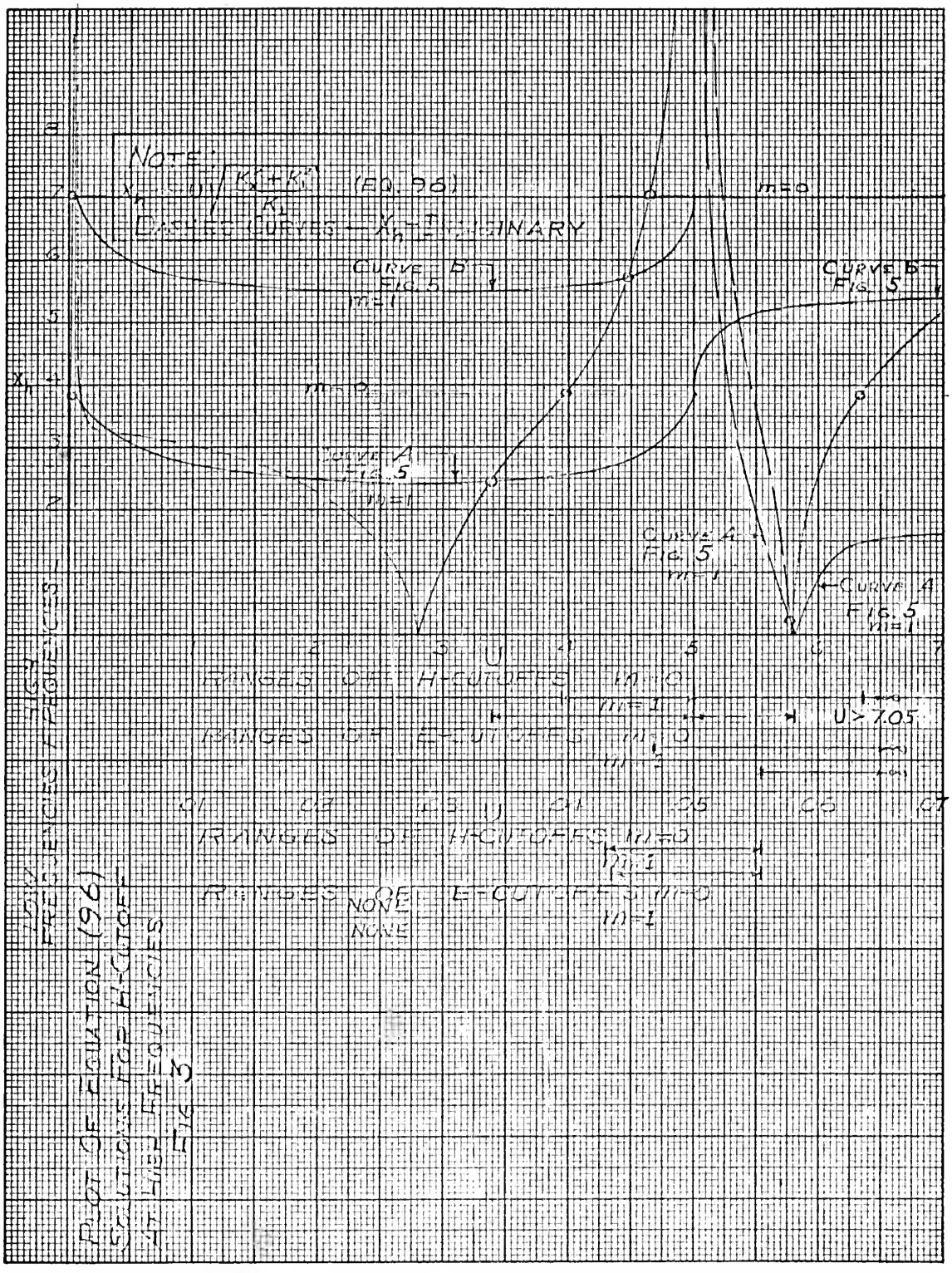
NOTE:
$X_h = \sqrt{\frac{K_x^2 + K^2}{K_x}}$ (EQ. 96)
CURVES — X_h = TRIGINARY
CURVE A FIG. 5 m=1
CURVE B FIG. 5 m=1
CURVE A FIG. 5 m=0
CURVE B FIG. 5 m=0
CURVE A FIG. 5 m=1
CURVE A FIG. 5 m=1
U > 7.05
RANGES OF H-CUTOFFS m=0
RANGES OF H-CUTOFFS m=1
RANGES OF E-CUTOFFS m=0
RANGES OF E-CUTOFFS m=1
NONE
NONE
X_h
FREE FREQUENCIES
CUTOFF FREQUENCIES
FIG. 96 — EQUATION (96)

PLOT OF
EQUATION (65)
FOR FOLLOWING EQUATIONS
CURVES TRANSFERRED

PLOT OF EQUATION (9.5) FOR HIGH FREQUENCIES
FIG. 5
NOTE
CURVES TRANSFERRED TO FIG. 12

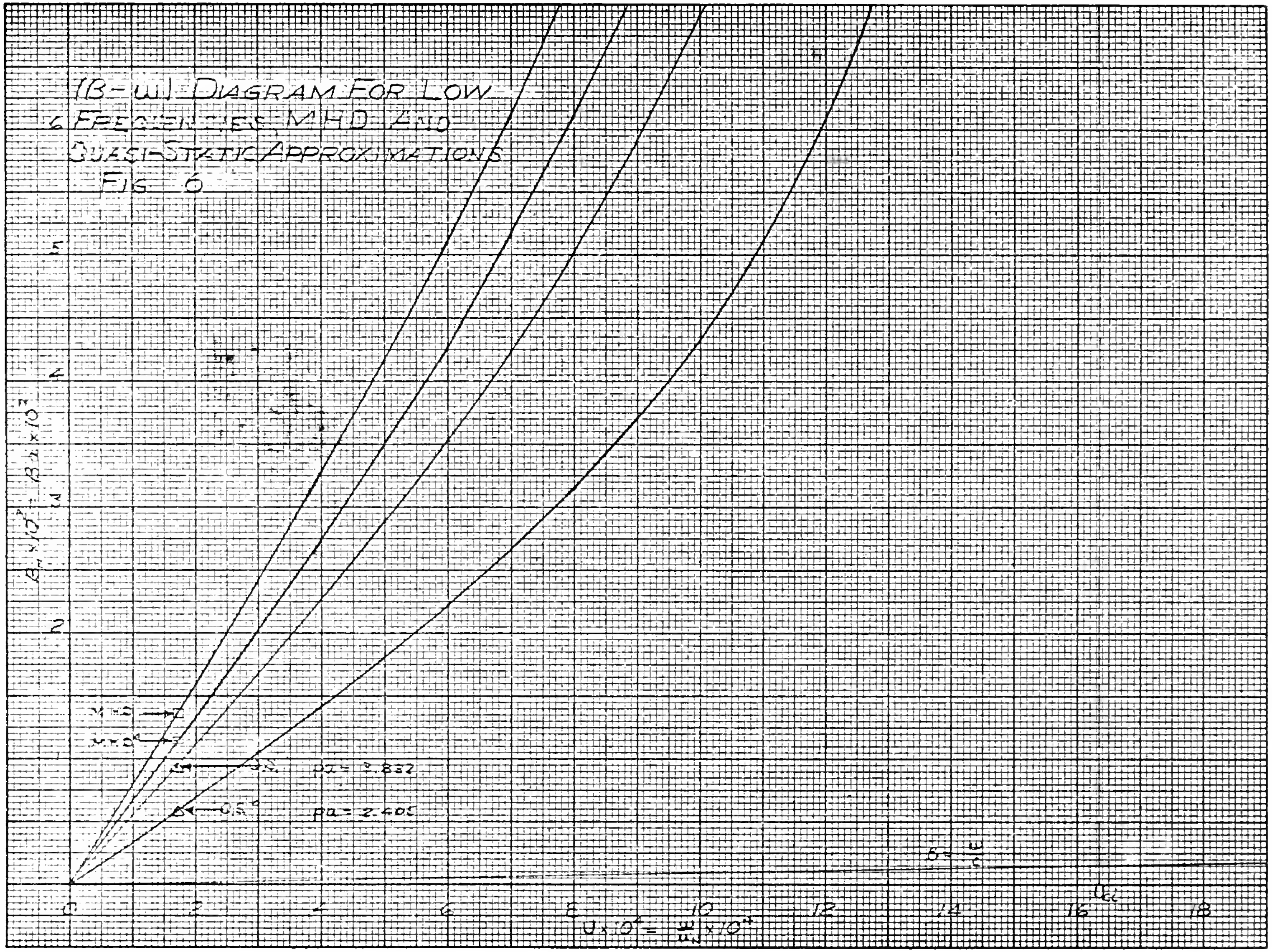

(B-ω) Diagram For Low Frequencies MHD And Quasi-Static Approximations
Fig. 6

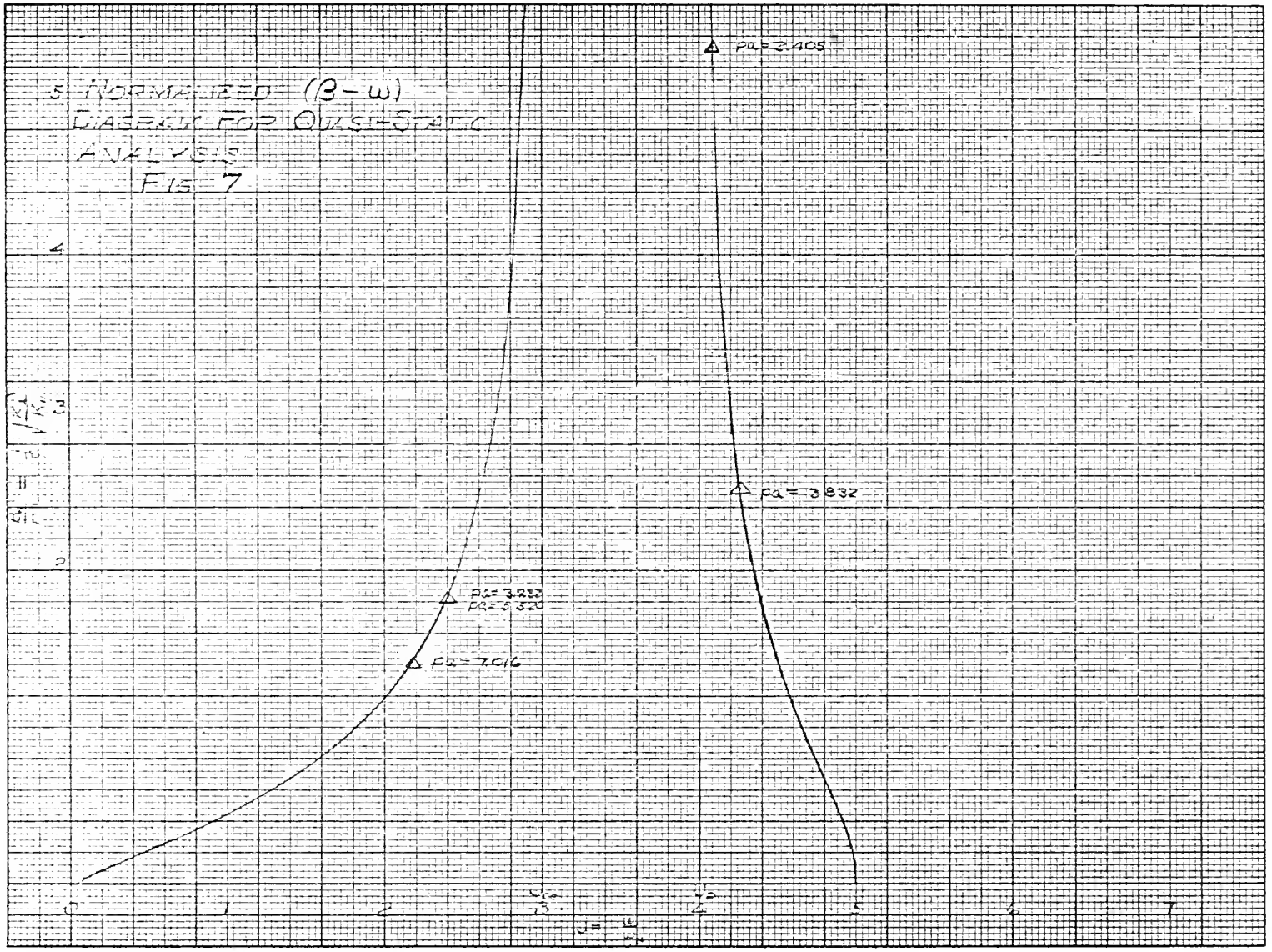
NORMALIZED (β − ω)
DIAGRAM FOR QUASI-STATIC
ANALYSIS
FIG 7
Pa = 2.405
Pa = 3.832
Pa = 3.832
Pa = 5.520
Pa = 7.016
0
1
2
3
4
5
6
7

MHD:

E-Wave (1.) pp. 169-172

$m = 0$

$u = 17 \times 10^{-5}$

$\beta_n = 1.141 \times 10^{-2}$

$p = 2.405/a$

$A(z,t) = A_1 e^{j(17\times10^{-5}\omega_n t - 1.141\times10^{-2}\frac{z}{a})}$

Complex Fields:

$\bar{E} = A(z,t)\ [-j795\ J_1(pr)\vec{1}_r + J_o(pr)\vec{1}_z]$

$\bar{H} = A(z,t)\ [-j103.8\ J_1(pr)\vec{1}_\phi]$

$\bar{J} = A(z,t)\ [23.7\ J_1(pr)\vec{1}_r + j2.38\ J_1(pr)\vec{1}_\phi - j4.99\times10^{+3}\ J_o(pr)\vec{1}_z]$

$\bar{J}_e = A(z,t)\ [+1.273\times10^{-2}\ J_1(pr)\vec{1}_r - j2.25\times10^{2}\ J_1(pr)\vec{1}_\phi - j4.99\times10^{+3}\ J_o(pr)\vec{1}_z]$

$\bar{J}_i = A(z,t)\ [23.7\ J_1(pr)\vec{1}_r + j2.27\times10^{2}\ J_1(pr)\vec{1}_\phi - j2.72\times10^{-4}\ J_o(pr)\vec{1}_z]$

$\rho = A(z,t)\ [-j3.38\times10^{-7}\ J_o(pr)]$

$\rho_e = A(z,t)\ [-j1.118\times10^{-3}\ J_o(pr)]$

$\rho_i = A(z,t)\ [+j1.118\times10^{-3}\ J_o(pr)]$

Quasi-Static: (1.) pp. 241-246, 253-254

$m = 0$

$u = 17 \times 10^{-5}$

$\beta_n = 5.87 \times 10^{-3}, \quad \beta = .1174$

$p = 2.405/a$

$A(z,t) = A_1 e^{j(17 \times 10^{-5} \omega_n t - 5.87 \times 10^{-3} z/a)}$

Complex Fields:

$$\bar{E} = A(x,t)\,[-j410\ J_1(pr)\vec{1}_r + J_o(pr)\vec{1}_z]$$

$$\bar{H} = A(z,t)\,[(-6.44 \times 10^{-5}\ J_1(pr) - 3.35 \times 10^{-5}\ \tfrac{r}{a})\vec{1}_r - j103.9\ J_1(pr)\vec{1}_\phi + j(2.64 \times 10^{-2}\ J_o(pr) - 1.142 \times 10^{-2})\vec{1}_z]$$

$$\bar{J} = A(z,t)\,[12.20\ J_1(pr)\vec{1}_r + j1.230\ J_1(pr)\vec{1}_\phi - j4.99 \times 10^{3}\ J_o(pr)\vec{1}_z]$$

$$\bar{J}_e = A(z,t)\,[6.56 \times 10^{-3}\ J_1(pr)\vec{1}_r - j1.159 \times 10^{2}\ J_1(pr)\vec{1}_\phi - j4.99 \times 10^{+3}\ J_o(pr)\vec{1}_z]$$

$$\bar{J}_i = A(z,t)\,[12.20\ J_1(pr)\vec{1}_r + j1.171 \times 10^{2}\ J_1(pr)\vec{1}_\phi - j2.272 \times 10^{-4}\ J_o(pr)\vec{1}_z]$$

$$\rho = A(z,t)\,[-j1.746 \times 10^{-7}\ J_o(pr)]$$

$$\rho_e = A(z,t)\,[-j5.75 \times 10^{-4}\ J_o(pr)]$$

$$\rho_i = A(z,t)\,[+j5.75 \times 10^{-4}\ J_o(pr)]$$

Note: Field Patterns Drawn For MHD Only

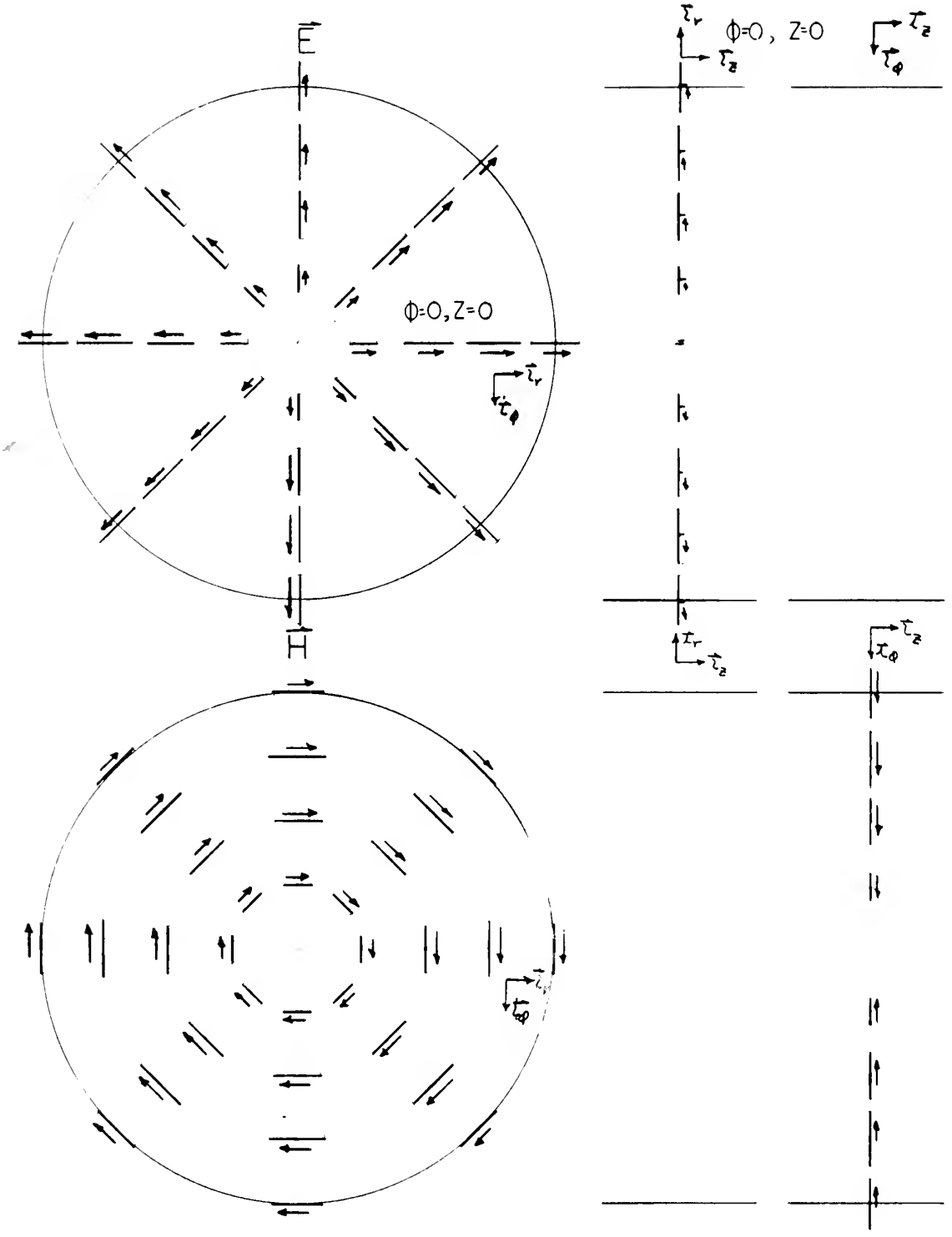
E
Φ=0, Z=0
H
Φ=0 , Z=0

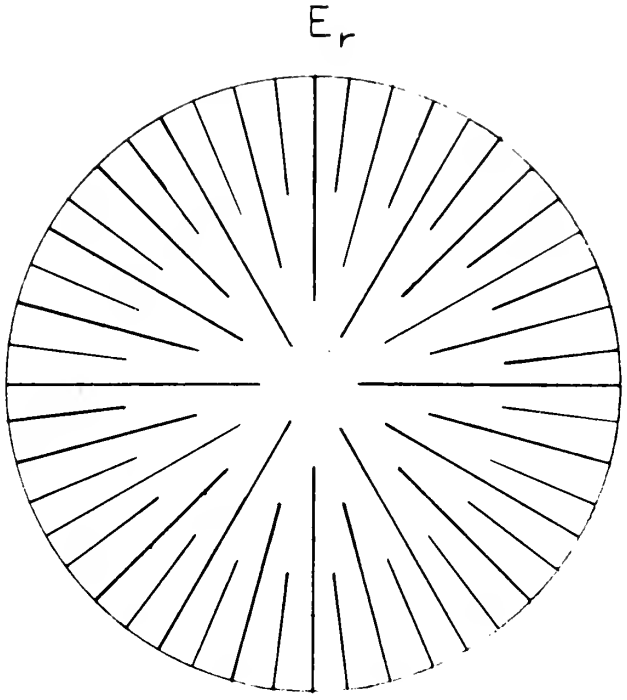
E_r

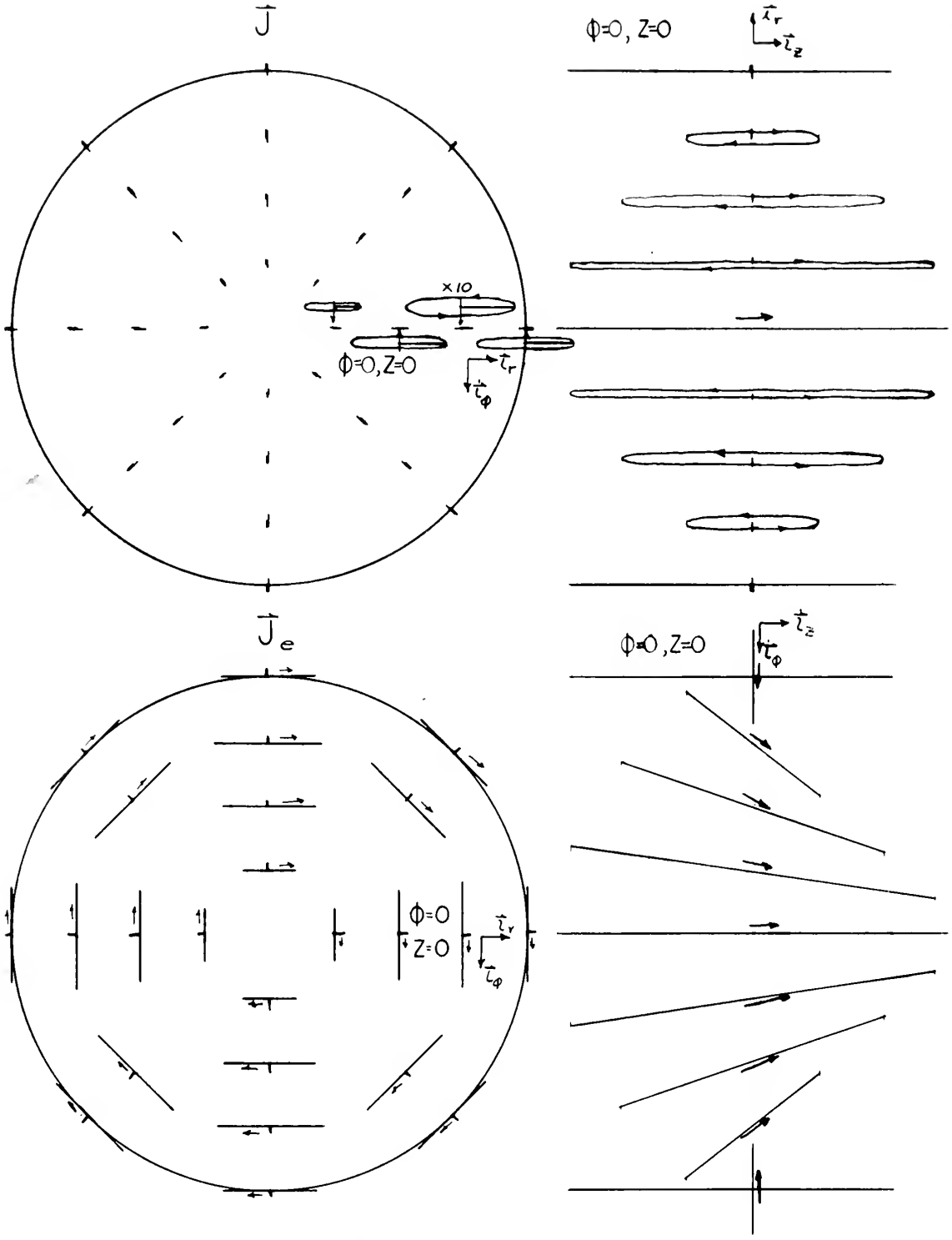
$\vec{J}$
Φ=0, Z=0
$\vec{i}_r$
$\vec{i}_z$
×10
Φ=0,Z=0
$\vec{i}_r$
$\vec{i}_\varphi$
$\vec{J}_e$
Φ=0 ,Z=0
$\vec{i}_z$
$\vec{i}_\varphi$
Φ=0
Z=0
$\vec{i}_r$
$\vec{i}_\varphi$

J_r

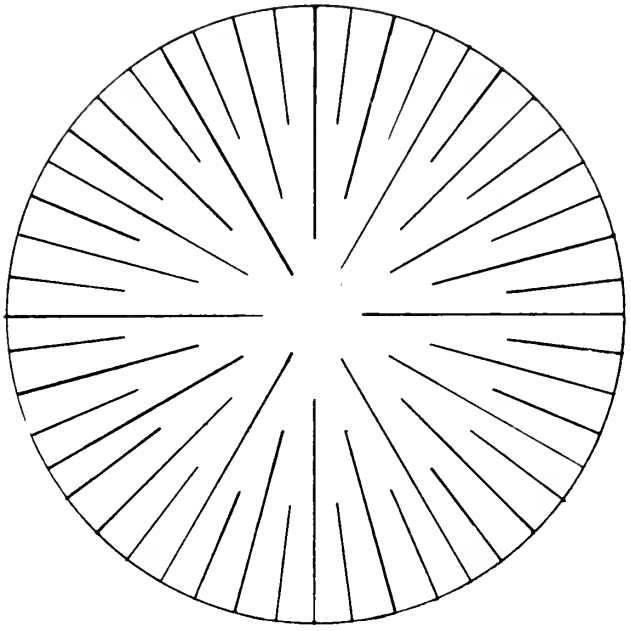

J_{er}

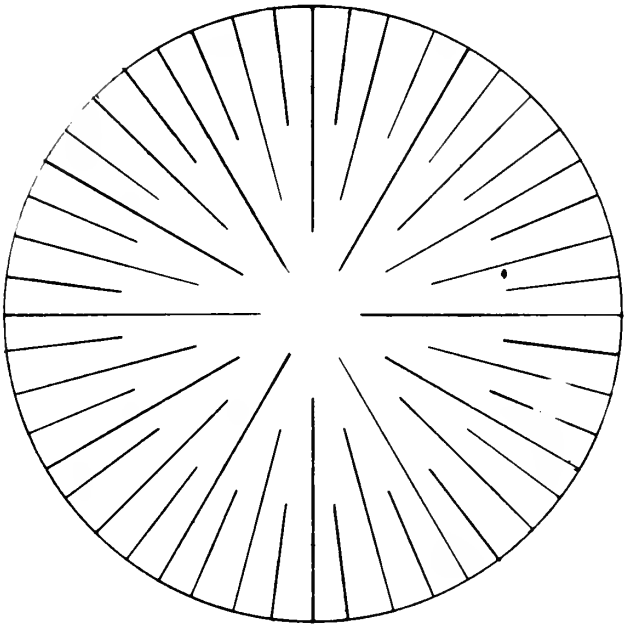

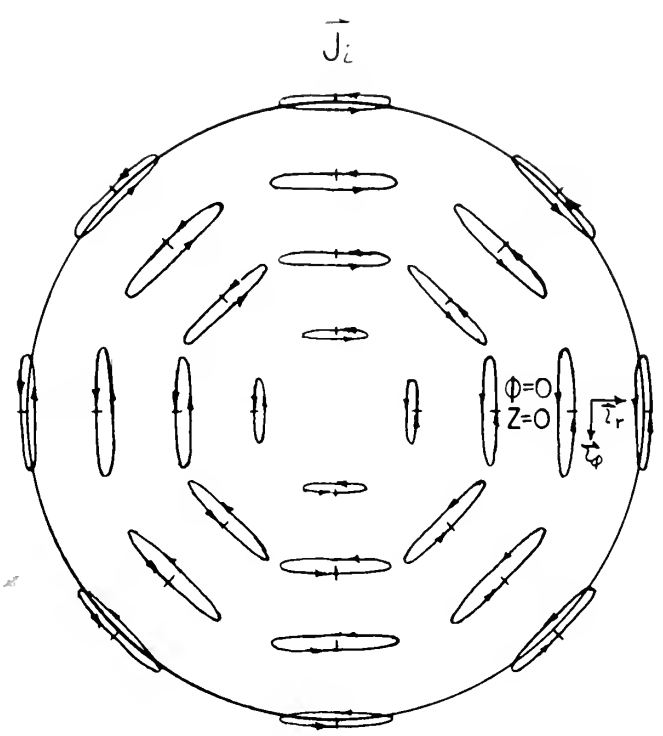

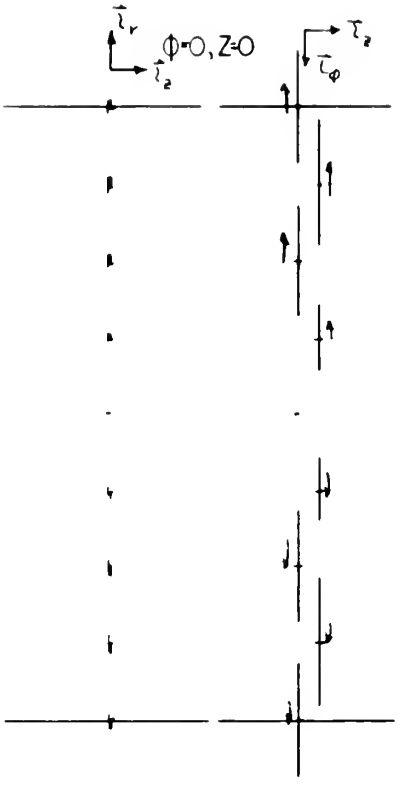

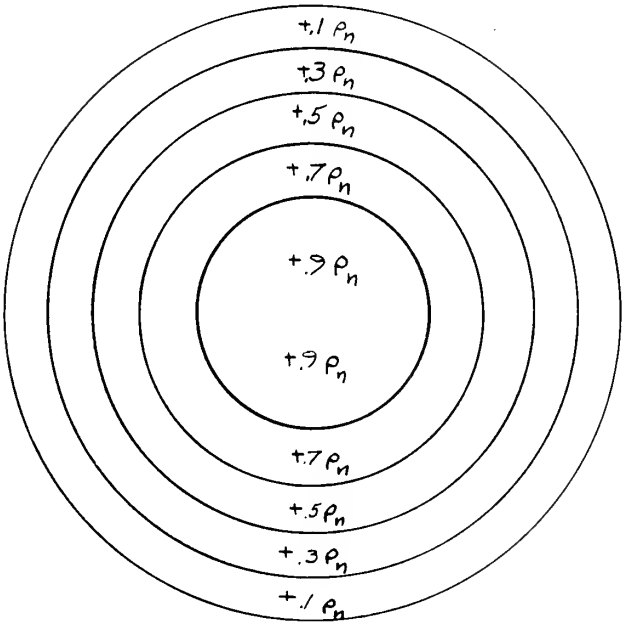

$\omega t = \frac{\pi}{2}$

$\rho = \rho_n$

$\rho_e = 3.31 \times 10^3 \rho_n$

$\rho_i = -3.31 \times 10^3 \rho_n$

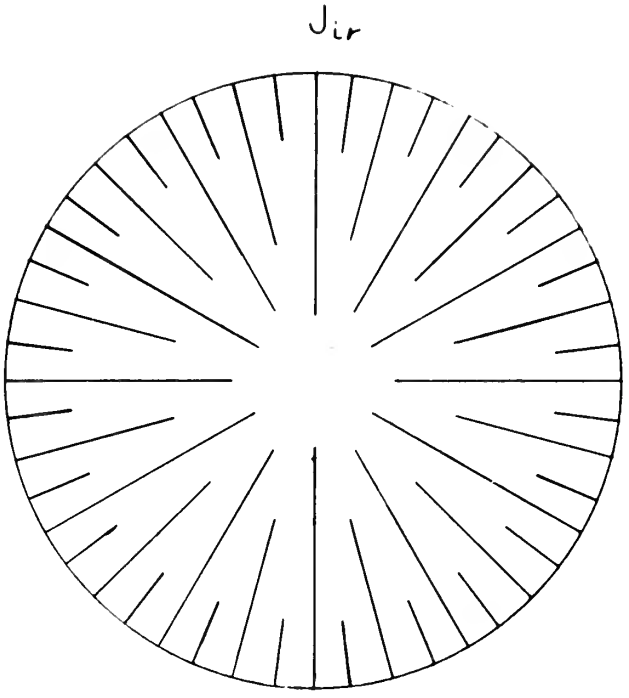
J_{ir}

MHD:

E-Wave (1.) pp. 169-172

$m = 1$

$u = 17\times10^{-5}$

$\beta_n = 1.353\times10^{-2}$

$p = 3.832/a$

$A(\phi,z,t) = A_1 e^{j(17\times10^{-5}\omega_n t - 1.353\times10^{-2} z/a)} e^{j\phi}$

Complex Fields:

$$\bar{E} = A(\phi,z,t)\left[j5.93\times10^{2}\left(J_o(pr) - \frac{J_1(pr)}{pr}\right)\vec{1}_r - 5.93\times10^{2}\,\frac{J_1(pr)}{pr}\,\vec{1}_\phi + J_1(pr)\vec{1}_z\right]$$

$$\bar{H} = A(\phi,z,t)\left[65.1\,\frac{J_1(pr)}{pr}\,\vec{1}_r + j65.1\left(J_o(pr) - \frac{J_1(pr)}{pr}\right)\vec{1}_\phi\right]$$

$$\bar{J} = A(\phi,z,t)\left[-17.63\,J_o(pr) + 15.85\,\frac{J_1(pr)}{pr}\right)\vec{1}_r - j\left(1.779\,J_o(pr) + 15.85\,\frac{J_1(pr)}{pr}\right)\vec{1}_\phi - j4.99\times10^{3}\,J_1(pr)\vec{1}_z\right]$$

$$\bar{J}_e = A(\phi,z,t)\left[-\left(9.49\times10^{-3}\,J_o(pr) - 1.672\times10^{2}\,\frac{J_1(pr)}{pr}\right)\vec{1}_r + j1.672\times10^{2}\left(J_o(pr) - \frac{J_1(pr)}{pr}\right)\vec{1}_\phi - j4.99\times10^{3}\,J_1(pr)\vec{1}_z\right]$$

$$\bar{J}_i = A(\phi,z,t)\left[\left(-17.62\,J_o(pr) - 1.519\times10^{2}\,\frac{J_1(pr)}{pr}\right)\vec{1}_r - j\left(1.697\times10^{2}\,J_o(pr) - 1.519\times10^{2}\,\frac{J_1(pr)}{pr}\right)\vec{1}_\phi - j2.72\times10^{-4}\,J_1(pr)\vec{1}_z\right]$$

$$\rho = A(\phi,z,t)\left[-j4.02\times10^{-7}\,J_1(pr)\right]$$

$$\rho_e = A(\phi,z,t)\left[-j1.324\times10^{-3}\,J_1(pr)\right]$$

$$\rho_i = A(\phi,z,t)\left[+j1.325\times10^{-3}\,J_1(pr)\right]$$

Quasi-Static: (1.) pp.241-246, 253-254

$m = 1$

$u = 17\times10^{-5}$

$\beta_n = 9.36\times10^{-3}$ $\beta = .1872$

$p = 3.83/a$

$A(\phi,z,t) = A_1 e^{j(17\times10^{-5}\omega_n t - 9.36\times10^{-3} z/a)} e^{j\phi}$

Complex Fields:

$$\bar{E} = A(\phi,z,t)\left[j409\left(J_o(pr) - \frac{J_1(pr)}{pr}\right)\vec{1}_r - 409\,\frac{J_1(pr)}{pr}\,\vec{1}_\phi + J_1(pr)\vec{1}_z\right]$$

$$\bar{H} = A(\phi,z,t)\left[65.1\,\frac{J_1(pr)}{pr}\,\vec{1}_r + j65.1\left(J_o(pr) - \frac{J_1(pr)}{pr}\right)\vec{1}_\phi + j1.652\times10^{-2}\,J_1(pr)\vec{1}_z\right]$$

$$\bar{J} = A(\phi,z,t)\left[\left(-12.19\,J_o(pr) + 10.95\,\frac{J_1(pr)}{pr}\right)\vec{1}_r - j\left(1.228\,J_o(pr) + 10.95\,\frac{J_1(pr)}{pr}\right)\vec{1}_\phi - j4.99\times10^{3}\,J_1(pr)\vec{1}_z\right]$$

$$\bar{J}_e = A(\phi,z,t)\left[-\left(6.54\times10^{-3}\,J_o(pr) - 1.156\times10^{2}\,\frac{J_1(pr)}{pr}\right)\vec{1}_r + j1.156\times10^{2}\left(J_o(pr) - \frac{J_1(pr)}{pr}\right)\vec{1}_\phi - j4.99\times10^{3}\,J_1(pr)\vec{1}_z\right]$$

$$\bar{J}_i = A(\phi,z,t)\left[\left(-12.19\,J_o(pr) - 1.048\times10^{2}\,\frac{J_1(pr)}{pr}\right)\vec{1}_r + j\left(-1.169\times10^{2}\,J_o(pr) + 1.048\times10^{2}\,\frac{J_1(pr)}{pr}\right)\vec{1}_\phi - 2.72\times10^{-4}\,J_1(pr)\vec{1}_z\right]$$

$$\rho = A(\phi,z,t)\left[-j2.77\times10^{-7}\,J_1(pr)\right]$$

$$\rho_e = A(\phi,z,t)\left[-j9.16\times10^{-4}\,J_1(pr)\right]$$

$$\rho_i = A(\phi,z,t)\left[j9.16\times10^{-4}\,J_1(pr)\right]$$

Note: Field Patterns Drawn For MHD Only

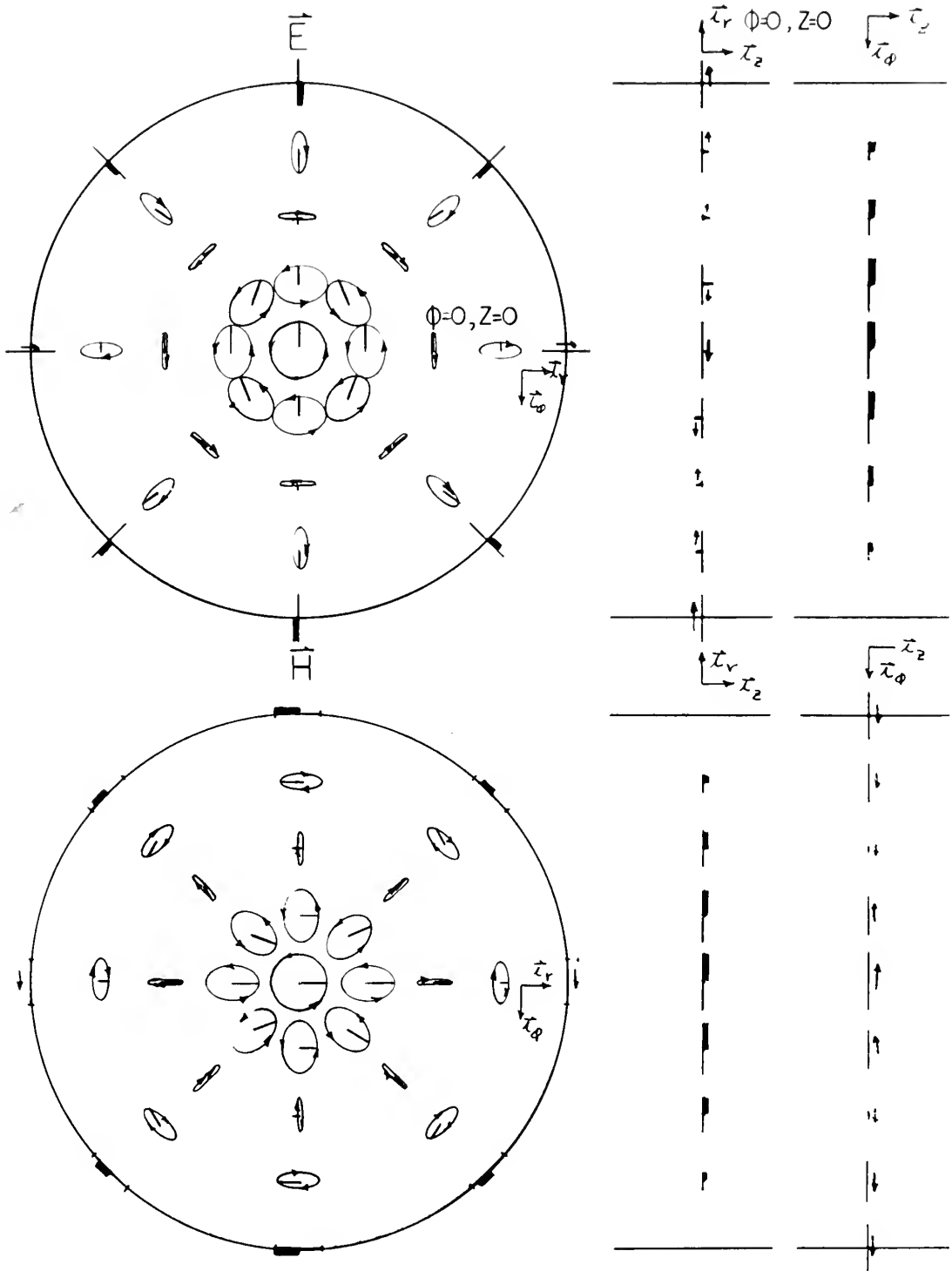
E
Φ=0, Z=0
H
Φ=0, Z=0

$\vec{E}_T$

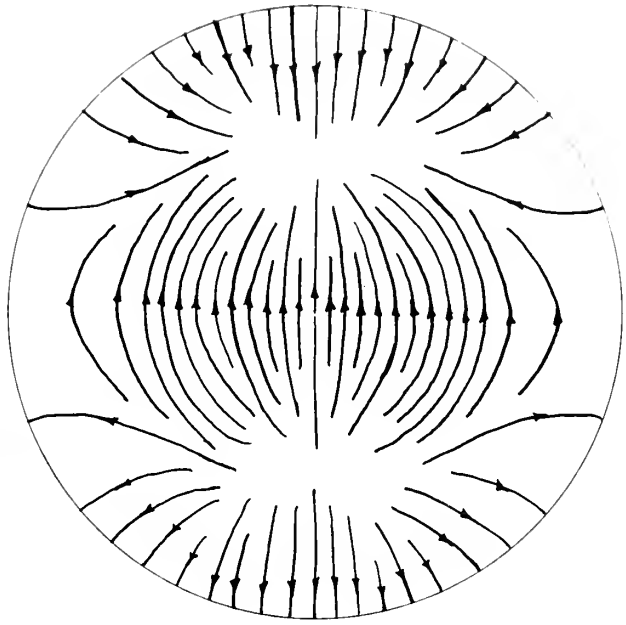

$\vec{H}_T$

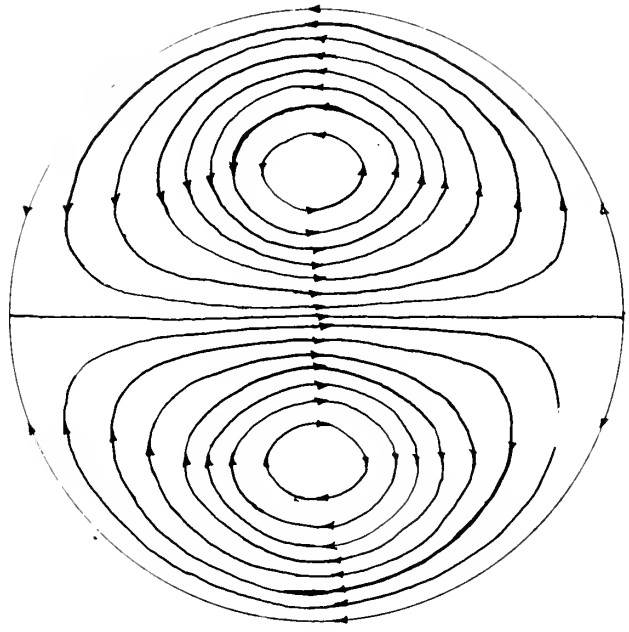

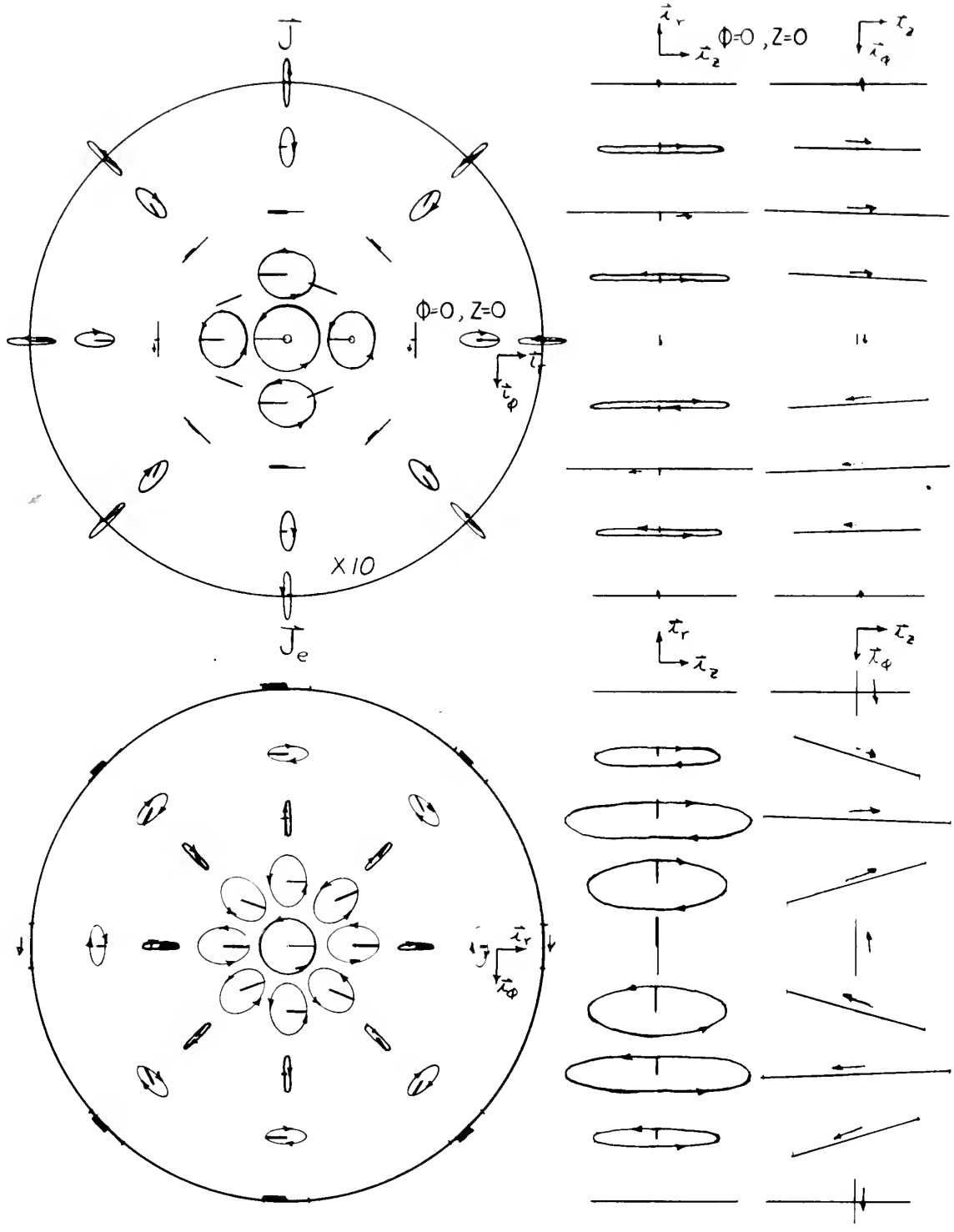
J
Φ=0 , Z=0
X10
J_e
Φ=0 , Z=0

$\vec{J}_T$

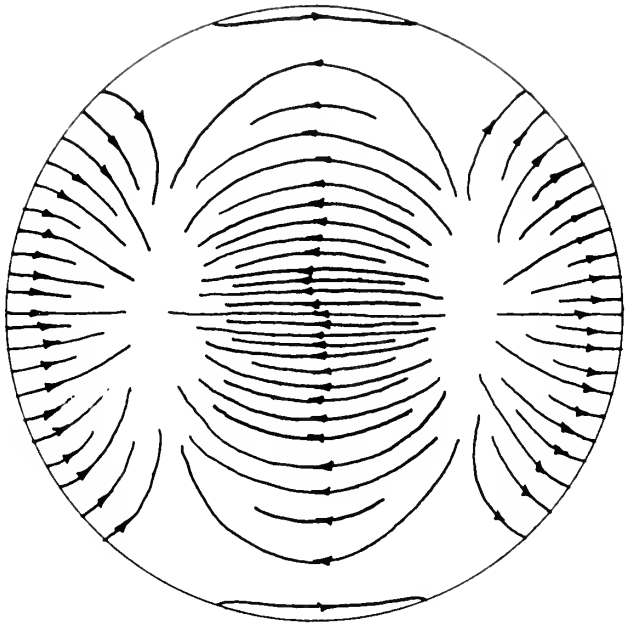

$\vec{J}_{eT}$

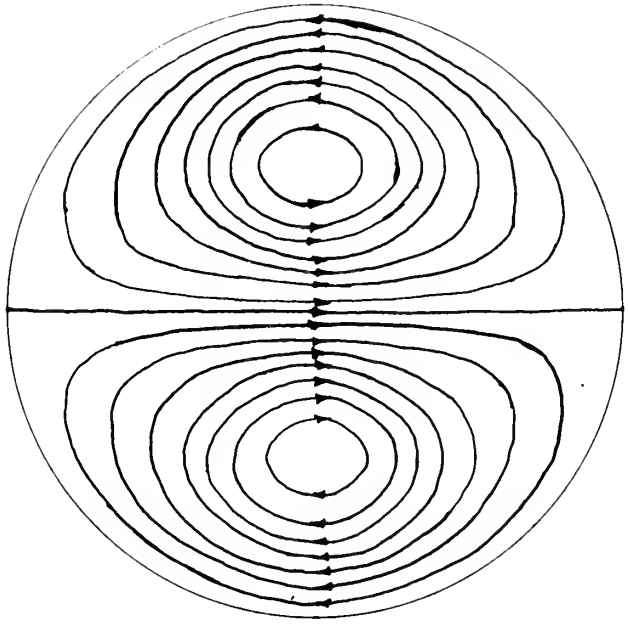

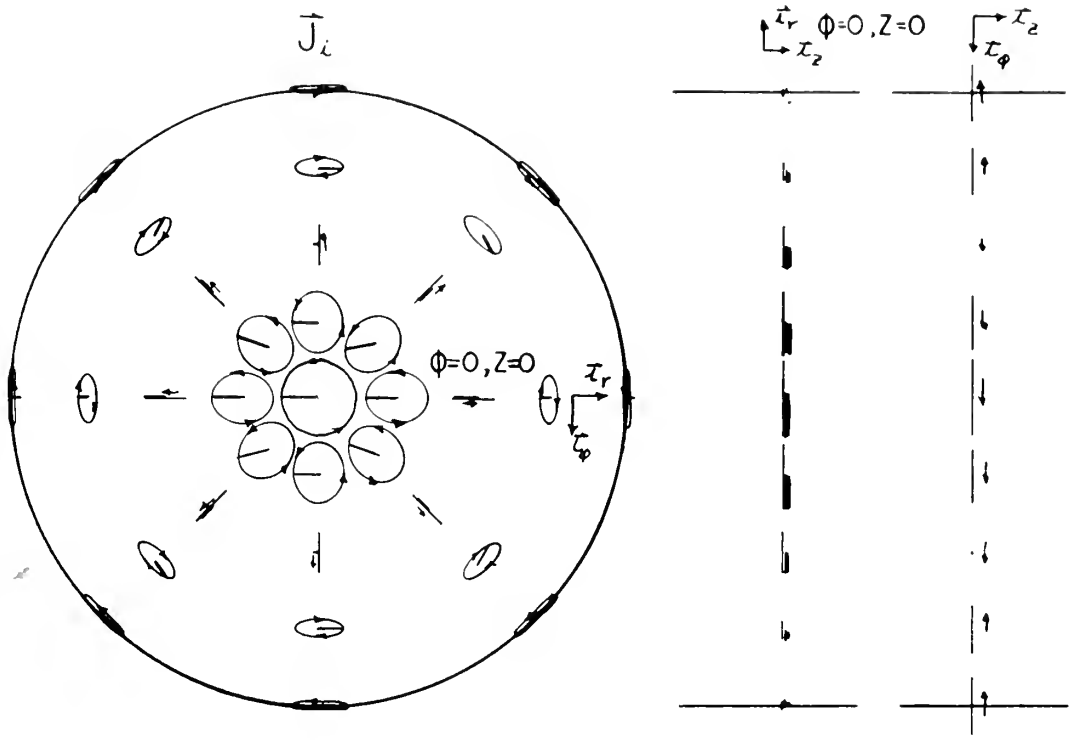

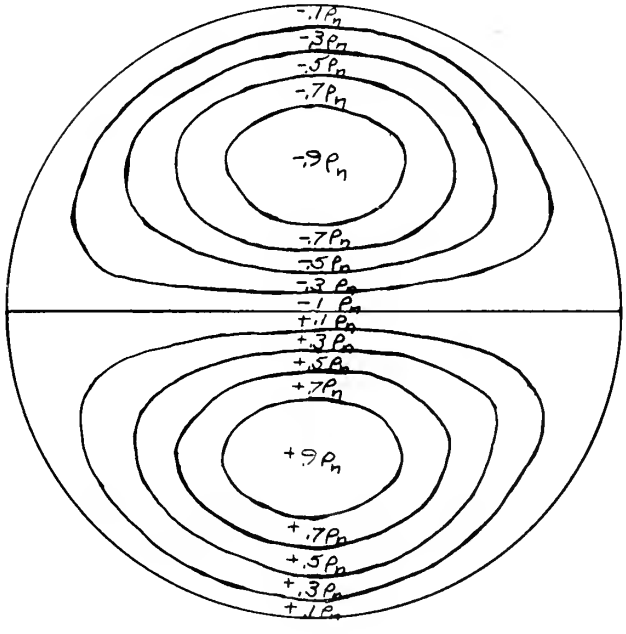

$\omega t = 0$

$\rho = \rho_n$

$\rho_e = 3.3 \times 10^3 \rho_n$

$\rho_i = -3.3 \times 10^3 \rho_n$

$\vec{J}_{iT}$

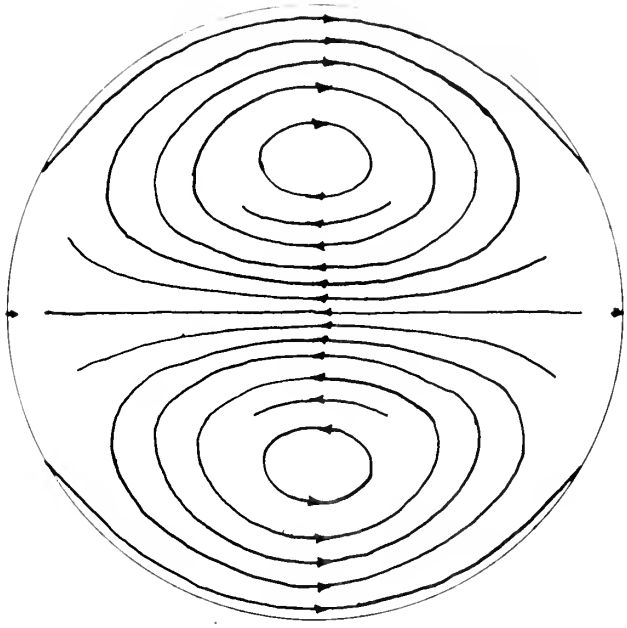

ELECTRON CYCLOTRON RESONANCE:

Quasi-Static Analysis

$m = 0$

$u = 2.4$

$\beta_n = 10.08$; $\beta = 201.6$

$p = \frac{5.52}{a}$

$A(z,t) = A_1 e^{j(2.4\omega_n t - 10.08 \frac{z}{a})}$

Complex Fields:

$$\bar{E} = A(z,t)\,[-j.547\,J_1(pr)\vec{1}_r + J_o(pr)\vec{1}_z]$$

$$\bar{H} = 10^{-3} x A(z,t)\,[(1.641\,J_1(pr) + 1.937x10^{-4} I_1(\beta r))\vec{1}_r - j2.05\,J_1(pr)\vec{1}_\phi - j(.898\,J_o(pr) + 1.937x10^{-4}\,I_o(\beta r))\vec{1}_z]$$

$$\bar{J} = A(z,t)\,[.344\,J_1(pr)\vec{1}_r - j.430\,J_1(pr)\vec{1}_\phi - j.354\,J_o(pr)\vec{1}_z]$$

$$\rho = A(z,t)\,[-j2.23x10^{-9}\,J_o(pr)]$$

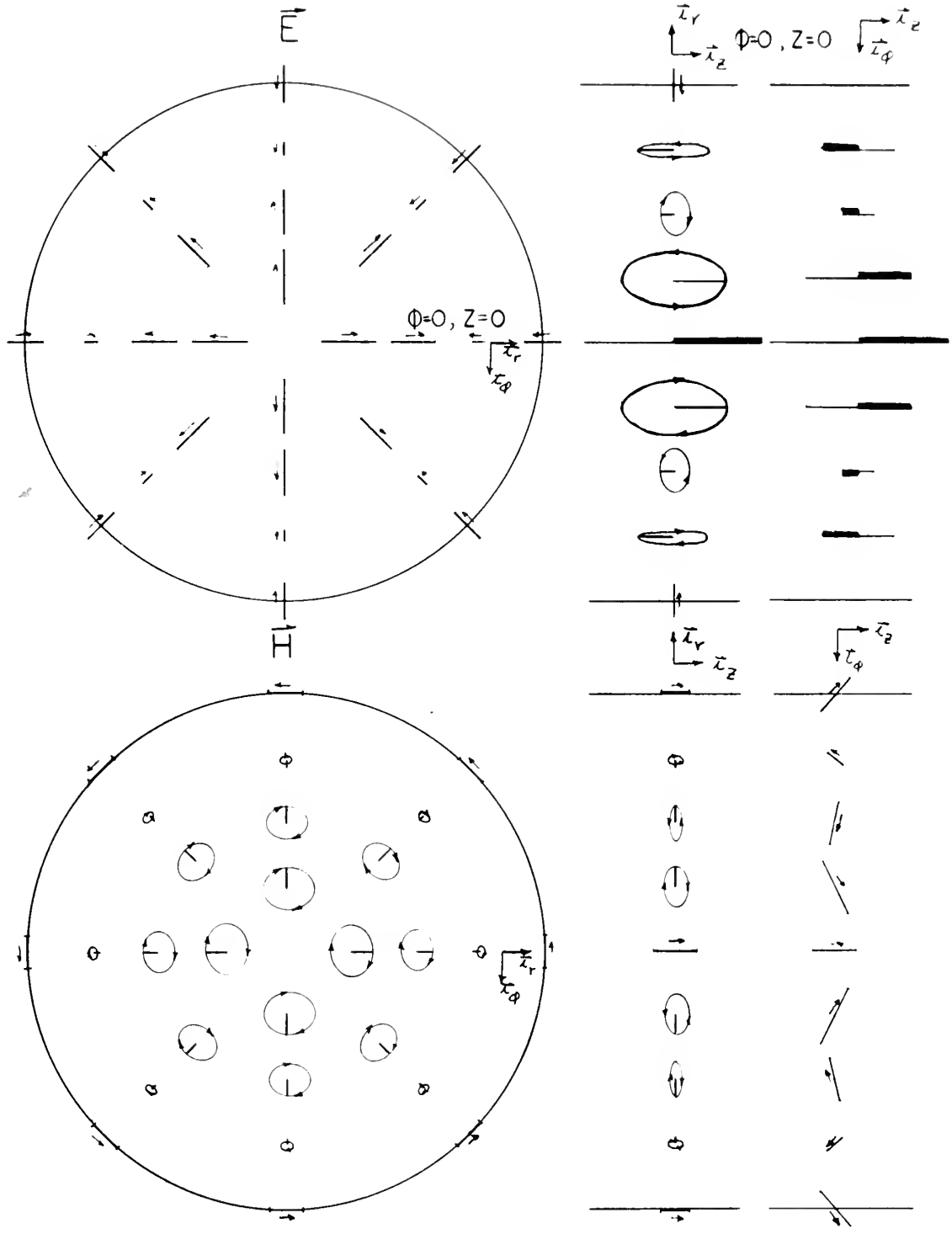
$\vec{E}$
$\Phi=0, Z=0$
$\vec{H}$
$\Phi=0, Z=0$

E_r

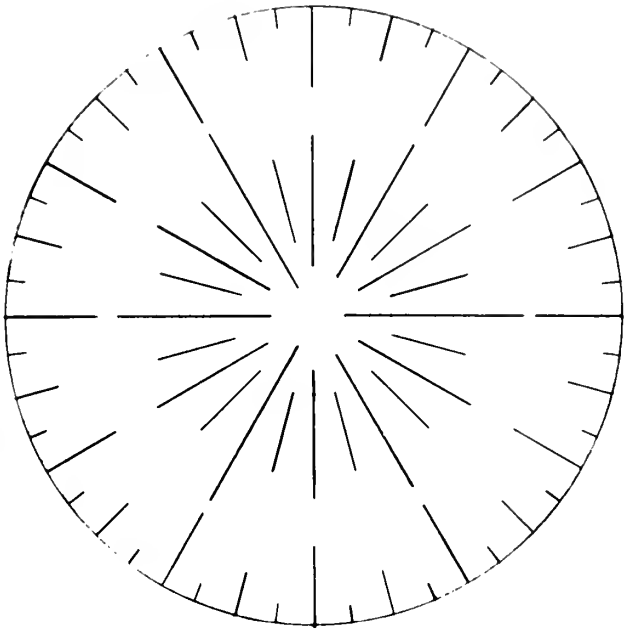

H_r

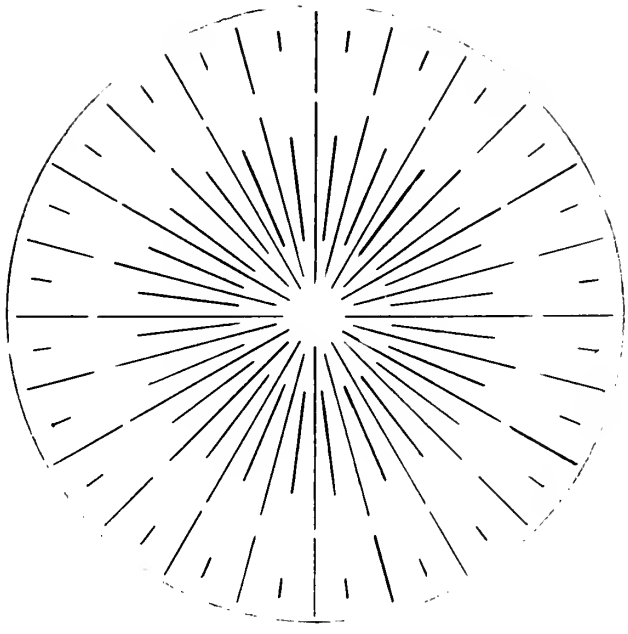

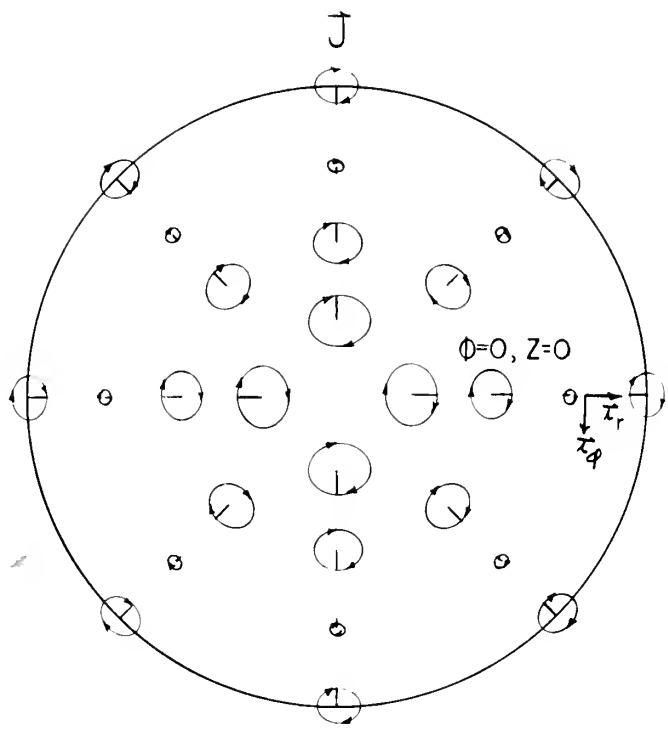

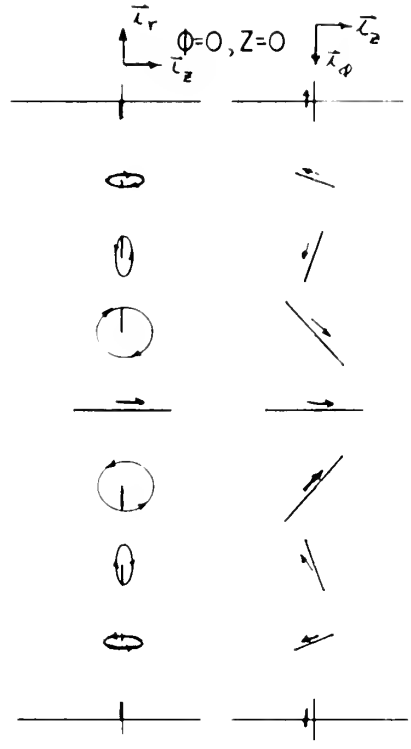

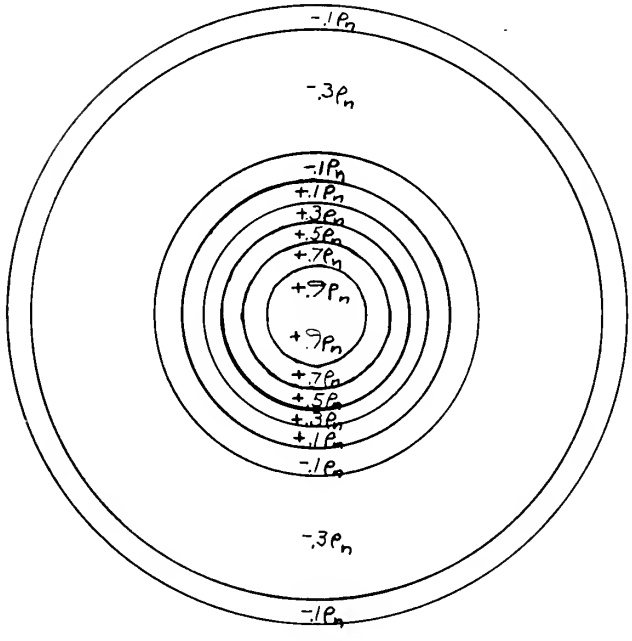

$\omega t = \frac{\pi}{2}$

$\rho = \rho_n$

$\rho_e = \rho_n$

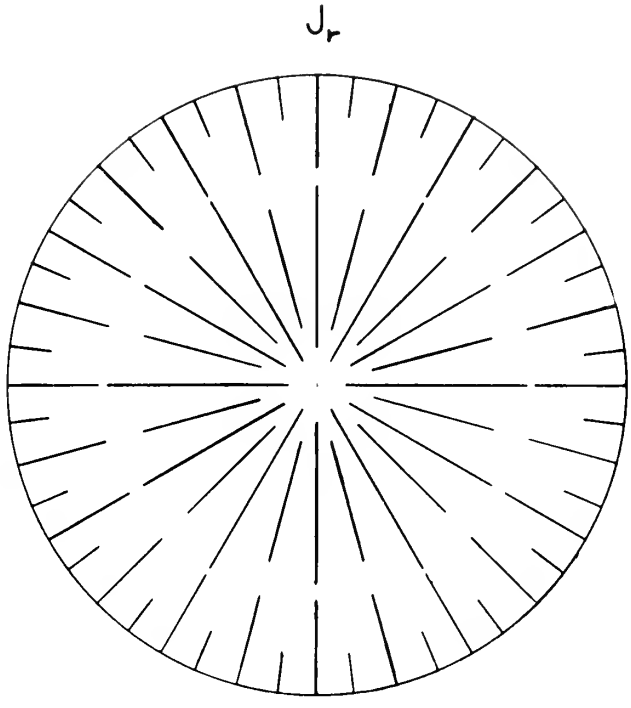
J_3

ELECTRON CYCLOTRON RESONANCE:

Quasi-Static Analysis

$m = 1$

$u = 2.4$

$\beta_n = 7.01$; $\beta = 140.2$

$p = \frac{3.83}{a}$

$A(\phi,z,t) = A_1 e^{j(2.4\omega_n t - 7.01 \frac{z}{a})} e^{j\phi}$

Complex Fields:

$$\bar{E} = A(\phi,z,t)\left[j.547\left(J_o(pr) - \frac{J_1(pr)}{pr}\right)\vec{1}_r - .547\,\frac{J_1(pr)}{pr}\,\vec{1}_\phi + J_1(pr)\vec{1}_z\right]$$

$$\bar{H} = 10^{-3}\,A(\phi,z,t)\left[\left(-2.36\,J_o(pr) + 5.31\,\frac{J_1(pr)}{pr} - 6.44\times10^{-3}\left(I_o(\beta r) - \frac{I_1(\beta r)}{\beta r}\right)\right)\vec{1}_r + j\left(2.95\,J_o(pr) - 5.31\,\frac{J_1(pr)}{pr} - 6.44\times10^{-3}\,\frac{I_1(\beta r)}{\beta r}\right)\vec{1}_\phi - j\left(1.292\,J_1(pr) - 6.44\times10^{-3}\,I_1(\beta r)\right)\vec{1}_z\right]$$

$$\bar{J} = A(\phi,z,t)\left[\left(-.344\,J_o(pr) + .744\,\frac{J_1(pr)}{pr}\right)\vec{1}_r + j\left(.430\,J_o(pr) - .744\,\frac{J_1(pr)}{pr}\right)\vec{1}_\phi - j.1937\,J_1(pr)\vec{1}_z\right]$$

$$\rho = A(\phi,z,t)\left[-j1.611\times10^{-9}\,J_1(pr)\right]$$

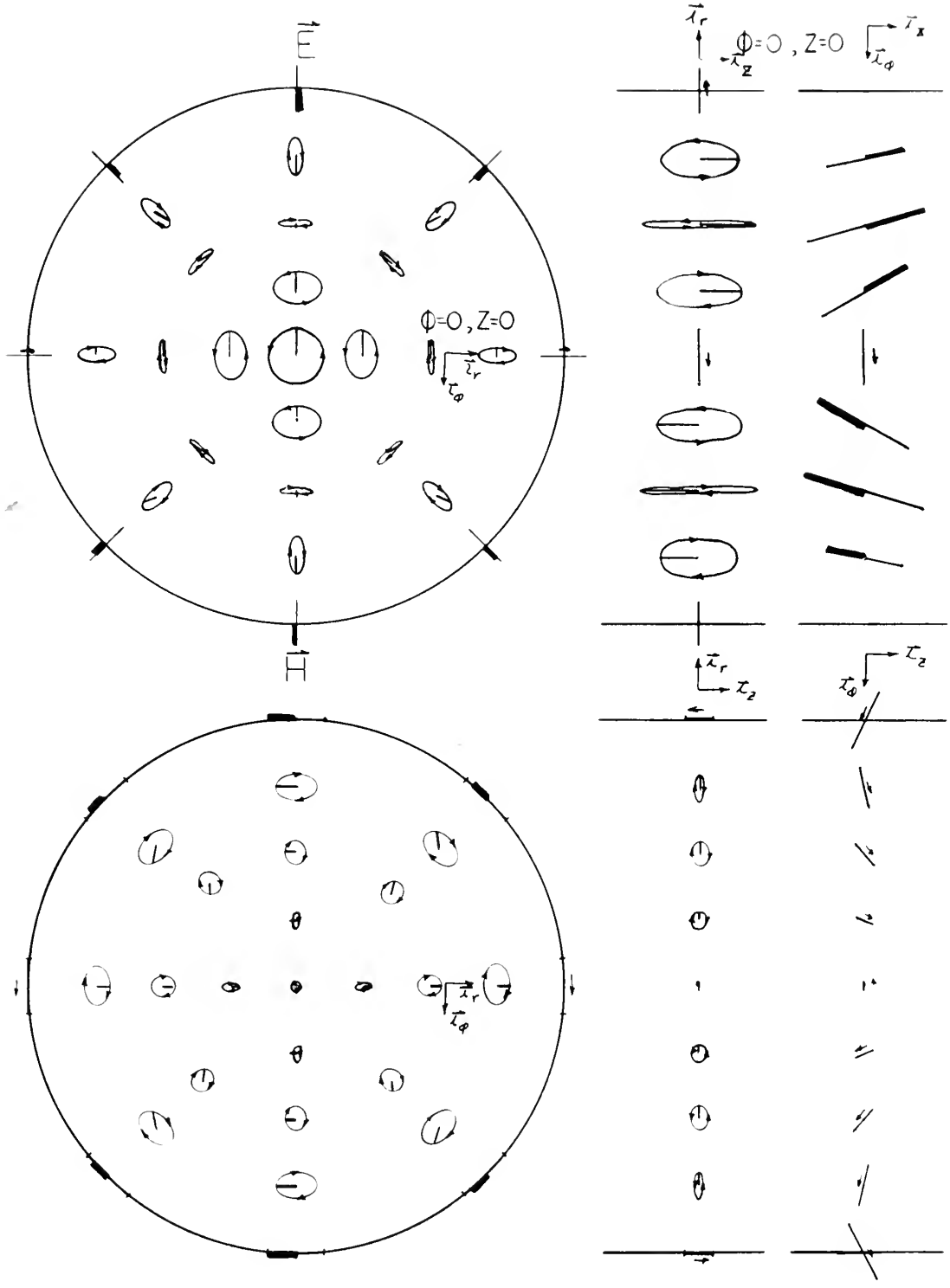
E
Φ=0, Z=0
H
Φ=0 , Z=0

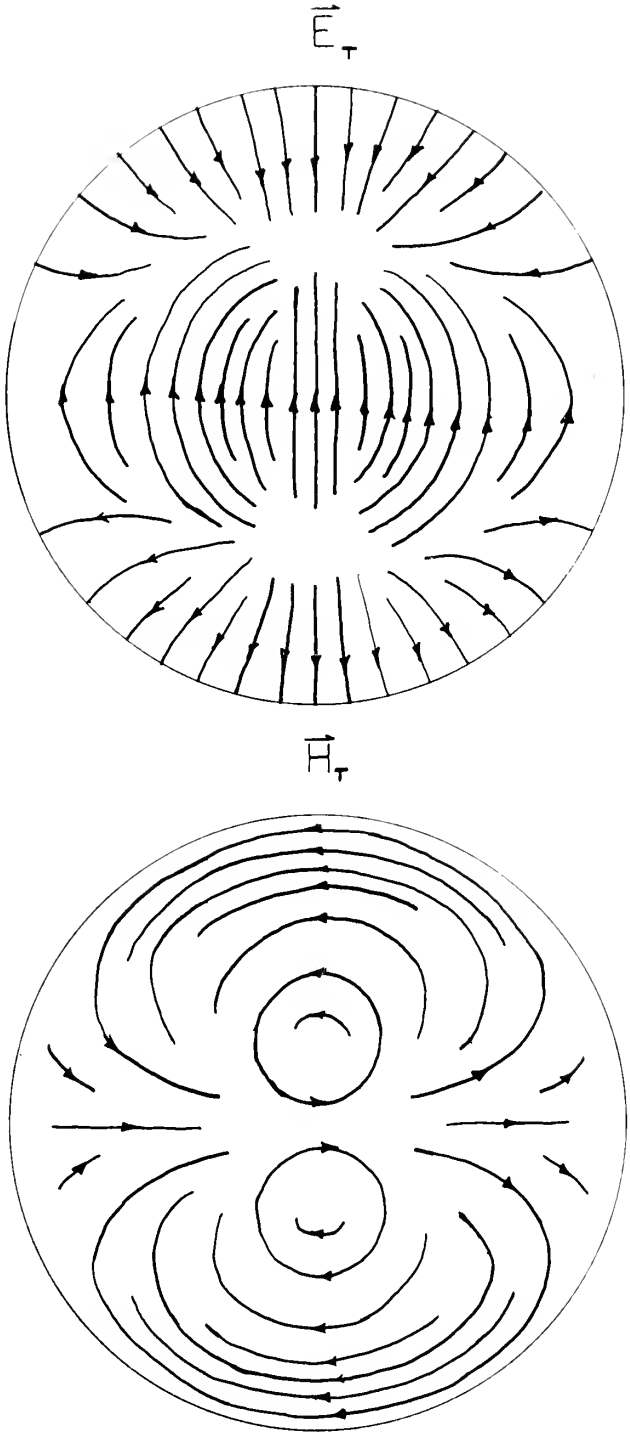
$\vec{E}_T$
$\vec{H}_T$

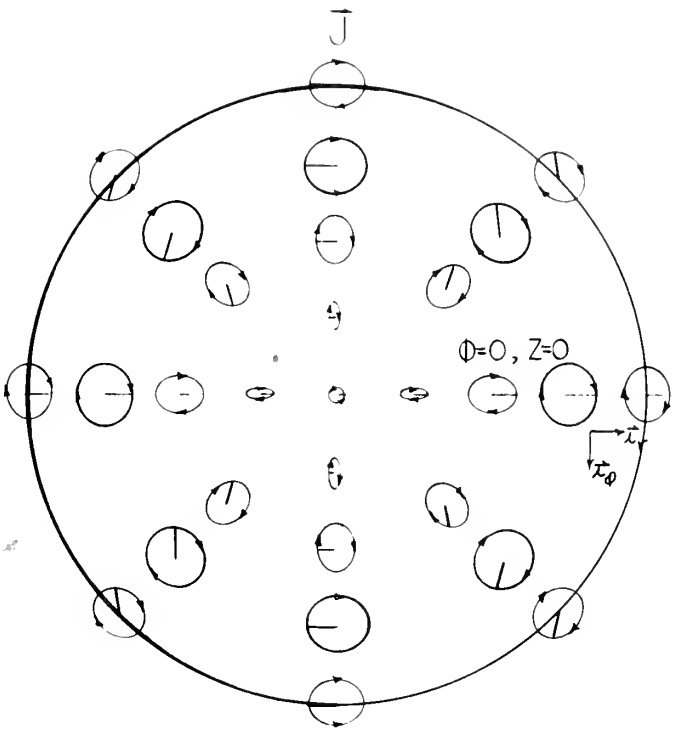

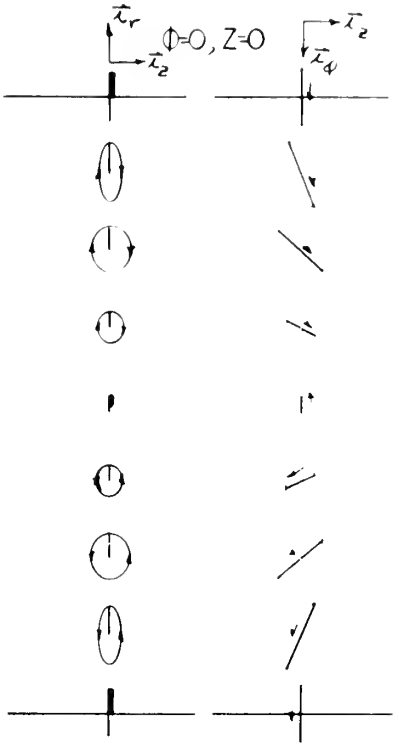

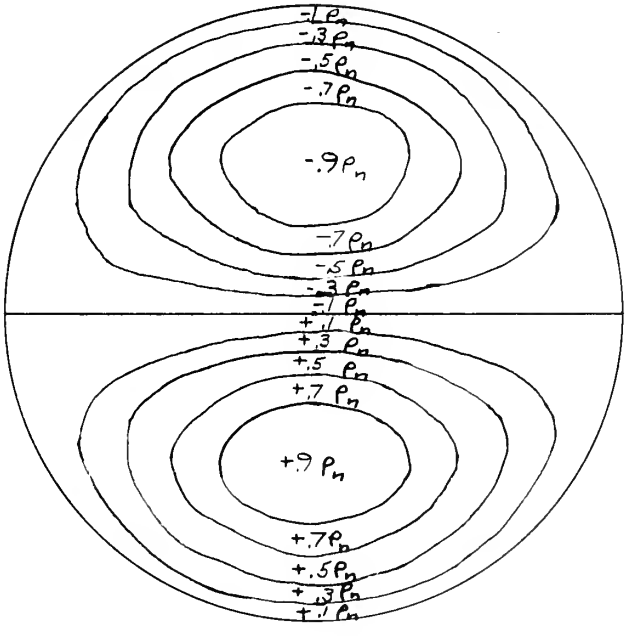

$\omega t = 0$
$\rho = \rho_n$
$\rho_e = \rho_n$

$\vec{J}_T$

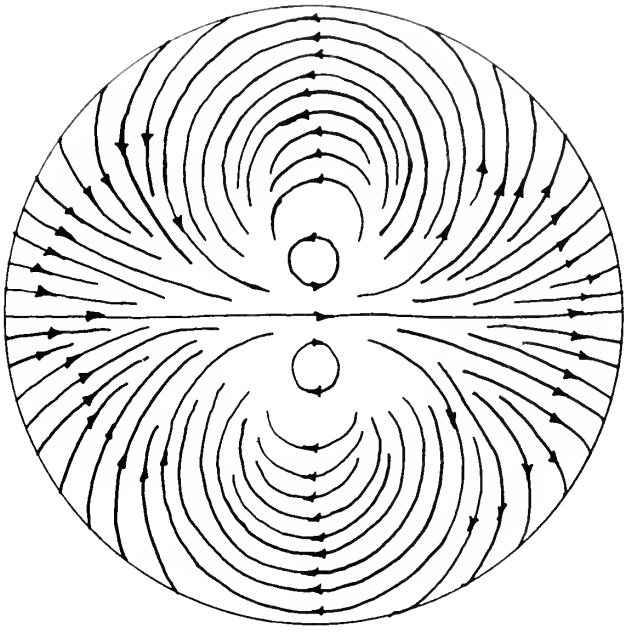

ELECTRON CYCLOTRON RESONANCE:

Quasi-Static Analysis

$m = 1 \qquad p = \frac{7.016}{a}$

$u = 2.18$

$\beta_n = 9.93 \quad \beta = 198.6$

$A(\phi,z,t) = A_1 e^{j(2.18\omega_n t - 9.93 \frac{z}{a})} e^{j\phi}$

Complex Fields:

$$\bar{E} = A(\phi,z,t)\left[j.707\left(J_o(pr) - \frac{J_1(pr)}{pr}\right)\vec{1}_r - .707\,\frac{J_1(pr)}{pr}\,\vec{1}_\phi + J_1(pr)\vec{1}_r\right]$$

$$\bar{H} = 10^{-3} x A(\phi,z,t)\left[\left(-1.425\,J_o(pr) + 3.38\,\frac{J_1(pr)}{pr} + 1.794x10^{-4}\left(I_o(\beta r) - \frac{I_1(\beta r)}{\beta r}\right)\vec{1}_r + j\left(1.962\,J_o(pr) - 3.38\,\frac{J_1(pr)}{pr} + 1.794x10^{-4}\,\frac{I_1(\beta r)}{\beta r}\right)\vec{1}_\phi - j\left(1.003\,J_1(pr) + 1.794x10^{-4}\,I_1(\beta r)\right)\vec{1}_z\right]$$

$$\bar{J} = A(\phi,z,t)\left[\left(-.308\,J_o(pr) + .732\,\frac{J_1(pr)}{pr}\right)\vec{1}_r + j\left(.424\,J_o(pr) - .732\,\frac{J_1(pr)}{pr}\right)\vec{1}_\phi - j.390\,J_1(pr)\vec{1}_z\right]$$

$$\rho = A(\phi,z,t)\left[-j2.63x10^{-9}\,J_1(pr)\right]$$

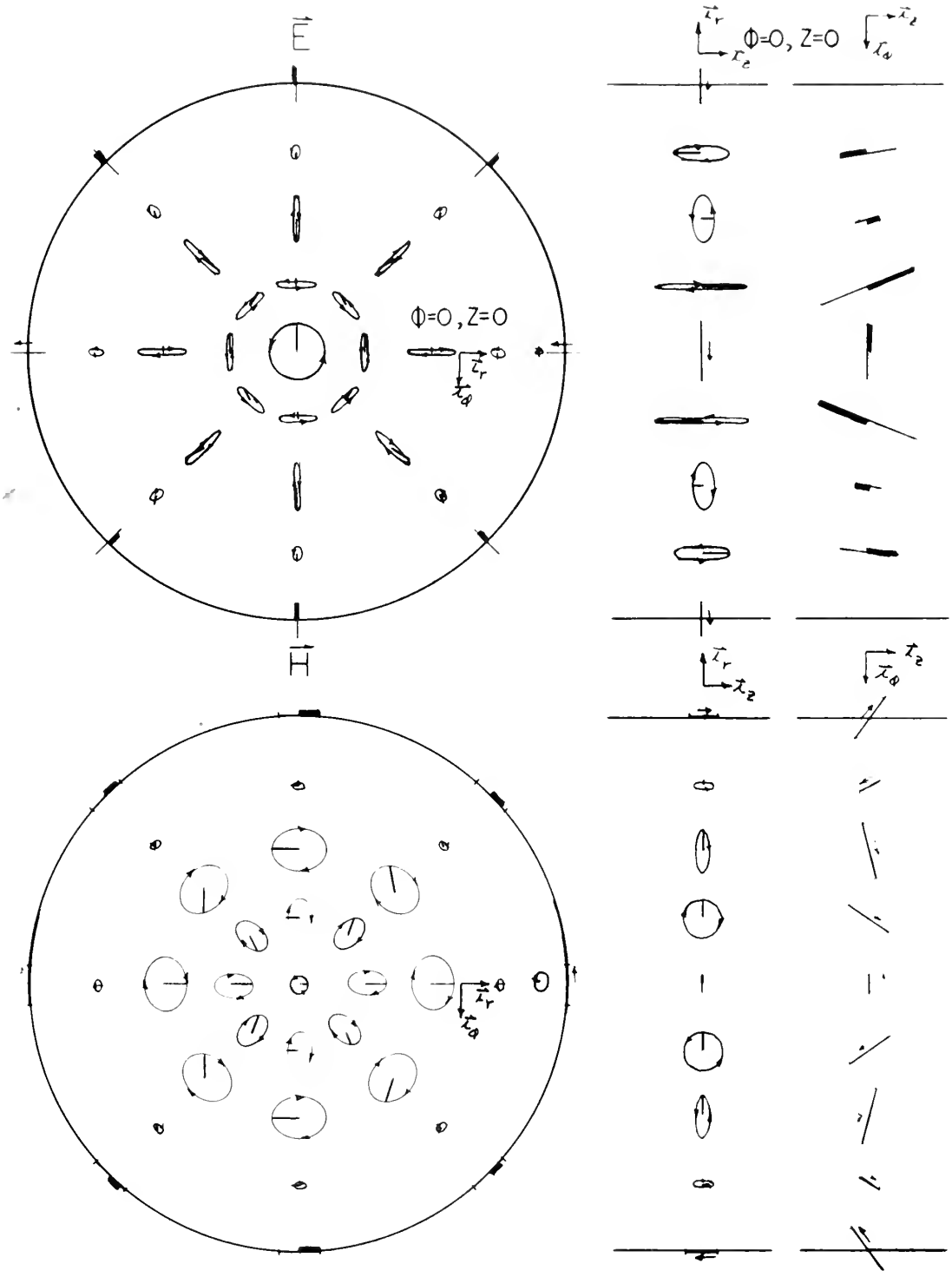
$\vec{E}$
$\Phi=0, Z=0$
$\vec{H}$
$\Phi=0, Z=0$

$\vec{E}_T$

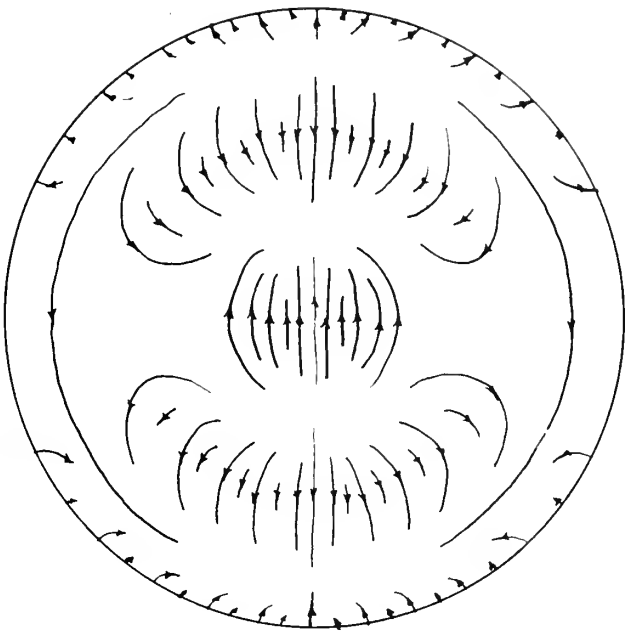

$\vec{H}_T$

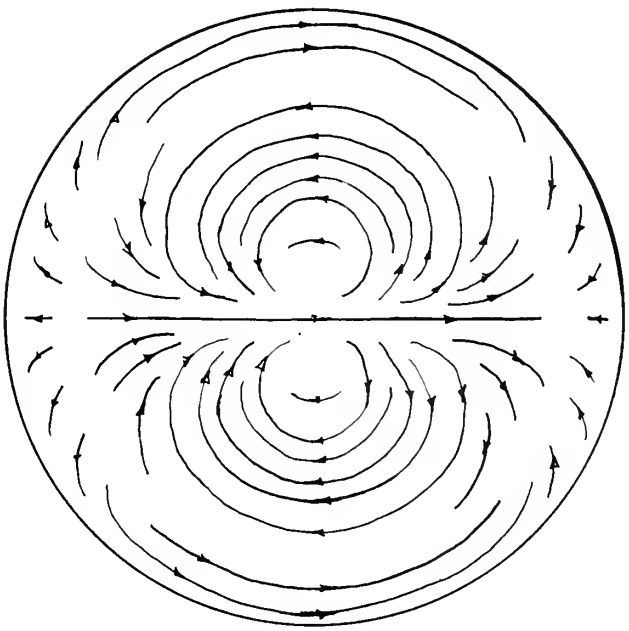

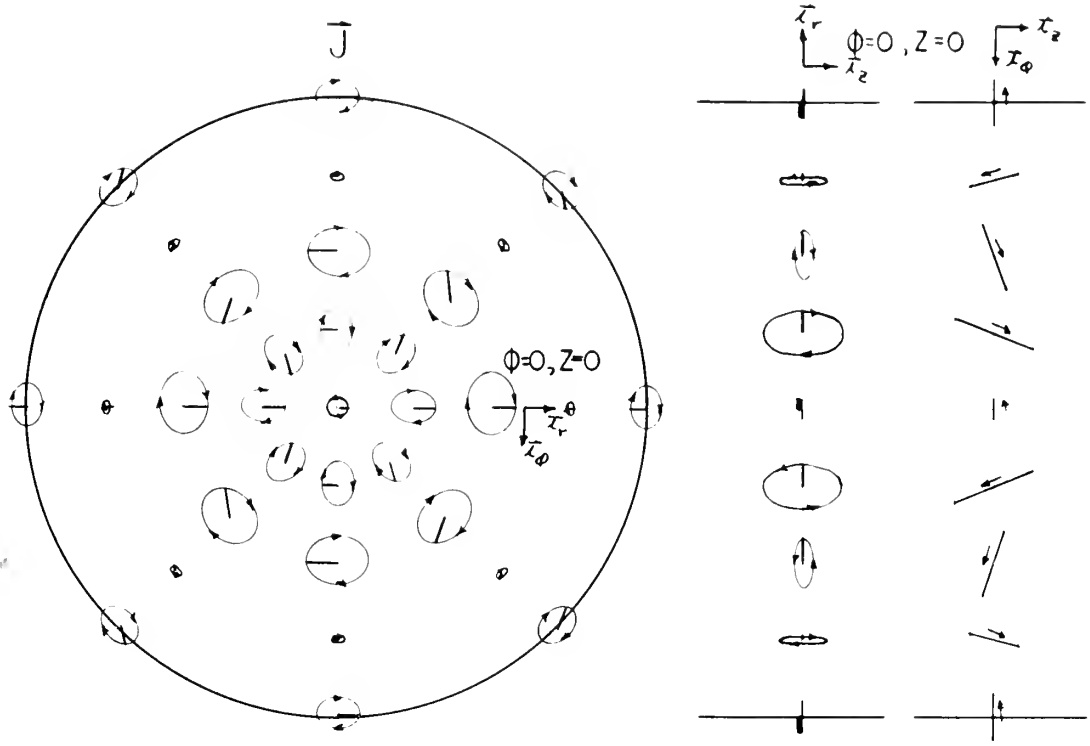

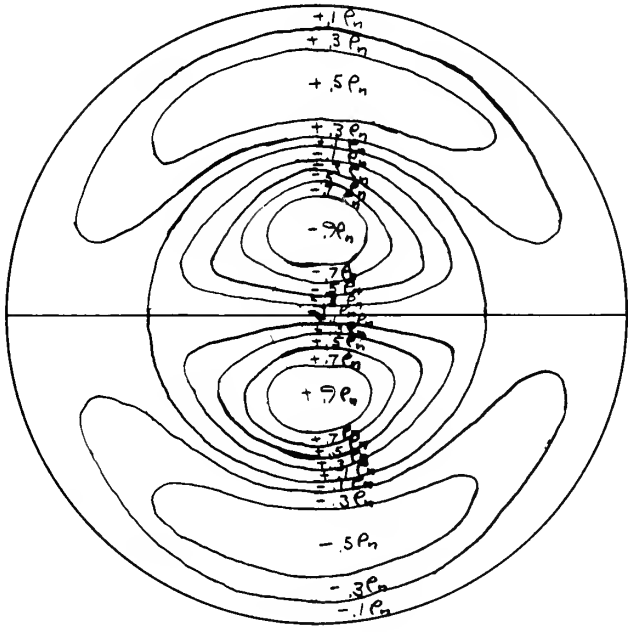

ωt = 0
ρ = ρn
ρe = ρn

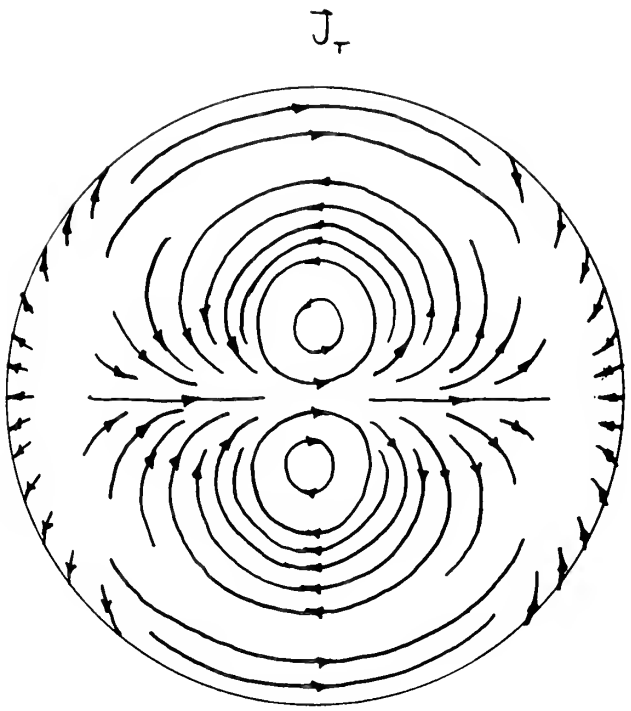
J_r

PLASMA RESONANCE: (1.) pp. 162-164

Exact Analysis

$m = 0$

$u = 4.08$

$\beta_n = 10.53$

$p_1 = \frac{2.45}{a}$

$p_2 = j\frac{9.72}{a} = jQ_2$

$A(z,t) = A_1 e^{j(4.08\,\omega_n t - 10.53\,\frac{z}{a})}$

Complex Fields:

$$\bar{E} = A(z,t)\,[-j2.09\text{x}10^{-1}(J_1(p_1 r) - 6.35\text{x}10^{-5} I_1(Q_2 r))\vec{I}_r + 3.94\text{x}10^{-2}(J_1(p_1 r) - 2.49\text{x}10^{-4} I_1(Q_2 r))\vec{I}_\phi + (J_o(p_1 r) + 1.427\text{x}10^{-5} I_o(Q_2 r))\vec{I}_z]$$

$$\bar{H} = A(z,t)\,[-2.71\text{x}10^{-4}(J_1(p_1 r) - 2.47\text{x}10^{-4} I_1(Q_2 r))\vec{I}_r + j1.722\text{x}10^{-4}(J_1(p_1 r) + 3.25\text{x}10^{-6} I_1(Q_2 r))\vec{I}_\phi + j6.25\text{x}10^{-5}(J_o(p_1 r) - 9.89\text{x}10^{-4} I_o(Q_2 r))\vec{I}_z]$$

$$\bar{J} = A(z,t)\,[-8.15\text{x}10^{-2}(J_1(p_1 r) - 3.36\text{x}10^{-5} I_1(Q_2 r))\vec{I}_r + j5.17\text{x}10^{-2}(J_1(p_1 r) + 3.9\text{x}10^{-7} I_1(Q_2 r))\vec{I}_\phi - j2.08\text{x}10^{-1}(J_o(p_1 r) + 1.427\text{x}10^{-5} I_o(Q_2 r))\vec{I}_z]$$

$$\rho = A(z,t)\,[-j\text{x}10^{-9}(1.948\, J_o(p_1 r) + 3.76\text{x}10^{-6} I_o(Q_2 r))]$$

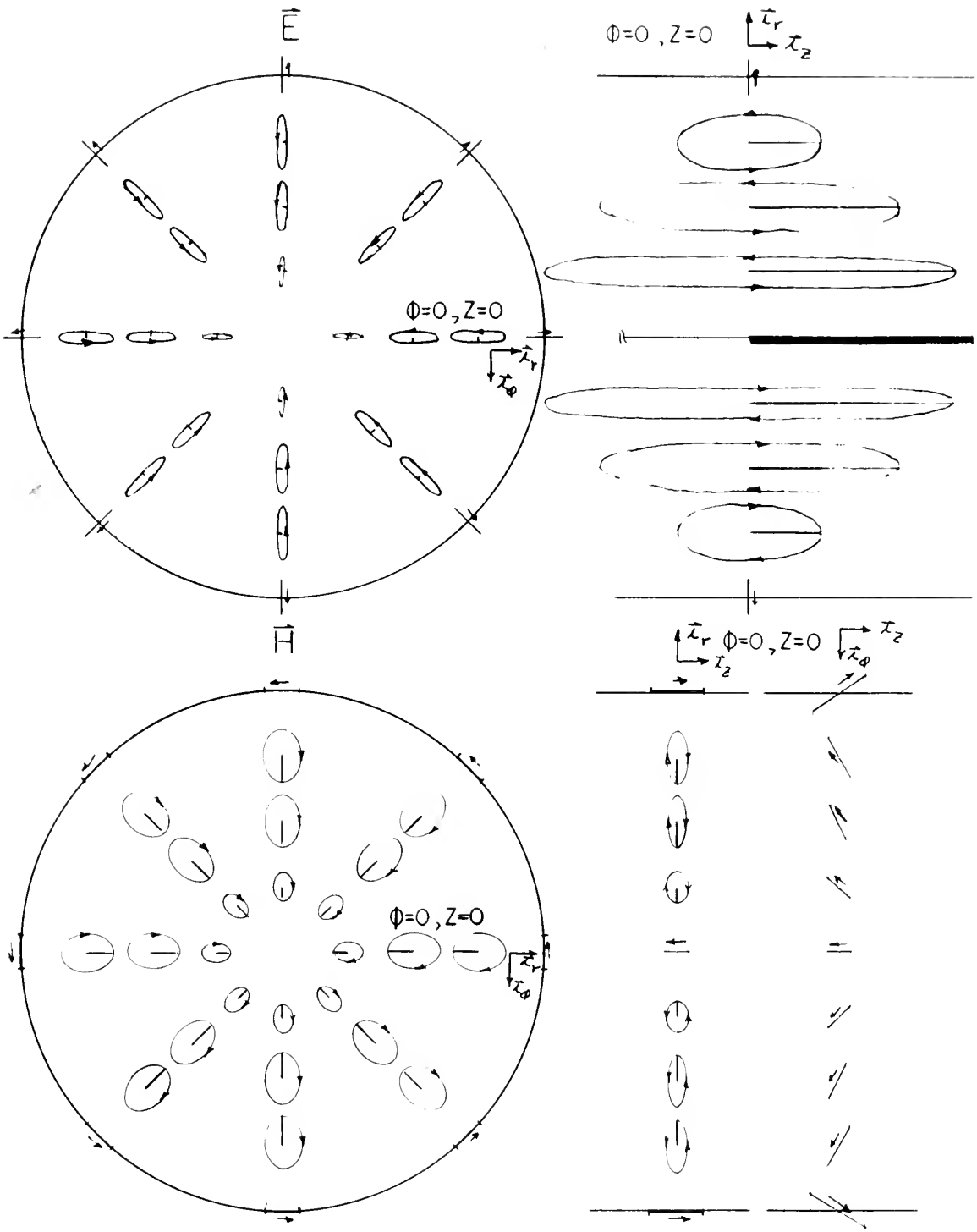
$\vec{E}$
Φ=0, Z=0
$\vec{r}_r$
$\vec{r}_\phi$
Φ=0 , Z=0
$\vec{r}_r$
$\vec{r}_z$
$\vec{H}$
Φ=0, Z=0
$\vec{r}_r$
$\vec{r}_\phi$
$\vec{r}_r$ Φ=0, Z=0 $\vec{r}_z$
$\vec{r}_z$
$\vec{r}_\phi$

E_r

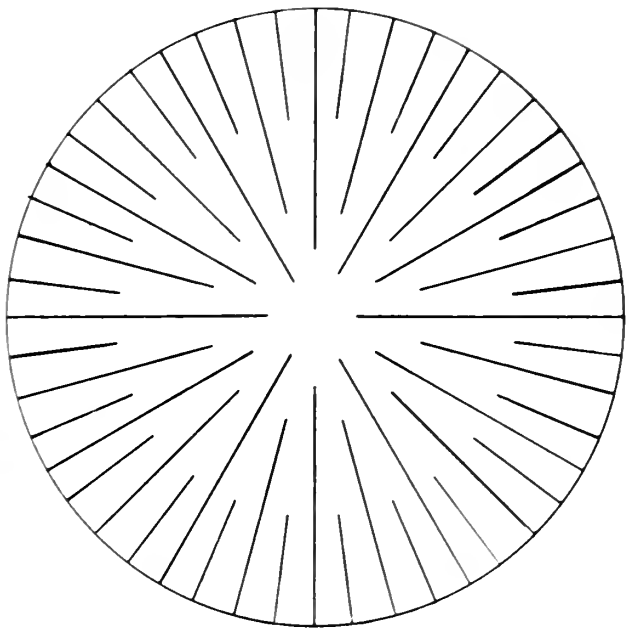

H_r

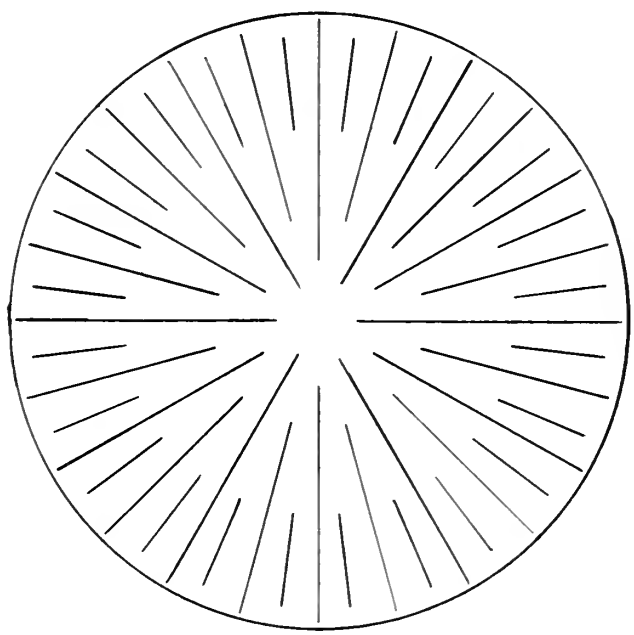

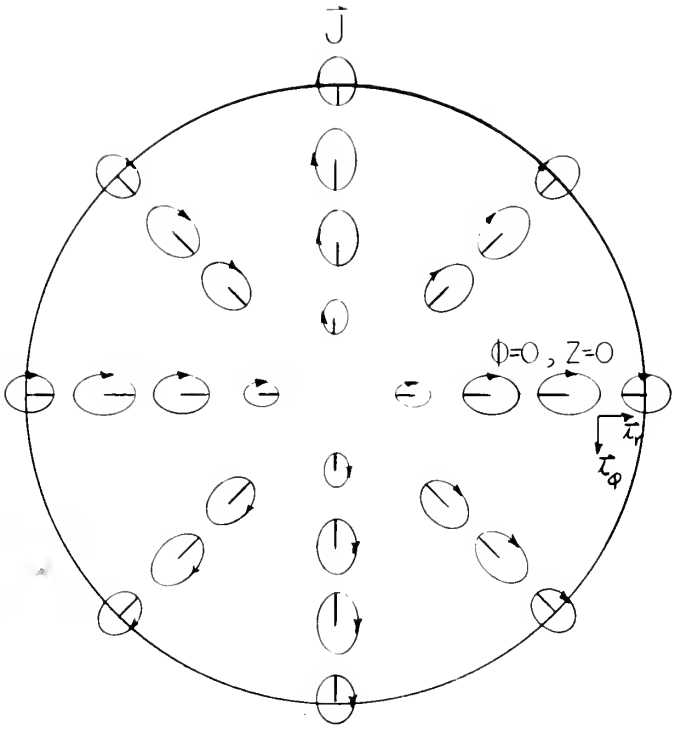

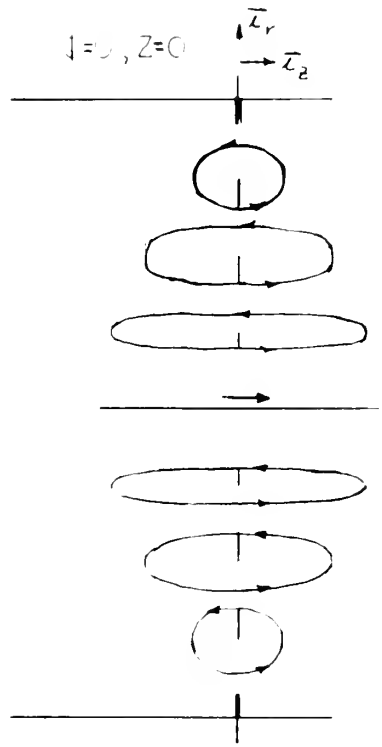

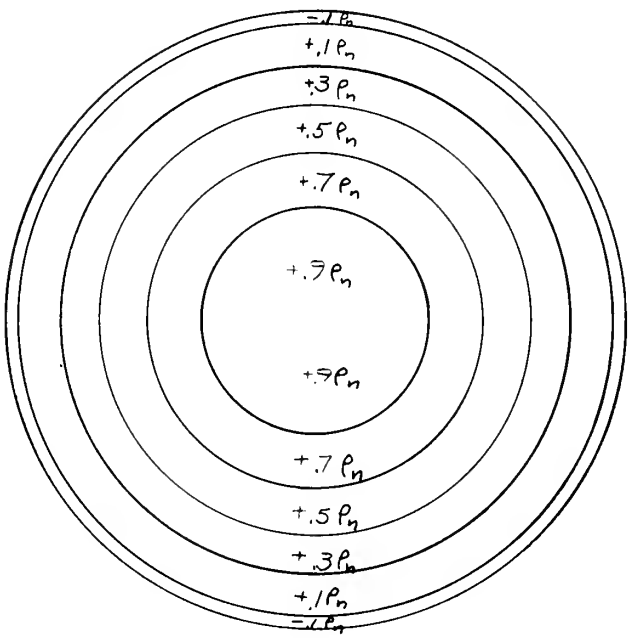

$\omega t = \frac{\pi}{2}$

$\rho = \rho_n$

$\rho_e = \rho_n$

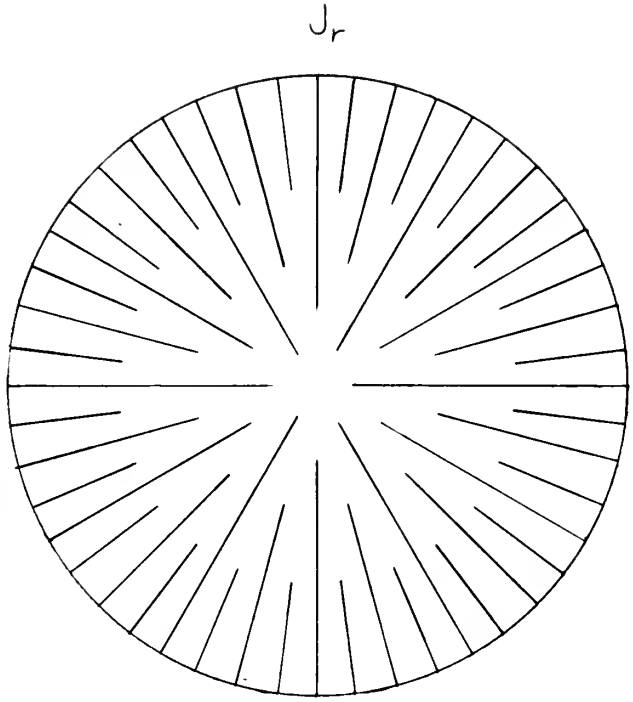
J_r

PLASMA RESONANCE:

Quasi-Static Analysis

$m = 0$

$u = 4.08$

$\beta_n = 8.23 \quad ; \quad \beta = 164.6$

$$A(z,t) = A_1 e^{j(4.08\,\omega_n t - 8.23\,\frac{z}{a})}$$

Complex Fields:

$$\bar{E} = A(z,t)\,[-j2.92\times10^{-1}\,J_1(pr)\vec{1}_r + J_o(pr)\vec{1}_r]$$

$$\bar{H} = A(z,t)\,[-5.69\times10^{-4}(J_1(pr) - 1.045\times10^{-3}\,I_1(\beta r))\vec{1}_r$$
$$+j4.20\times10^{-4}\,J_1(pr)\vec{1}_\phi$$
$$+j6.92\times10^{-5}(J_o(pr) - 8.61\times10^{-3}\,I_o(\beta r))\vec{1}_z]$$

$$\bar{J} = A(x,t)\,[-1.322\times10^{-1}\,J_1(pr)\vec{1}_r + j9.72\times10^{-2}\,J_1(pr)\vec{1}_\phi$$
$$-j.208\,J_o(pr)\vec{1}_z]$$

$$\rho = A(z,t)\,[-j1.58\times10^{-9}\,J_o(pr)]$$

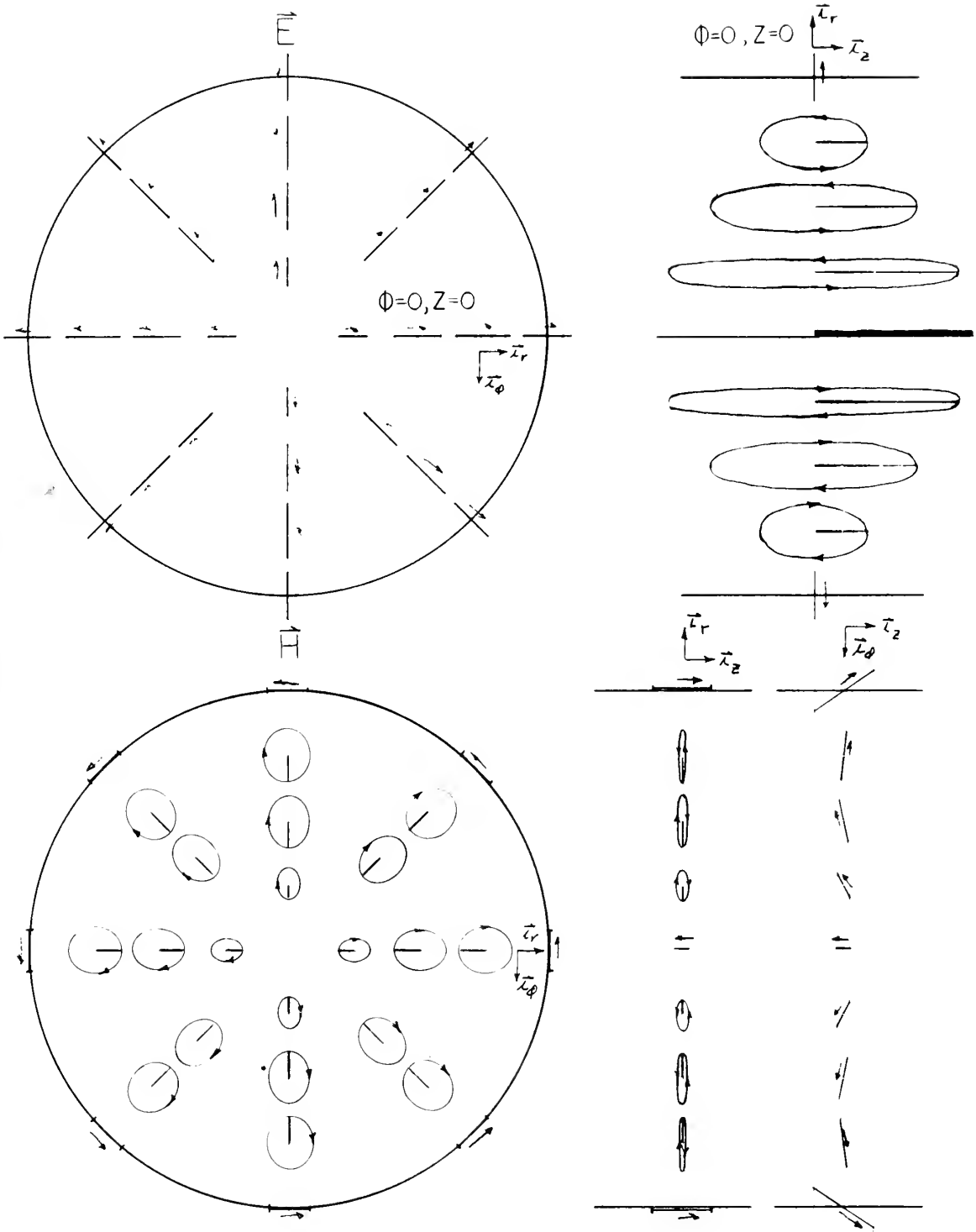
$\vec{E}$
$\Phi=0, Z=0$
$\vec{\iota}_r$
$\vec{\iota}_\phi$
$\vec{H}$
$\Phi=0, Z=0$
$\vec{\iota}_r$
$\vec{\iota}_z$
$\vec{\iota}_r$
$\vec{\iota}_z$
$\vec{\iota}_z$
$\vec{\iota}_\phi$

E_r

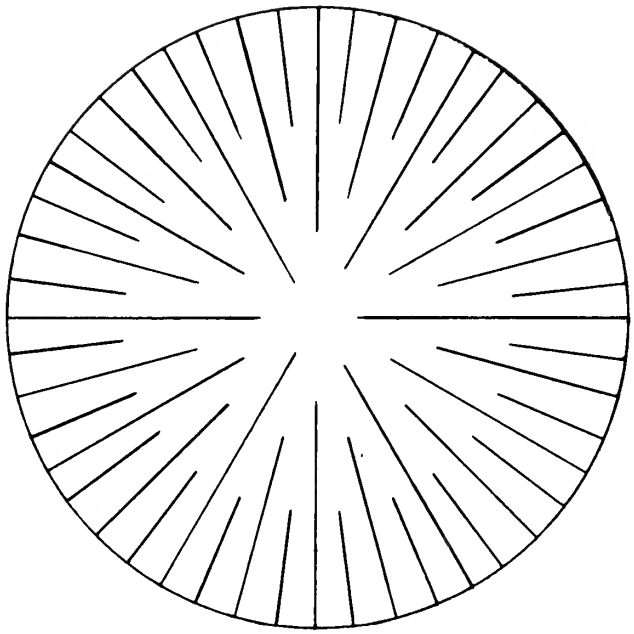

H_r

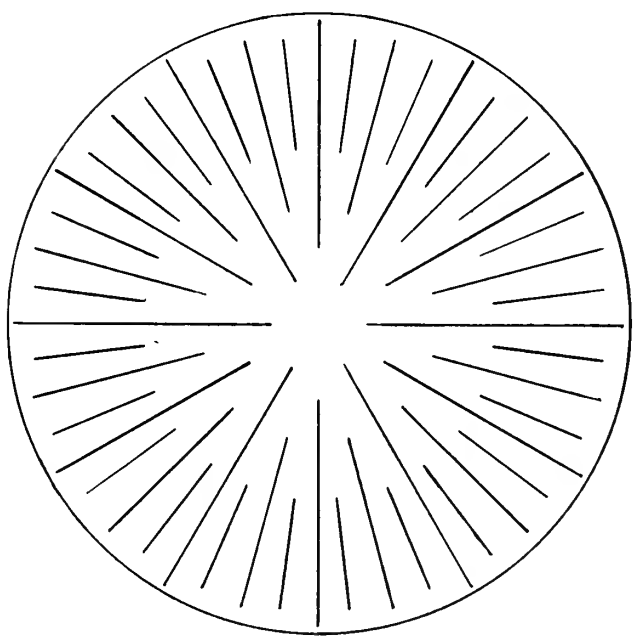

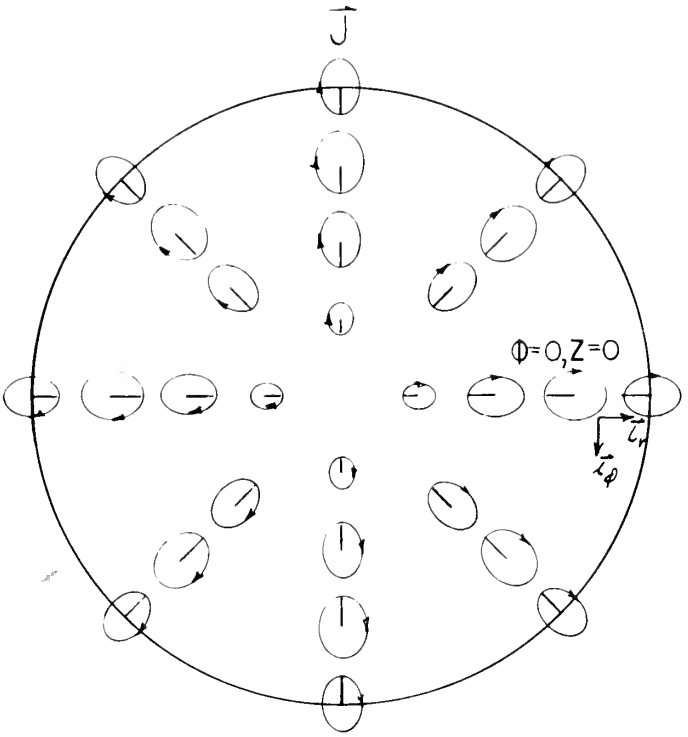

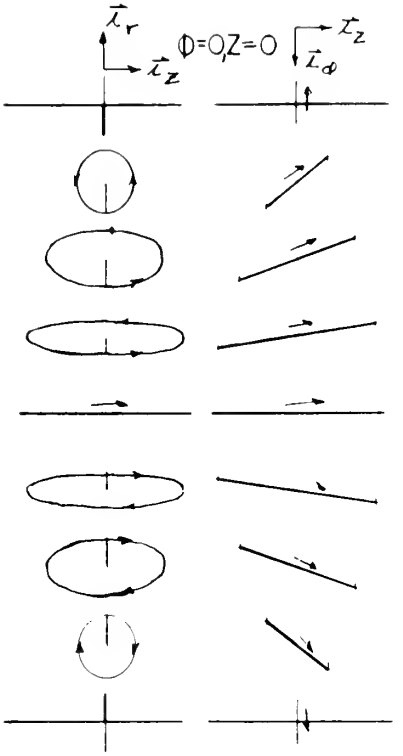

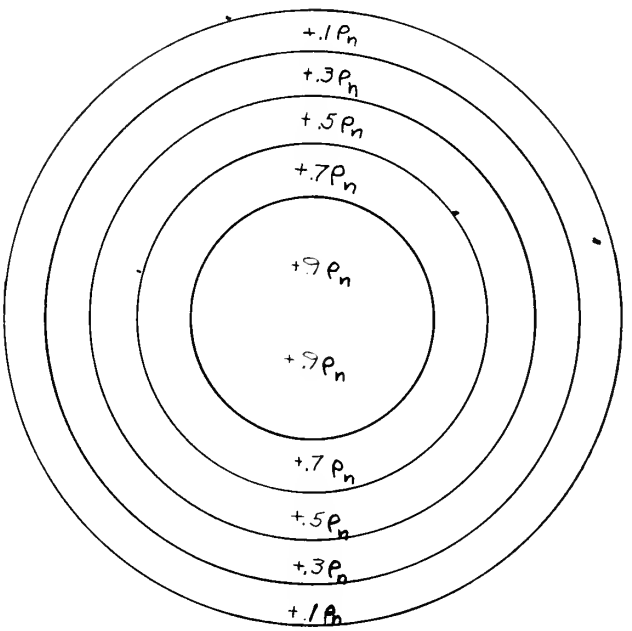

$\omega t = \frac{\pi}{2}$

$\rho = \rho_n$

$\rho_e = \rho_n$

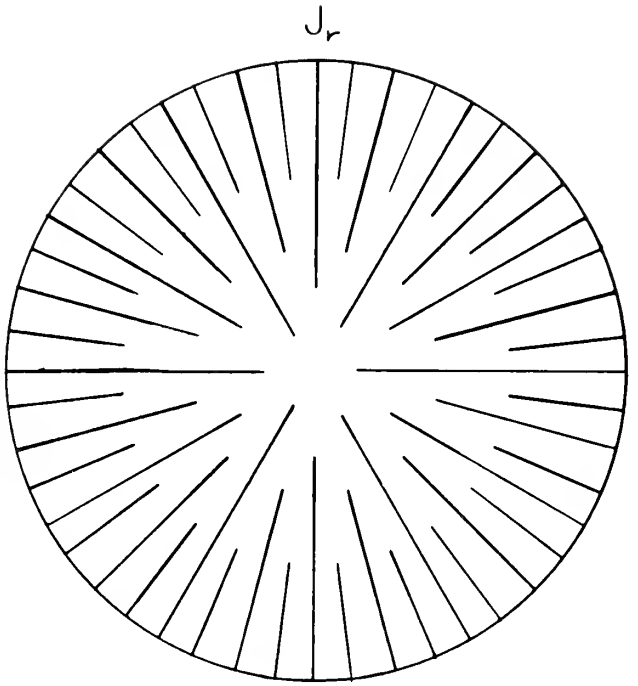
J_r

PLASMA RESONANCE - FAST WAVE:

Exact Analysis

$m = 0$

$u = 4.154$

$\beta_n = 4.00$

$p_1 = 3.149/a$

$p_2 = j1.874/a = j\, q_2$

$A(z,t) = A_1 e^{j(4.154\,\omega_n t - 4\,\frac{z}{a})}$

Complex Fields:

$$\bar{E} = A(z,t)\,[j(-.686\,J_1(pr) + .0927\,I_1(q_2r))\vec{1}_r + (.393\,J_1(p_1r) - .0782\,I_1(q_2r))\vec{1}_\phi + (J_o(p_1r) + .1464\,I_o(q_2r))\vec{1}_z]$$

$$\bar{H} = 10^{-3}xA(z,t)\,[-1.006\,J_1(p_1r) + .1997\,I_1(q_2r))\vec{1}_r + j(.252\,J_1(p_1r) + .0620\,I_1(q_2r))\vec{1}_\phi + j(.795\,J_o(p_1r) - .0937\,I_o(q_2r))\vec{1}_z]$$

$$\bar{J} = A(z,t)\,[-.1717\,J_1(p_1r) + .01545\,I_1(q_2r))\vec{1}_r + j(.0437\,J_1(p_1r) + .00475\,I_1(q_2r))\vec{1}_\phi - j(.204\,J_o(p_1r) + .0300\,I_o(q_2r))\vec{1}_z]$$

$$\rho = A(z,t)\,[-j10^{-9}(1.090\,J_o(p_1r) + .0728\,I_o(q_2r))]$$

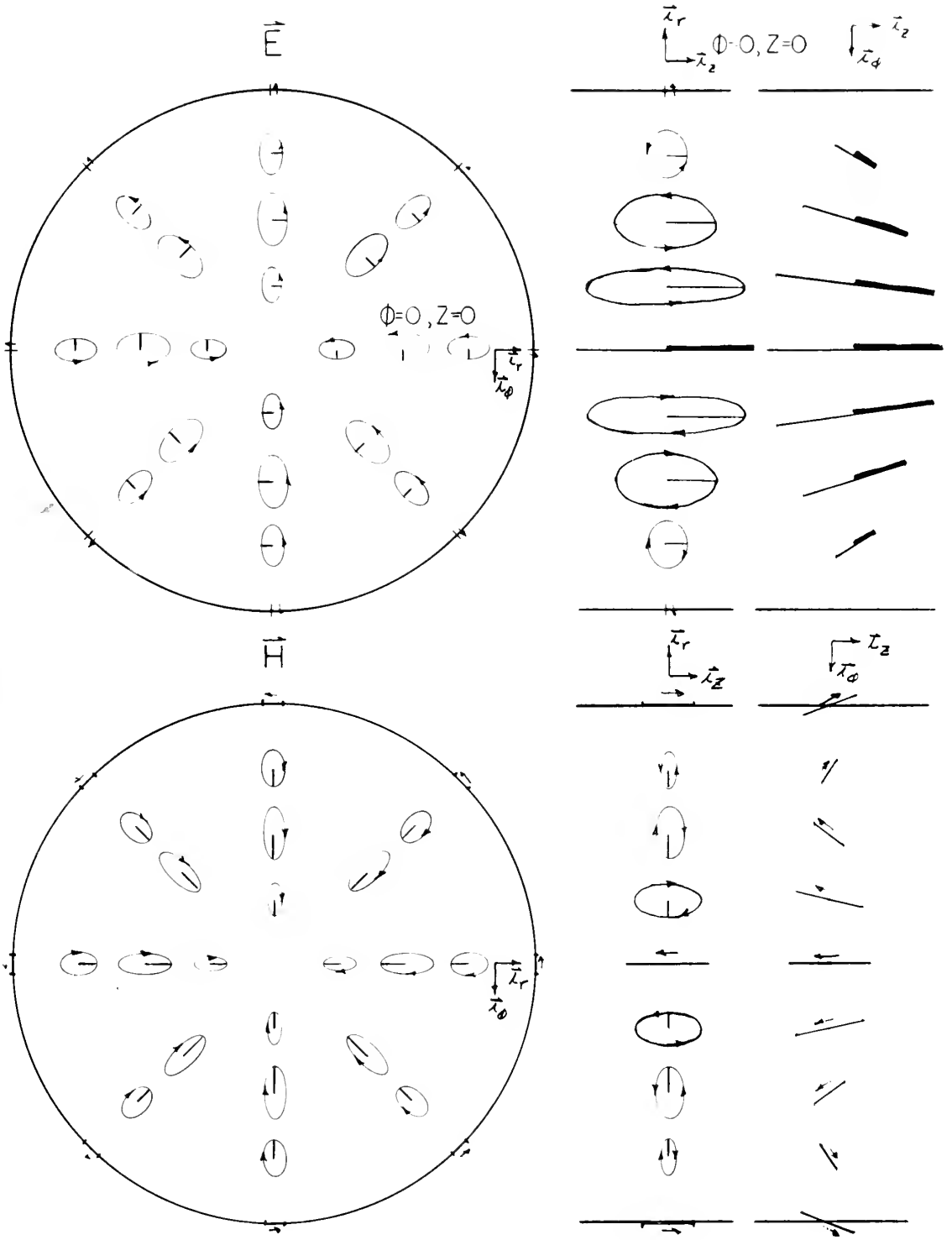
$\vec{E}$
$\Phi=0, Z=0$
$\vec{H}$
$\Phi=0, Z=0$

E_r

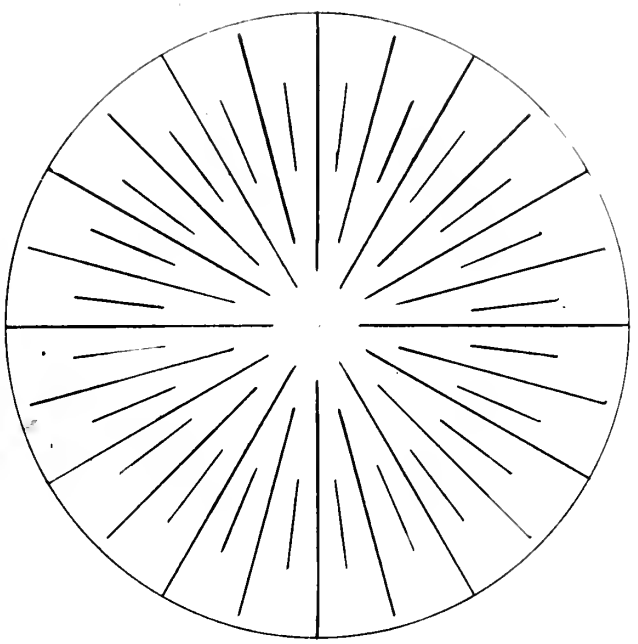

H_r

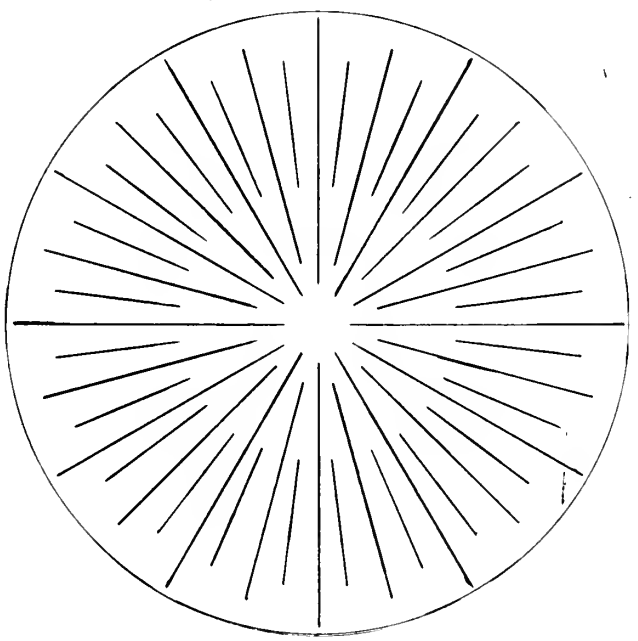

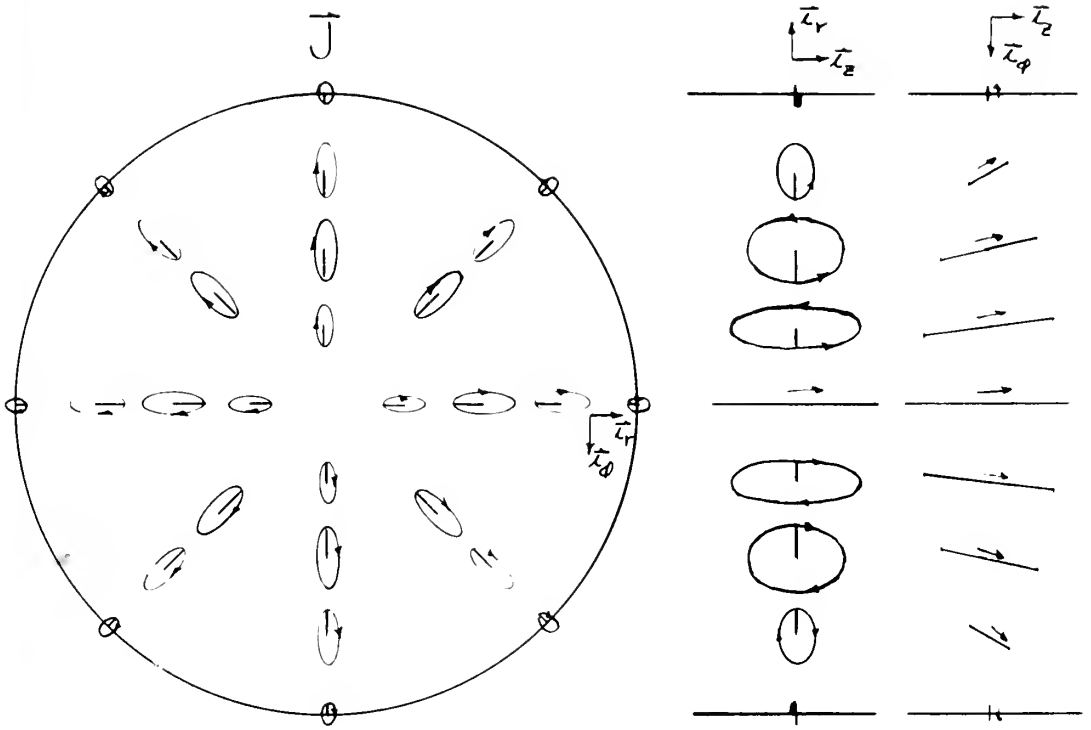

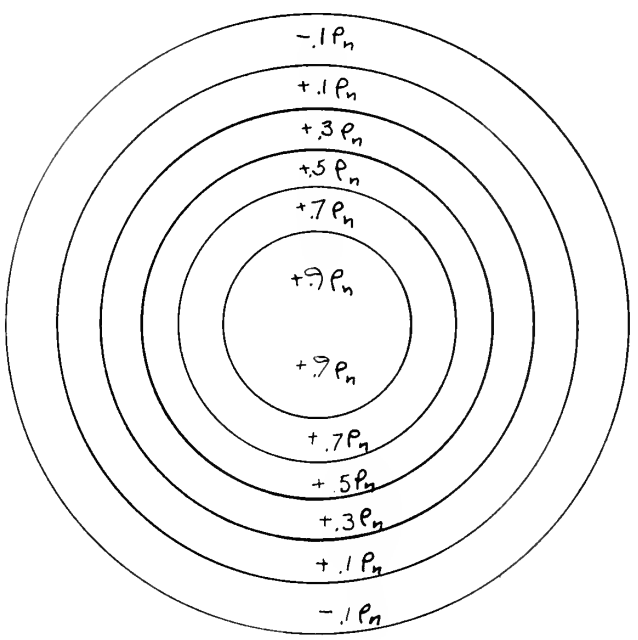

$\omega t = \frac{\pi}{2}$

$\rho_e = \rho_n$

$\rho = \rho_n$

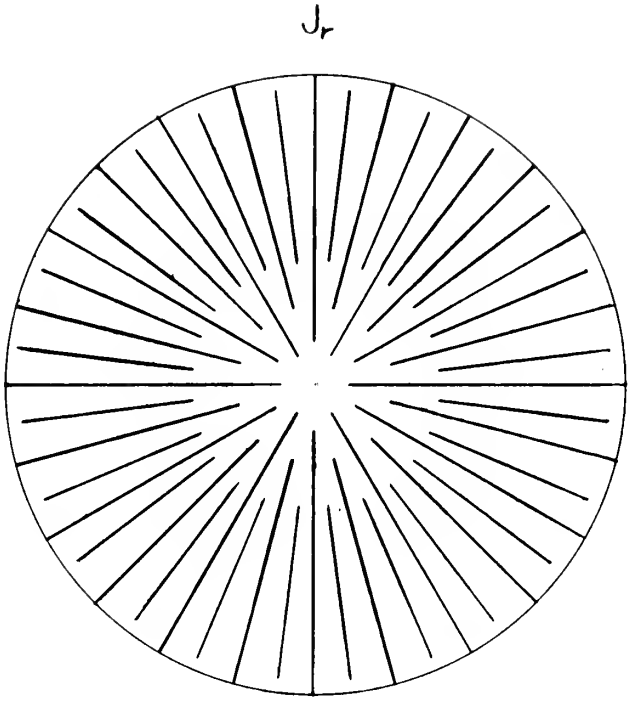
J_r

PLASMA RESONANCE:

Quasi-Static Analysis

$m = 1$

$u = 4.26$

$\beta_n = 9.62 \quad ; \quad \beta = 192.4$

$p = \frac{3.83}{a}$

$A(\phi, z, t) = A_1 e^{j(4.26\,\omega_n t - 9.62\,\frac{z}{a})} e^{j\phi}$

Complex Fields:

$$\bar{E} = A(\phi,z,t)\,[j.398(J_o(pr) - \frac{J_1(pr)}{pr})\vec{1}_r - .398\,\frac{J_1(pr)}{pr}\,\vec{1}_\phi + J_1(pr)\vec{1}_z]$$

$$\bar{H} = 10^{-3} x A(\phi,z,t)\,[(.497\,J_o(pr) - .847\,\frac{J_1(pr)}{pr} + 1.129x10^{-4}[I_o(\beta r) - \frac{I_1(\beta r)}{\beta r}])\vec{1}_r - j(.350\,J_o(pr) - .847\,\frac{J_1(pr)}{pr} - 1.129x10^{-4}\,\frac{I_1(\beta r)}{\beta r})\vec{1}_\phi + j(.1977\,J_1(pr) - 1.129x10^{-4}\,I_1(\beta r))\vec{1}_z]$$

$$\bar{J} = A(\phi,z,t)\,[(.1571\,J_o(pr) - .268\,\frac{J_1(pr)}{pr})\vec{1}_r - j(.1108\,J_o(pr) - .268\,\frac{J_1(pr)}{pr})\vec{1}_\phi - j.1992\,J_1(pr)\vec{1}_z]$$

$$\rho = A(\phi,z,t)\,[-j1.970x10^{-9}\,J_1(pr)]$$

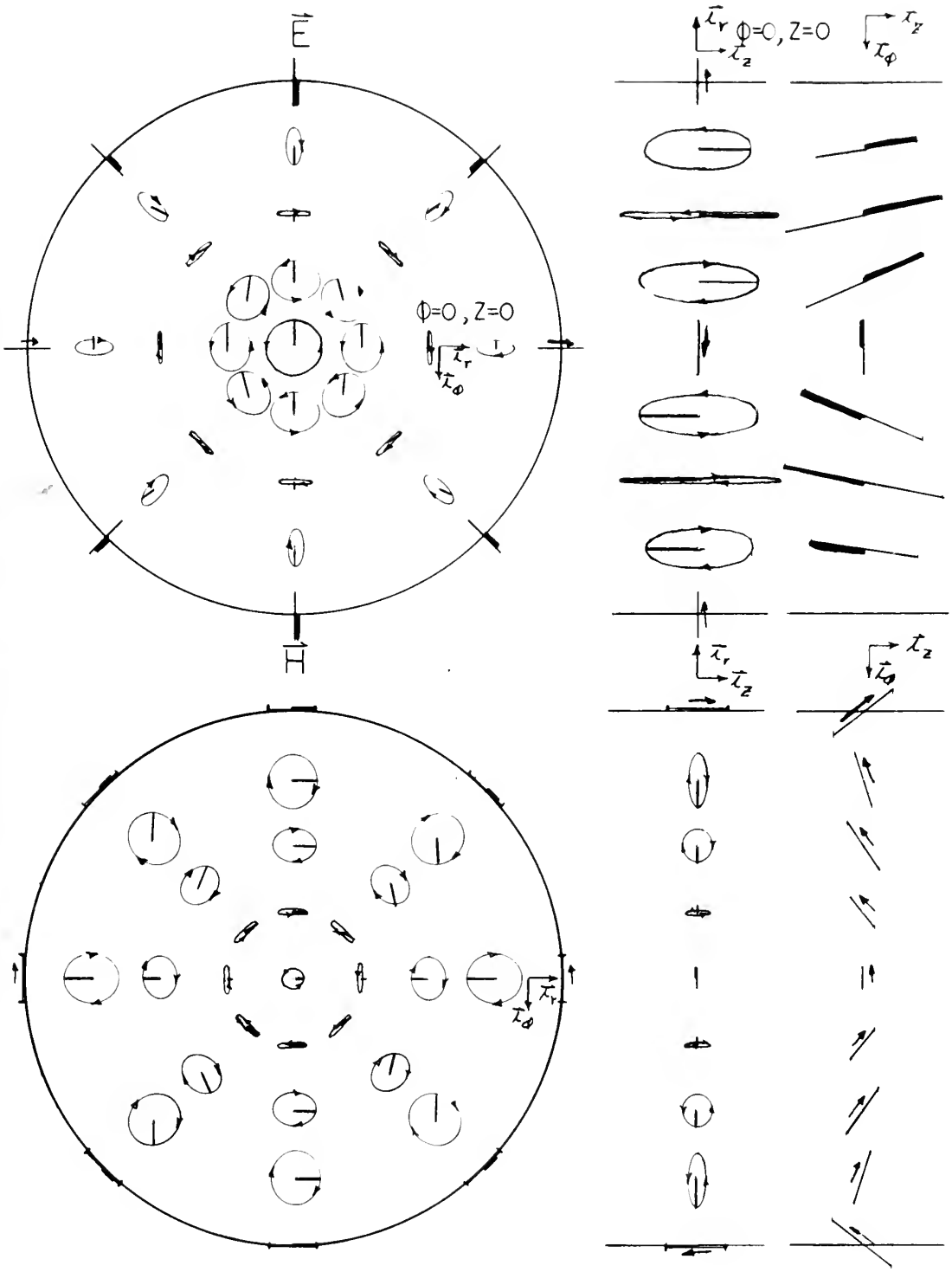
E
H
Φ=0, Z=0
Φ=0, Z=0

$\vec{E}_T$

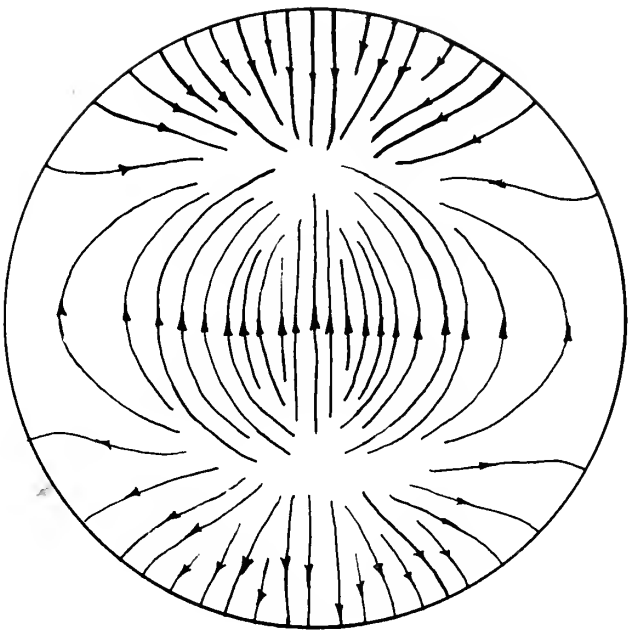

$\vec{H}_T$

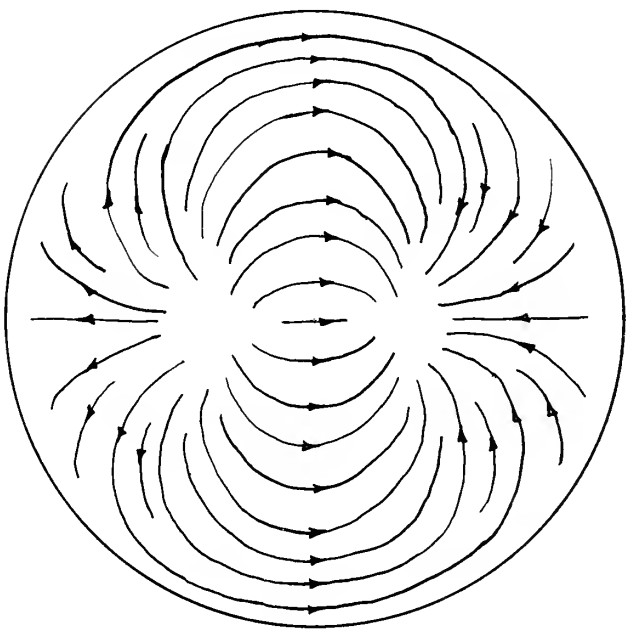

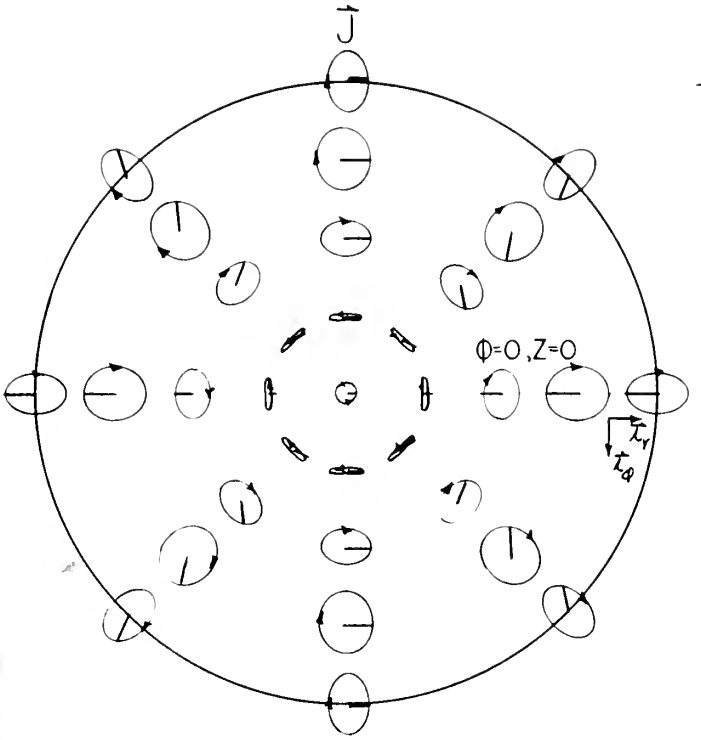

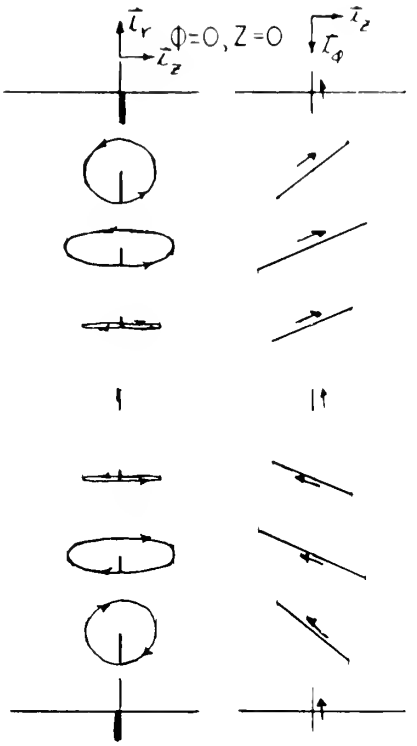

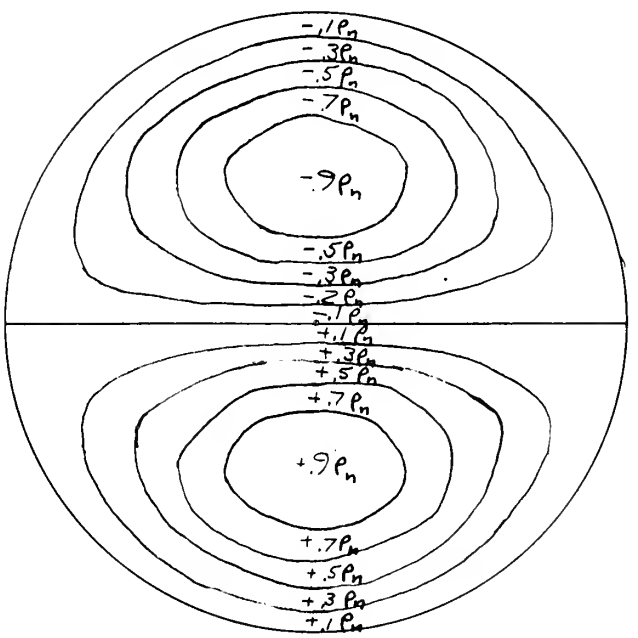

$\omega t = 0$

$\rho = \rho_n$

$\rho_e = \rho_n$

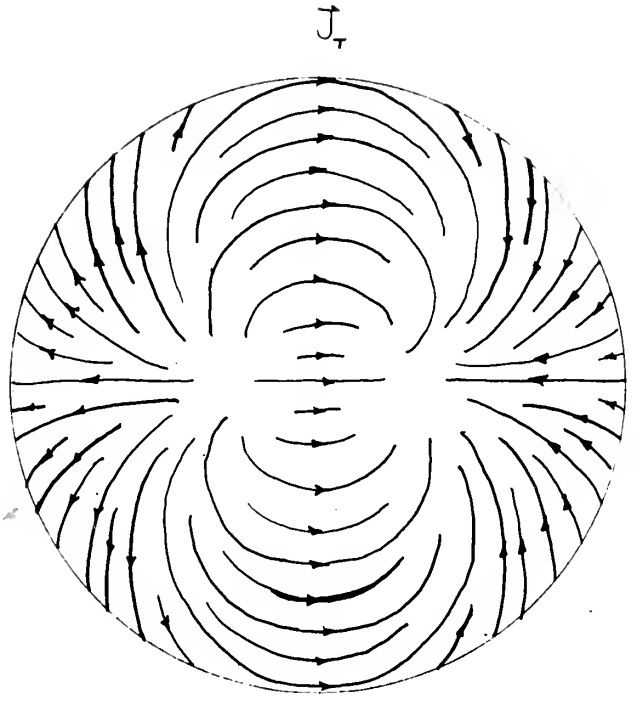
J_T

CUTOFF FIELDS:

E-Wave

$m = 0$

$u = 4.67$

$p = \frac{2.405}{a}$

$A(t) = A_1 e^{j4.67\omega_n t}$

Complex Fields:

$\overline{E} = A(t)\ [J_o(pr)\vec{1}_z]$

$\overline{H} = A(t)\ [j.1367\ J_1(pr)\vec{1}_\phi]$

$\overline{J} = A(t)\ [-j.1818\ J_o(pr)\vec{1}_z]$

$\overline{J}_e = A(t)\ [-j.1818\ J_o(pr)\vec{1}_z]$

$\overline{J}_i = A(t)\ [-j9.89x10^{-5}\ J_o(pr)\vec{1}_z]$

$\rho = 0$

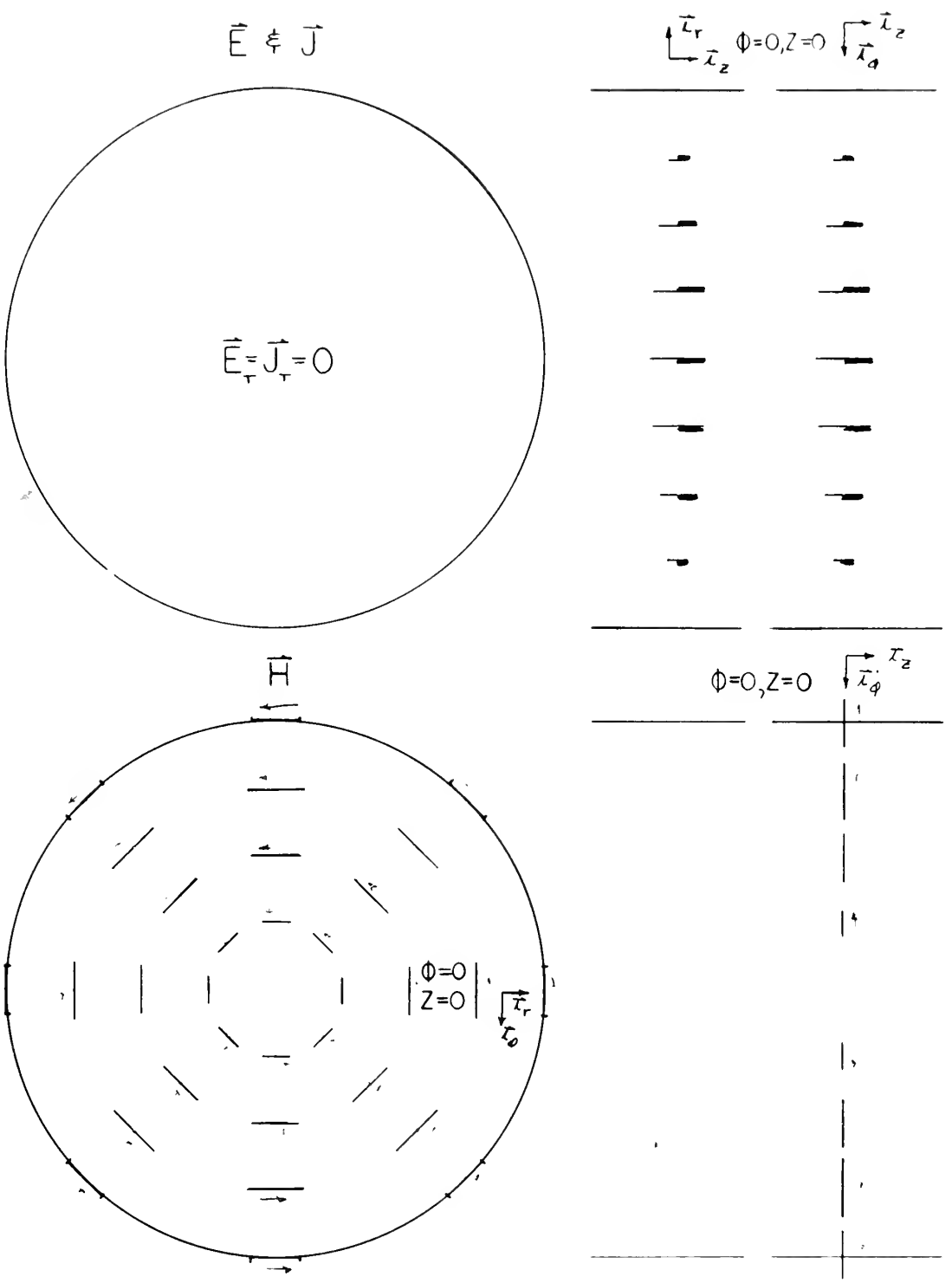
$\vec{E}$ & $\vec{J}$
$\vec{E}_T = \vec{J}_T = 0$
$\vec{H}$
$\Phi=0$
$Z=0$
$\vec{\iota}_r$
$\vec{\iota}_\theta$
$\vec{\iota}_r$ $\vec{\iota}_z$ $\Phi=0, Z=0$ $\vec{\iota}_z$ $\vec{\iota}_\theta$
$\Phi=0, Z=0$ r_z $\vec{\iota}_\varphi$

CUTOFF FIELDS:

E-Wave

$m = 1$

$u = 5.54$

$p = \frac{3.83}{a}$

$A(\phi,t) = A_1 e^{j5.54\omega_n t}\, e^{j\phi}$

Complex Fields:

$\overline{E} = A(\phi,t)\,[J_1(pr)\vec{1}_z]$

$\overline{H} = 1.833\times10^{-3}\, A(\phi,t)\,[-\frac{J_1(pr)}{pr}\vec{1}_r - j(J_o(pr) - \frac{J_1(pr)}{pr})\vec{1}_\phi]$

$\overline{J} = A(\phi,t)\,[-j.1534\, J_1(pr)\vec{1}_z]$

$\rho = 0$

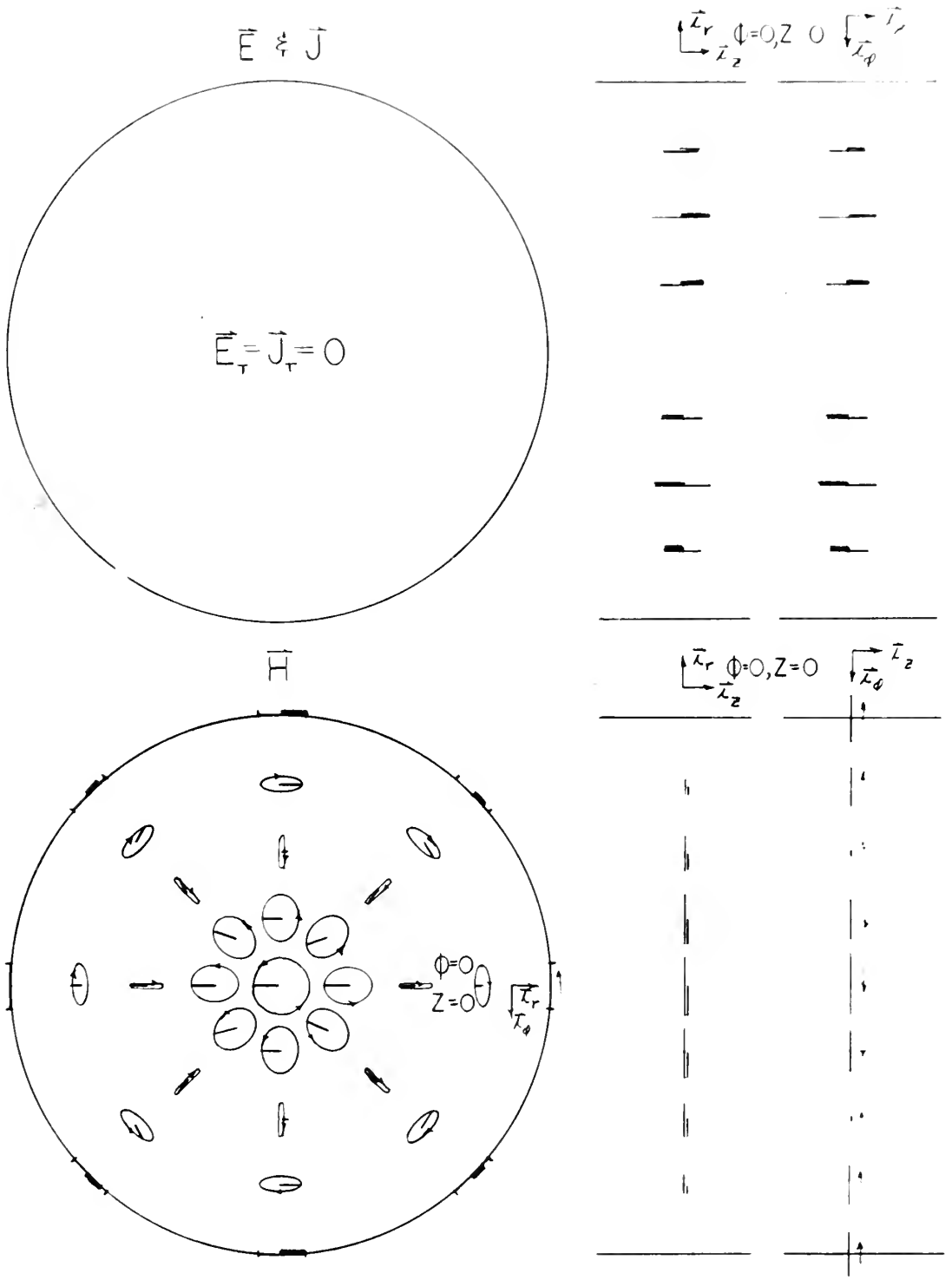
$\vec{E}$ & $\vec{J}$
$\vec{E}_\tau = \vec{J}_\tau = 0$
$\vec{H}$
$\Phi=0$
$Z=0$
$\vec{\iota}_r$ $\Phi=0, Z=0$ $\vec{\iota}_z$
$\vec{\iota}_r$ $\Phi=0, Z=0$ $\vec{\iota}_\phi$ $\vec{\iota}_z$

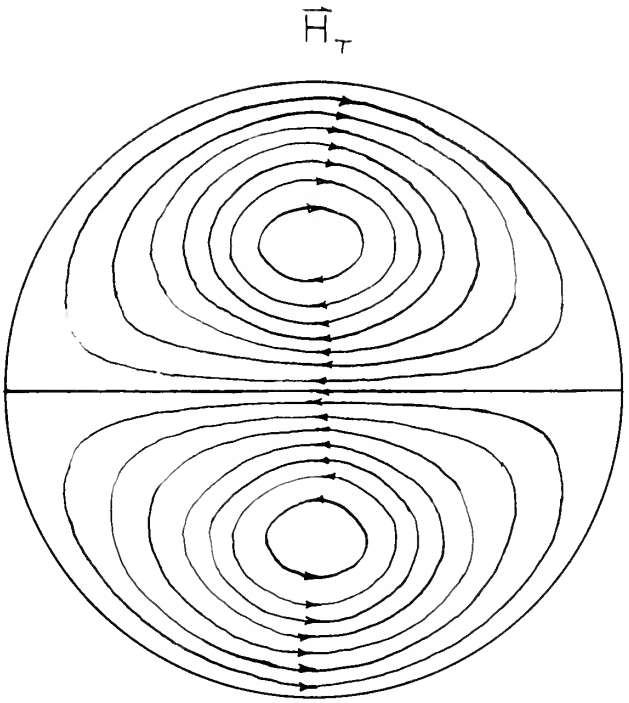
$\vec{H}_T$

CUTOFF FIELDS:

H-Wave

$m = 0$

$p = \frac{3.83}{a}$

Complex Fields:

(1.) $u_{co1} = .0430 \quad A(t) = A_1 e^{j.0430\omega_n t}$

$\bar{E} = A(t)\, J_1(pr)\, [2.72\times10^{2}\, \vec{i}_r - j4.23\, \vec{i}_\phi]$

$\bar{H} = A(t)\, J_o(pr)\vec{i}_z$

$\bar{J} = A(t)\, J_1(pr)\, [-j.619\, \vec{i}_r + 77.0\, \vec{i}_\phi]$

$\bar{J}_e = A(t)\, J_1(pr)\, [+j2.30\, \vec{i}_r - 77.0\, \vec{i}_\phi]$

$\bar{J}_i = A(t)\, J_1(pr)\, [-j2.92\, \vec{i}_r + 6.56\times10^{-2}\, \vec{i}_\phi]$

$\rho = A(t)\, J_o(pr)\, [1.83\times10^{-7}]$

(2.) $u_{co2} = 3.94 \quad A(t) = A_1 e^{j3.94\omega_n t}$

$\bar{E} = A(t)\, J_1(pr)\, [-4.98\, \vec{i}_r - j3.88\, \vec{i}_\phi]$

$\bar{H} = A(t)\, J_o(pr)\vec{i}_z$

$\bar{J} = A(t)\, J_1(pr)\, [j104.0\, \vec{i}_r - 4.46\, \vec{i}_\phi]$

$\rho = A(t)\, J_o(pr)\, [-3.37\times10^{-7}]$

(3.) $u_{co3} = 6.34 \quad A(t) = A_1 e^{j6.34\omega_n t}$

$\bar{E} = A(t)\, J_1(pr)\, [310\, \vec{i}_r - j624\, \vec{i}_\phi]$

$\bar{H} = A(t)\, J_o(pr)\vec{i}_z$

$\bar{J} = A(t)\, J_1(pr)\, [-j104.6\, \vec{i}_r - 133.2\, \vec{i}_\phi]$

$\rho = A(t)\, J_o(pr)\, [2.10\times10^{-7}]$

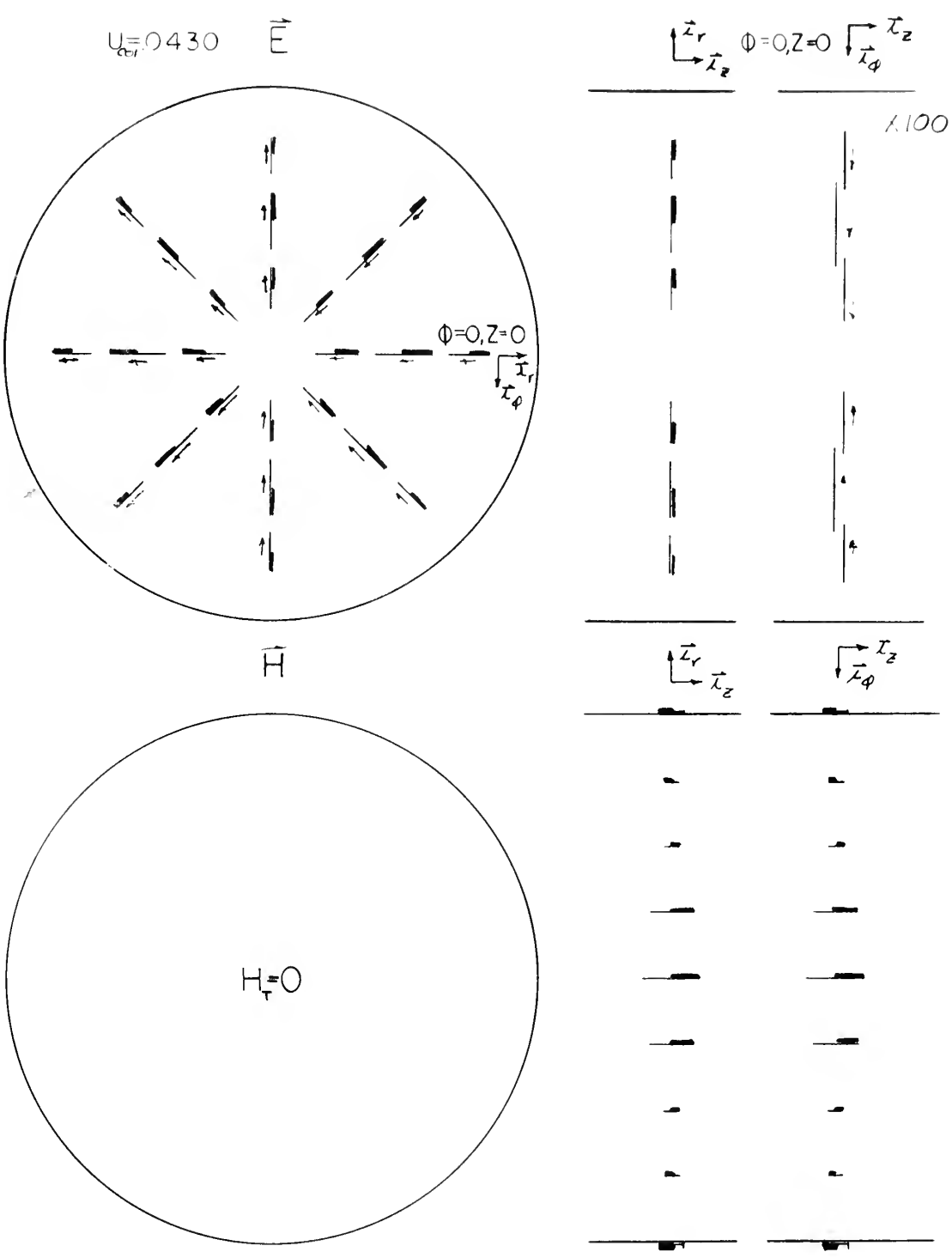
U_{ant}=0430
$\vec{E}$
$\vec{r}_r$ $\vec{r}_z$ Φ=0,Z=0 $\vec{r}_z$ $\vec{r}_\varphi$
X100
Φ=0,Z=0
$\vec{r}_r$
$\vec{r}_\varphi$
$\vec{H}$
$\vec{r}_r$ $\vec{r}_z$
$\vec{r}_z$ $\vec{r}_\varphi$
H_r=0

$U_{coi} = 0430$ $E_r \xi J_r \xi J_{er} \xi J_{ir}$

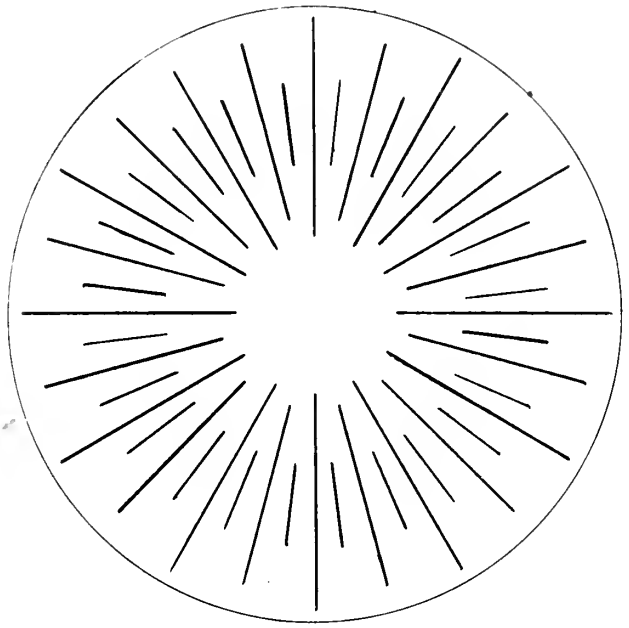

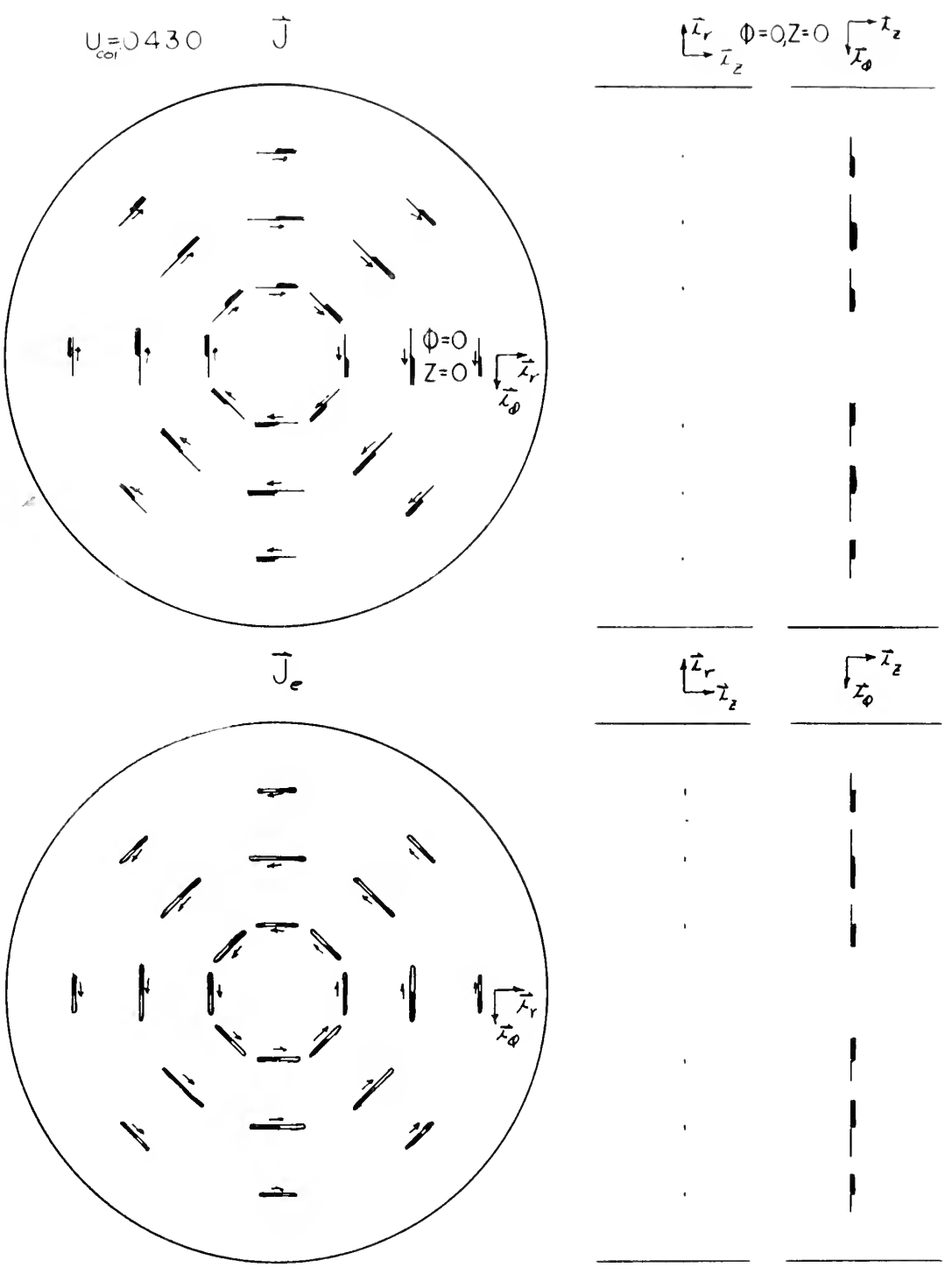
$U_{coil} = 0430$
$\vec{J}$
$\Phi = 0, Z = 0$
$\vec{J}_e$

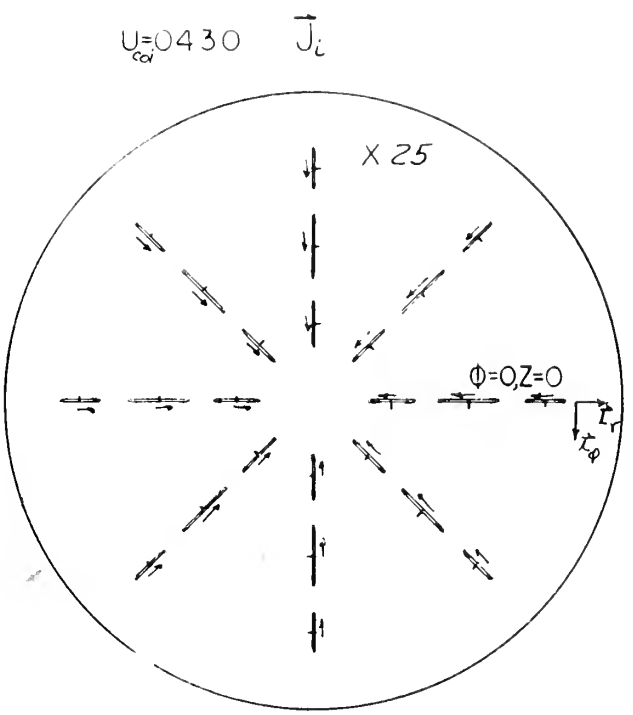

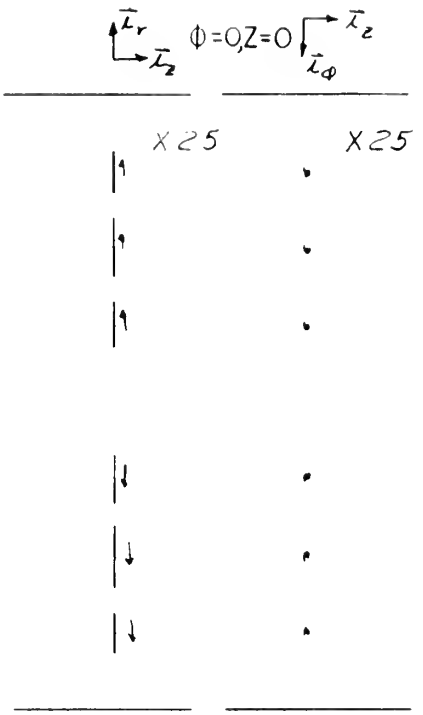

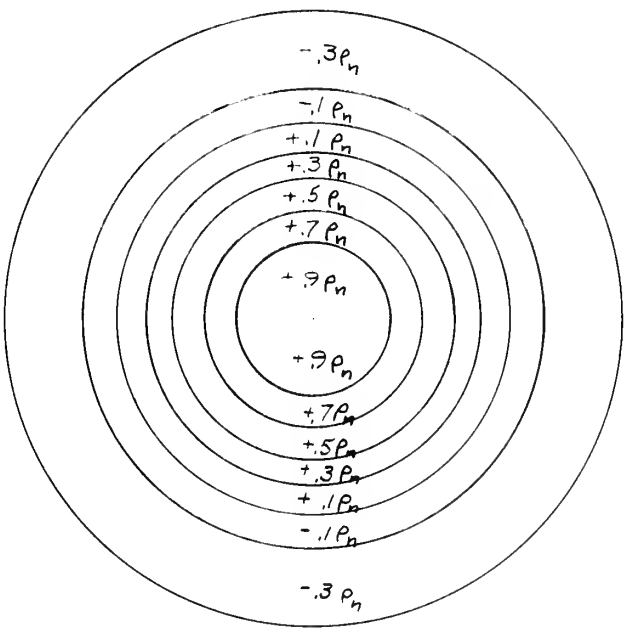

$t = 0$

$\rho = \rho_n$

$\rho_e = -3.71\,\rho_n$

$\rho_i = +4.71\,\rho_n$

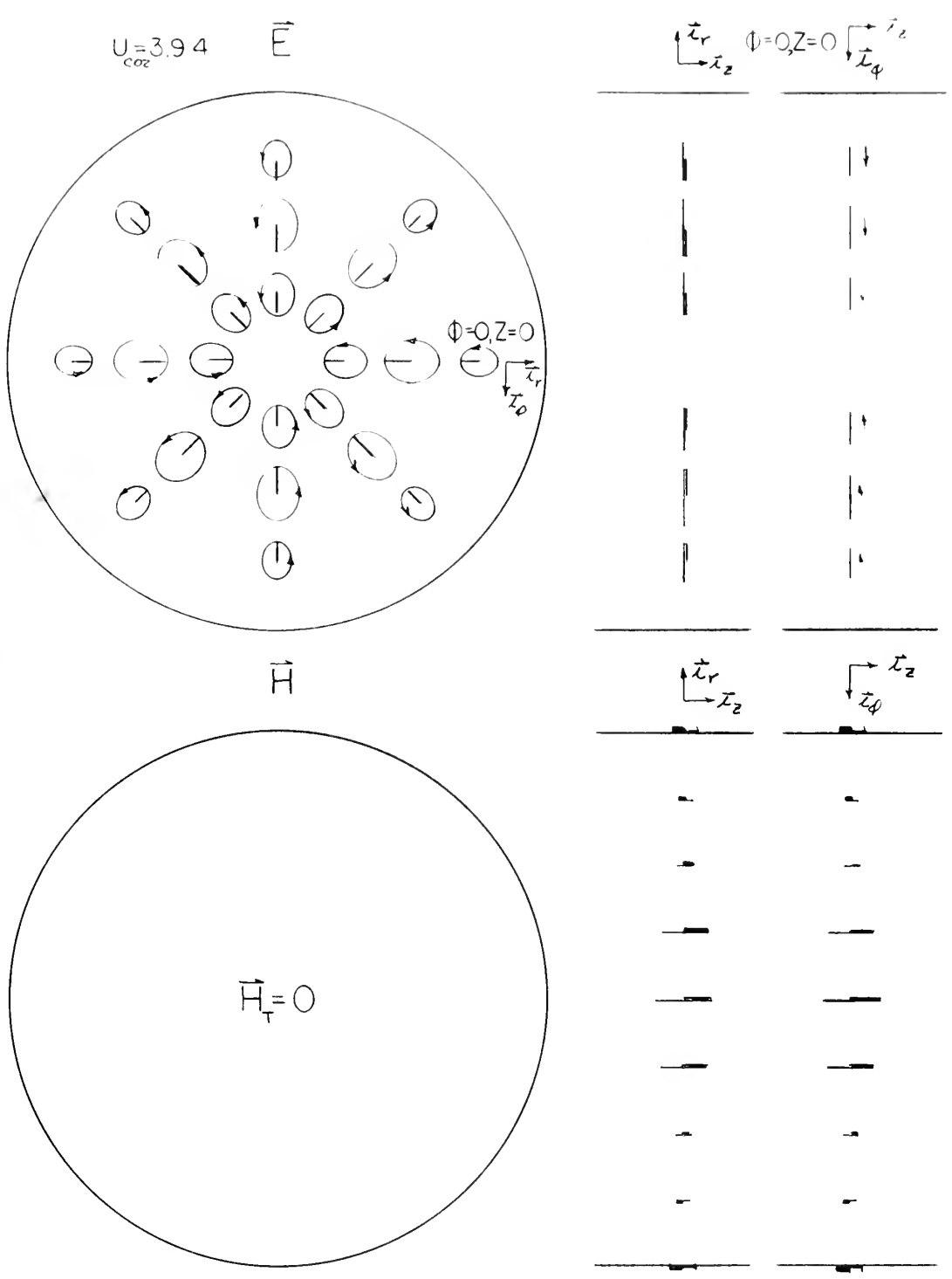
$U_{coz} = 3.94$
$\vec{E}$
$\Phi=0, Z=0$
$\vec{H}$
$\vec{H}_T = 0$

$U_{coz} = 3.94$ E_r & J_r

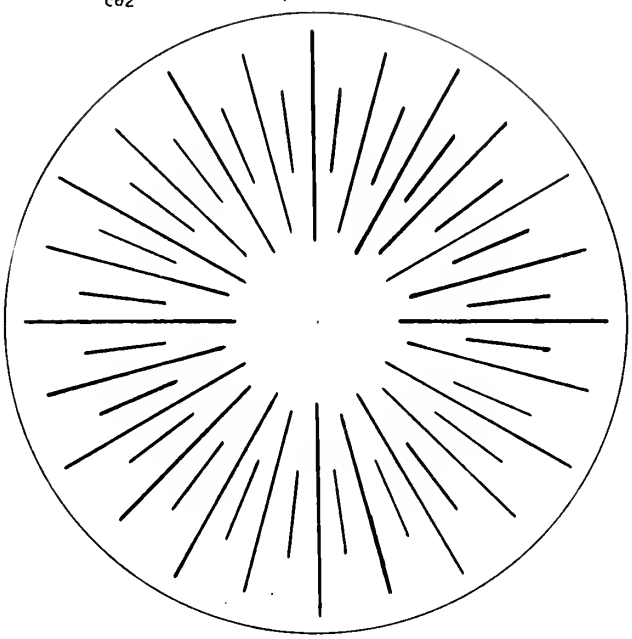

$U_{CO_2} = 3.94$ J

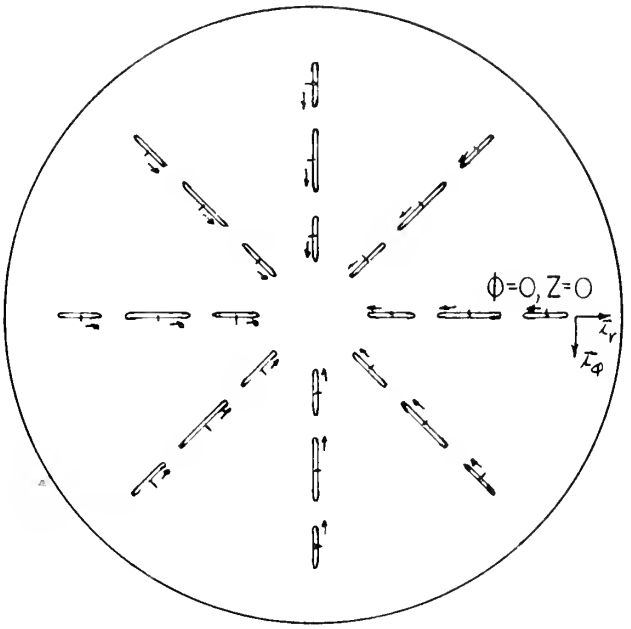

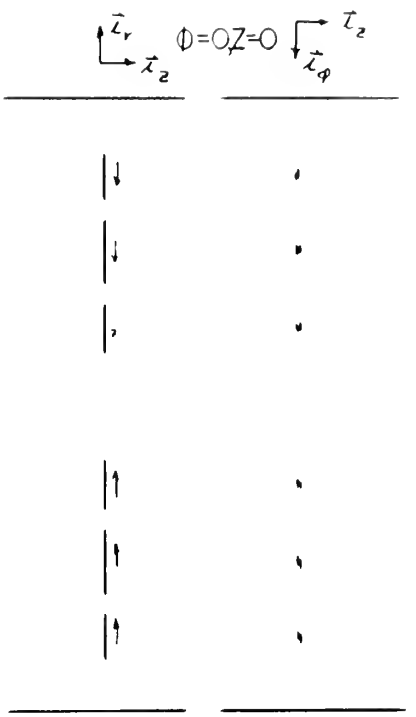

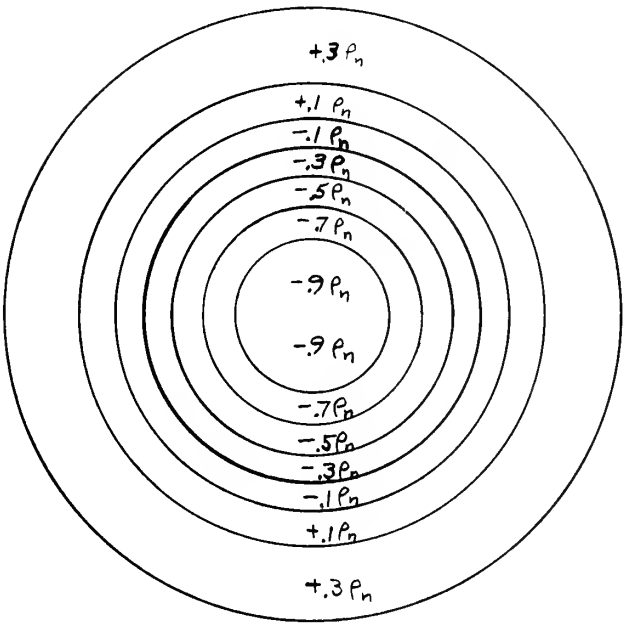

$t = 0$

$\rho = \rho_n$

$\rho_e = \rho_n$

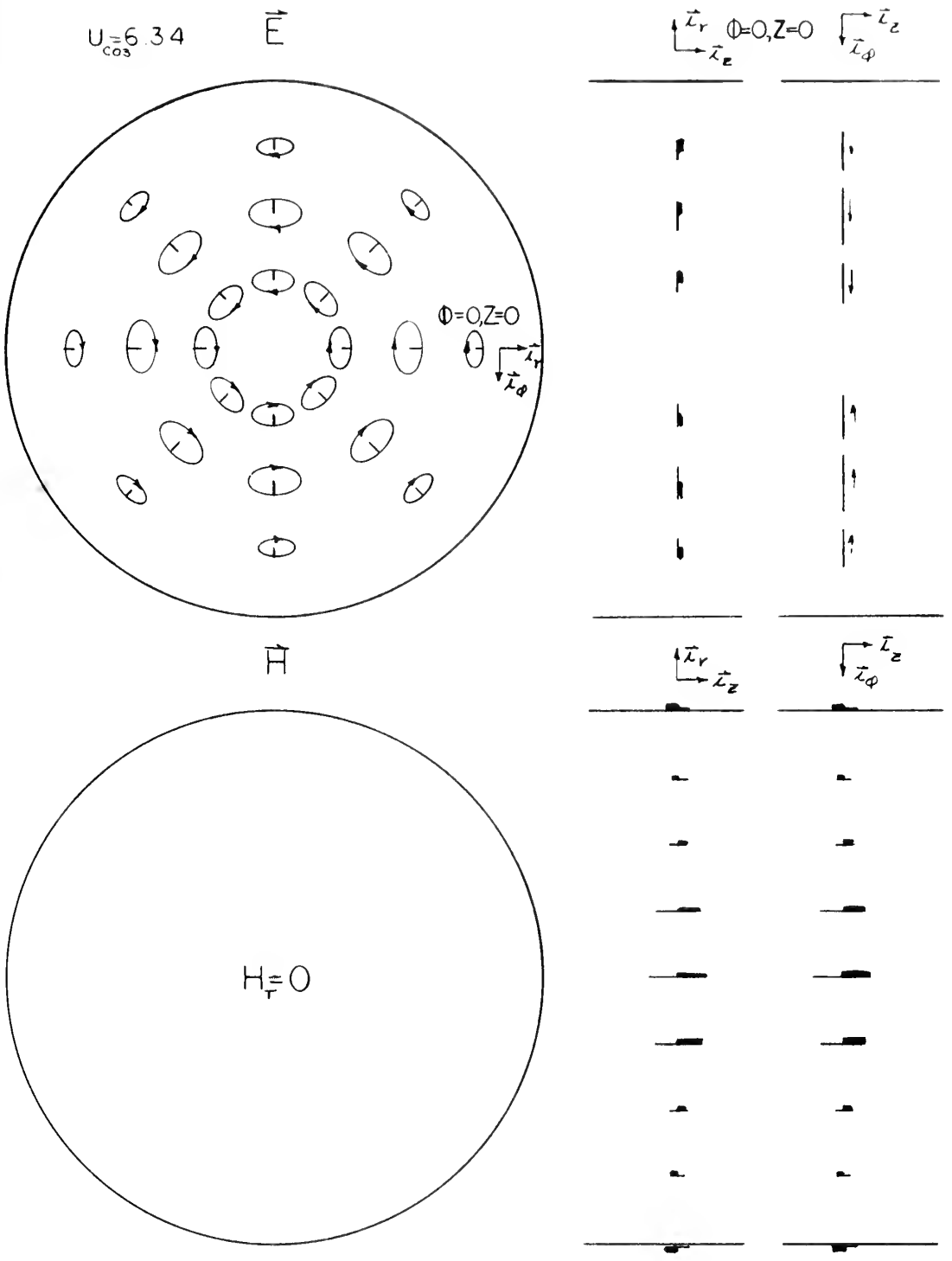
$U_{cos} = 6.34$
$\vec{E}$
$\Phi=0, Z=0$
$\vec{\imath}_r$
$\vec{\imath}_\Phi$
$\vec{\imath}_z$
$\vec{H}$
$H_r = 0$

$U = \frac{6.34}{\cos}$ $E_r = J_r$

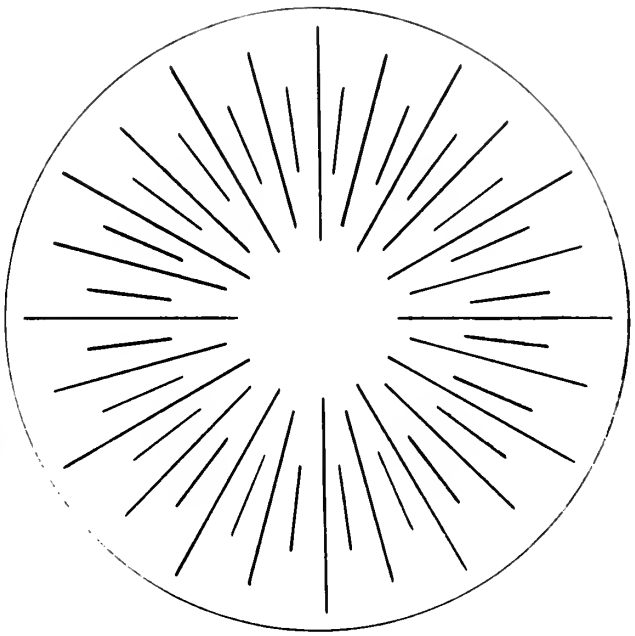

$U_{\varphi=0,3} = 6.34$ $\vec{J}$

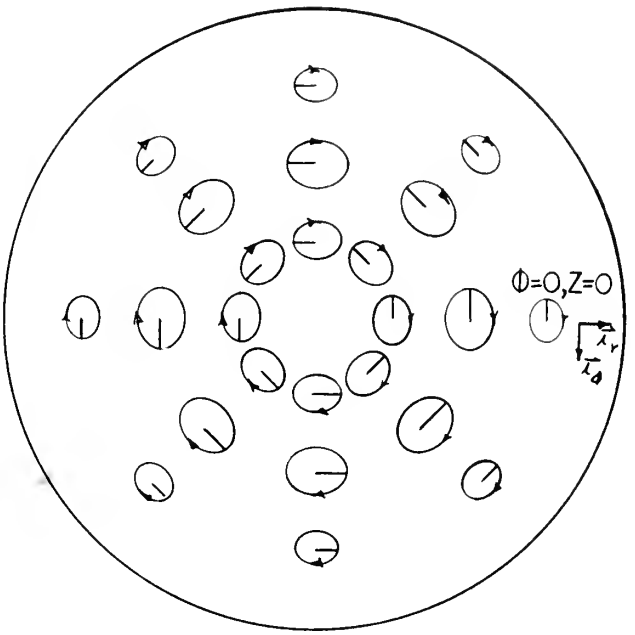

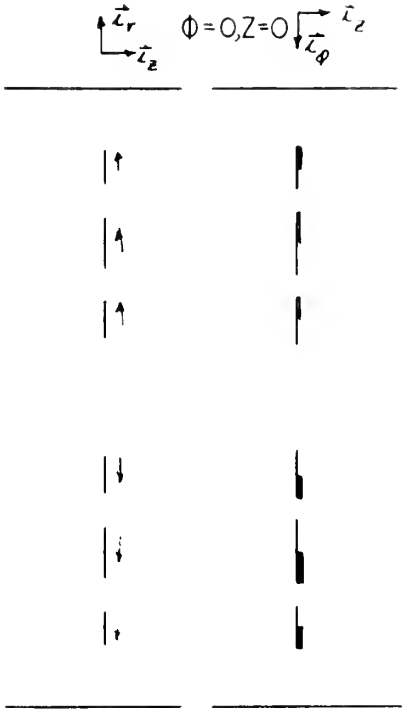

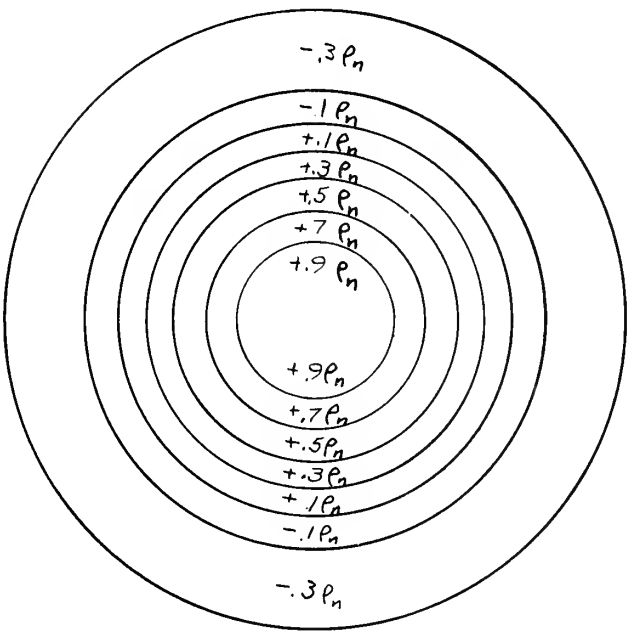

$t = o$

$\rho = \rho_n$

$\rho_e = \rho_n$

CUTOFF FIELDS:

H-Wave

$m = 1$

$u = .04326$

$A(\phi,t) = A_1 e^{j.0433\omega_n t}\, e^{j\phi}$

Complex Fields:

$$\bar{E} = A(\phi,t)\left[-(272\ J_o(pr) - 275\ \frac{J_1(pr)}{pr})\vec{I}_r + j(4.17\ J_o(pr) - 275\ \frac{J_1(pr)}{pr})\vec{I}_\phi\right]$$

$$\bar{H} = A(\phi,t)\left[J_1(pr)\vec{I}_z\right]$$

$$\bar{J} = A(\phi,t)\left[j(.615\ J_o(pr) + 76.5\ \frac{J_1(pr)}{pr})\vec{I}_r - (76.9\ J_o(pr) - 76.5\ \frac{J_1(pr)}{pr})\vec{I}_\phi\right]$$

$$\bar{J}_e = A(\phi,t)\left[-j(2.29\ J_o(pr) - 79.4\ \frac{J_1(pr)}{pr})\vec{I}_r - (76.9\ J_o(pr) - 79.4\ \frac{J_1(pr)}{pr})\vec{I}_\phi\right]$$

$$\bar{J}_i = A(\phi,t)\left[j(2.90\ J_o(pr) - 2.84\ \frac{J_1(pr)}{pr})\vec{I}_r - (6.52\times10^{-2}\ J_o(pr) + 2.84\ \frac{J_1(pr)}{pr})\vec{I}_\phi\right]$$

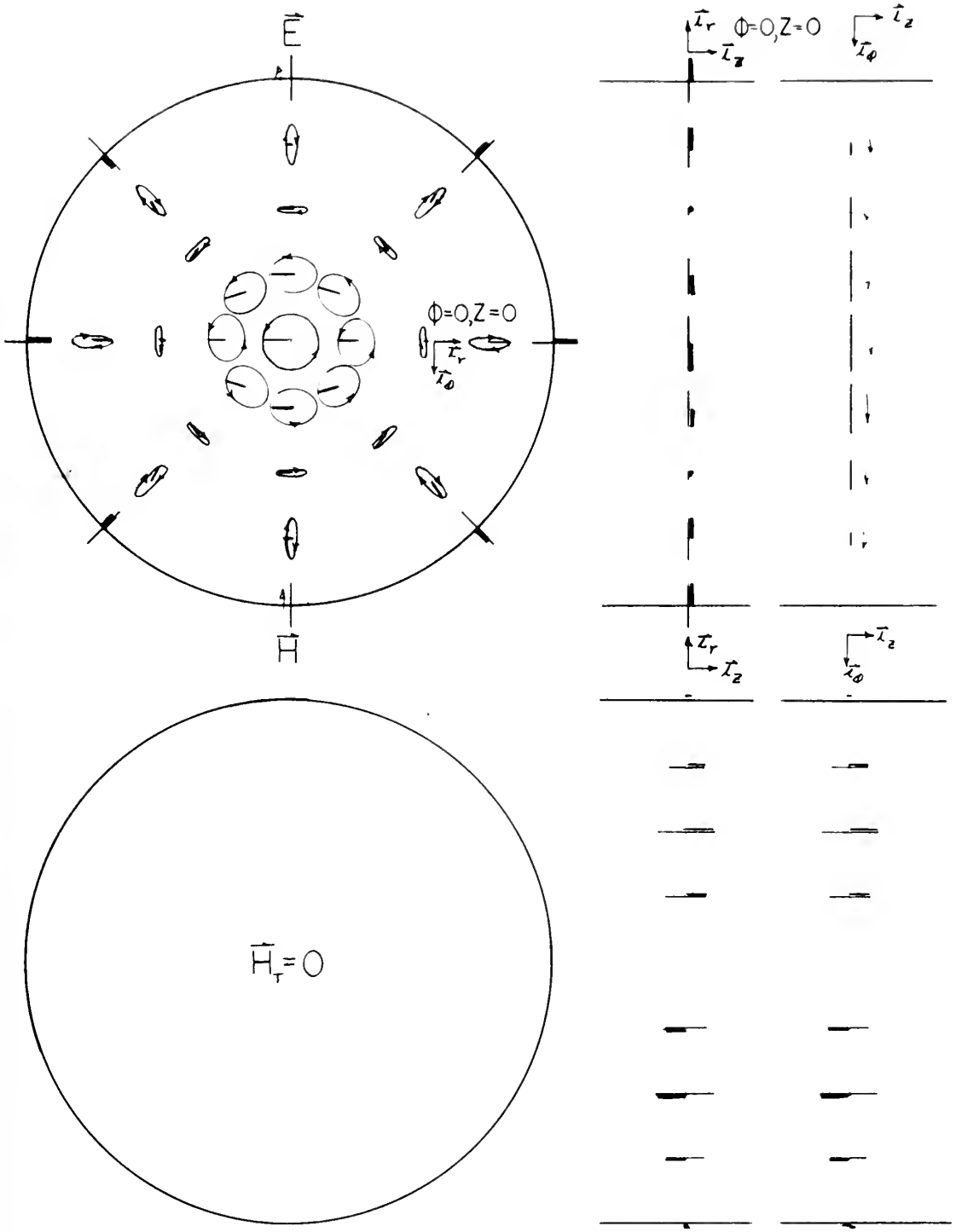
$\vec{E}$
$\vec{H}$
$\Phi=0, Z=0$
$\vec{r}_r$
$\vec{r}_\Phi$
$\vec{r}_z$
$\vec{H}_r=0$

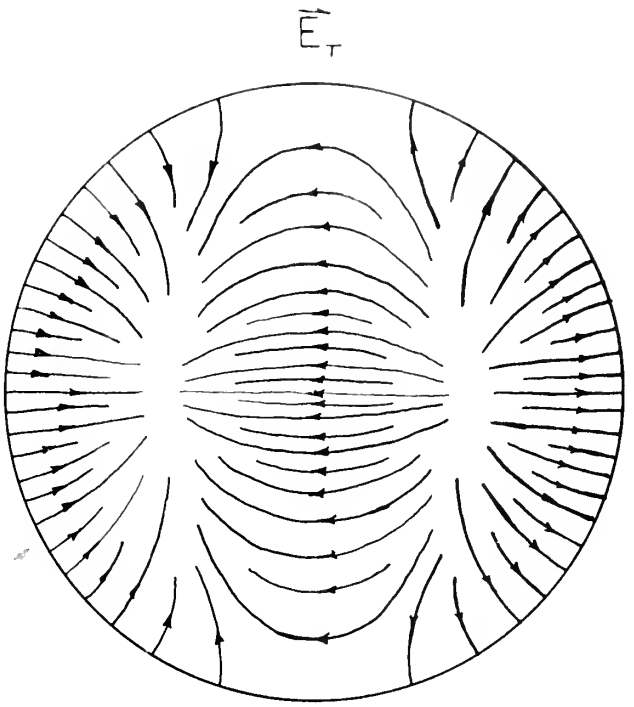
$\vec{E}_T$

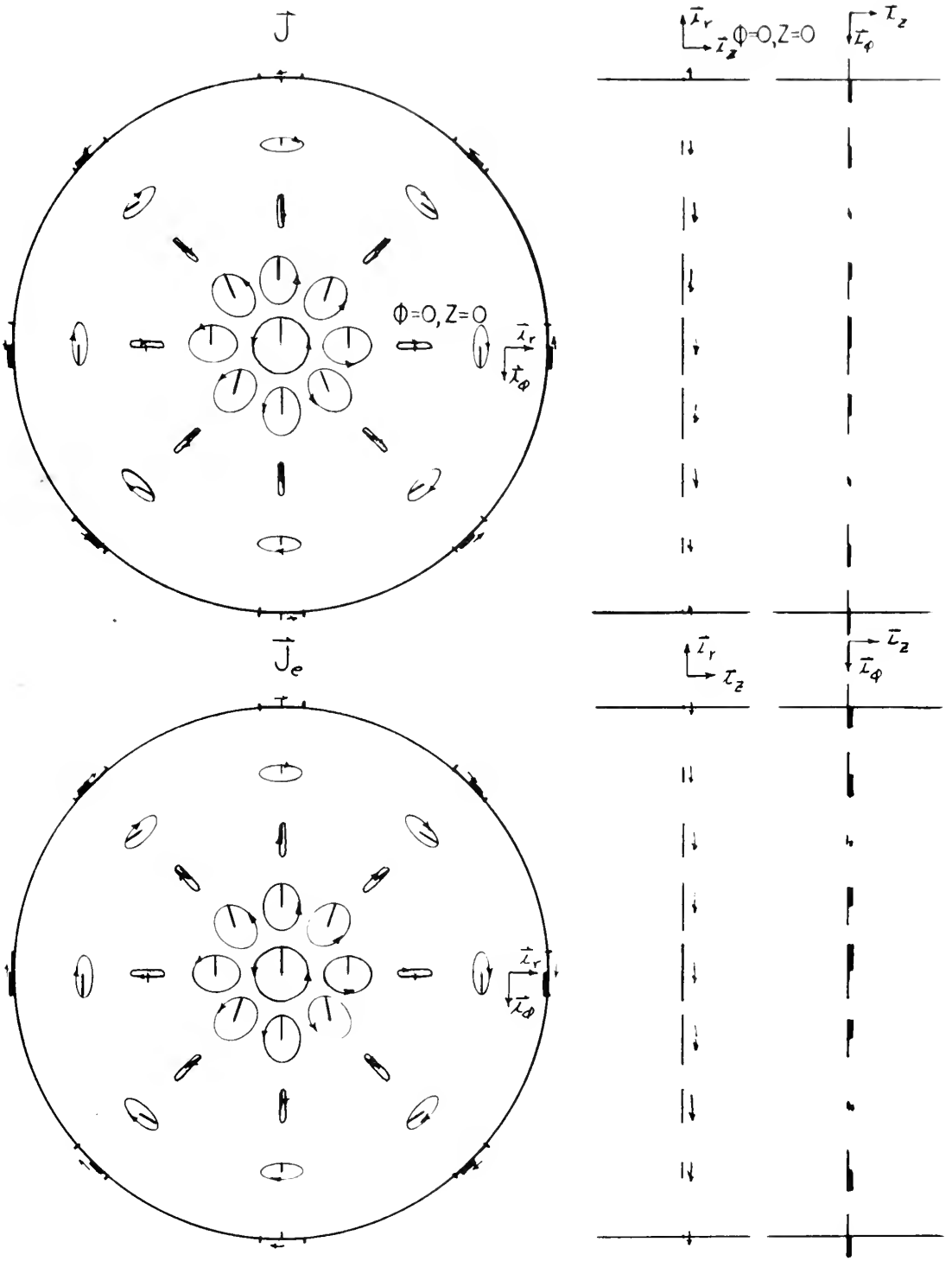
J
Φ=0, Z=0
$\vec{J}_e$
Φ=0, Z=0

$\vec{J}_T$

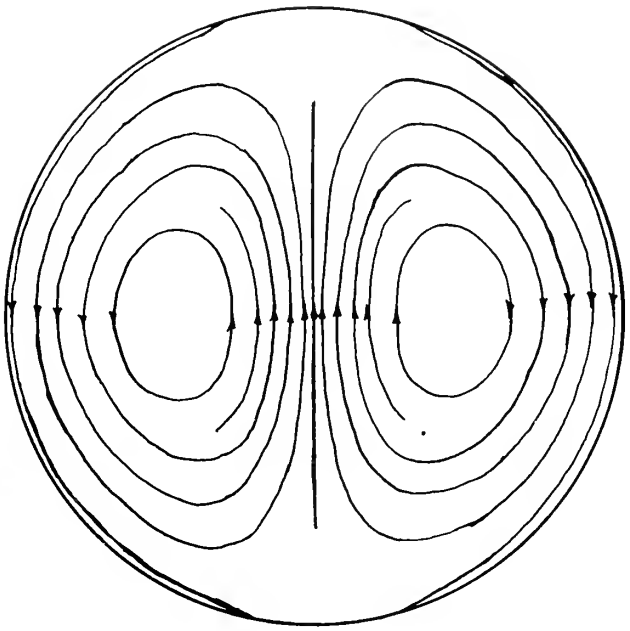

$\vec{J}_{eT}$

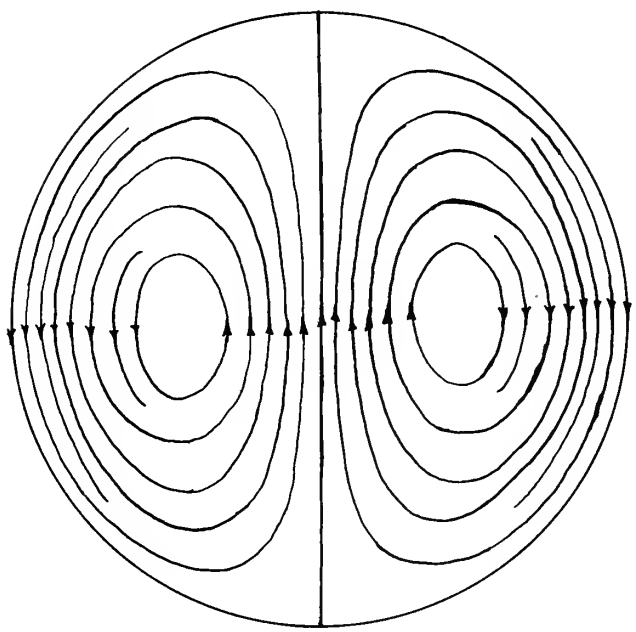

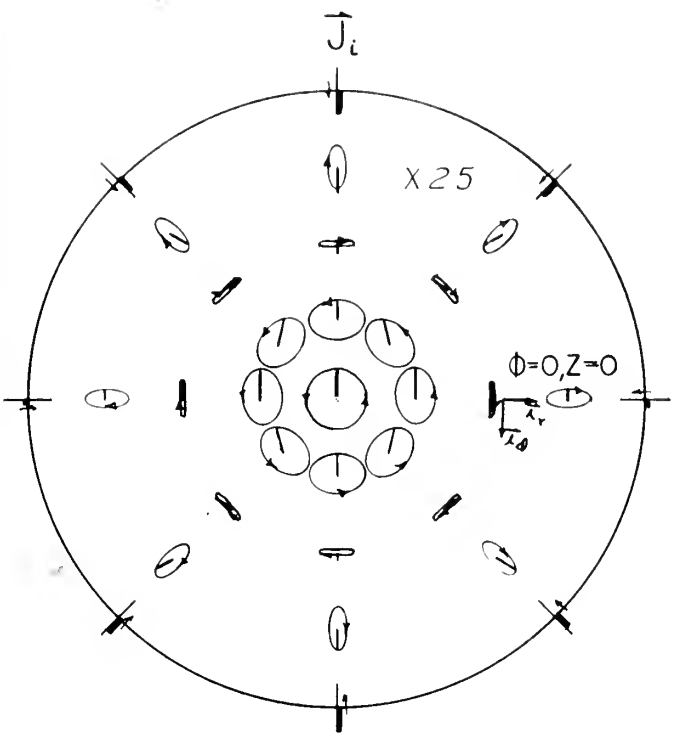

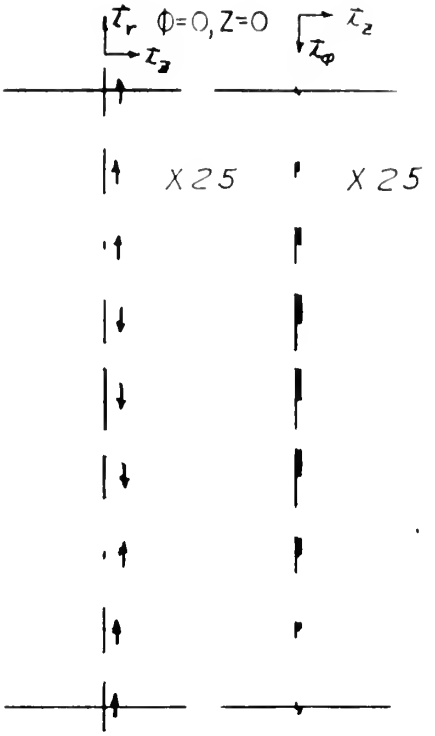

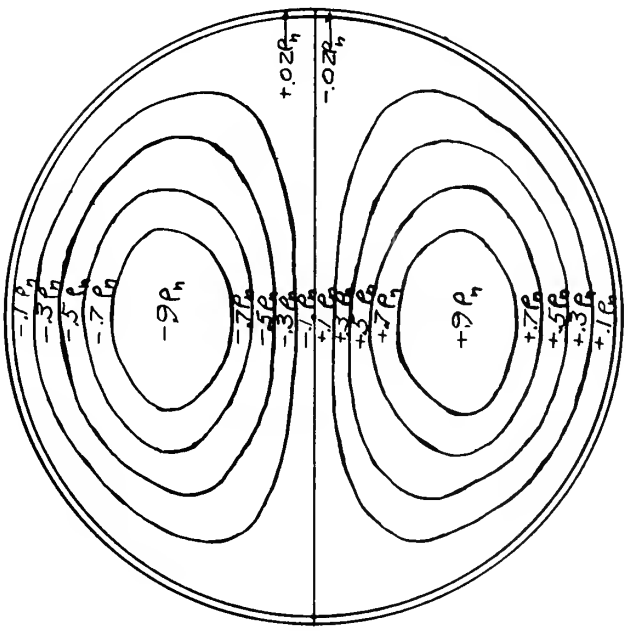

$t = 0$

$\rho = \rho_n$

$\rho_e = -3.72\,\rho_n$

$\rho_i = +4.72\,\rho_n$

$\vec{J}_{iT}$

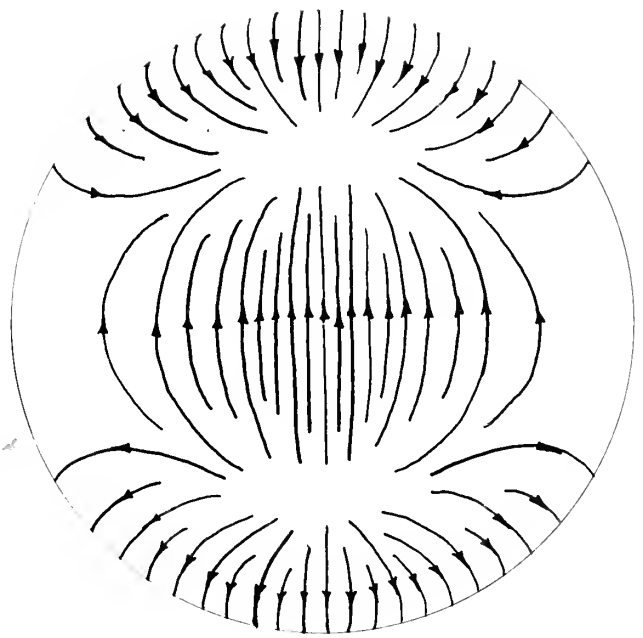

CUTOFF FIELDS:

H-Wave

$m = 1$

$u = 3.37$

$p = \frac{2.42}{a}$

$A(\phi,t) = A_1 e^{j3.37\omega_n t}\, e^{j\phi}$

Complex Fields:

$$\bar{E} = A(\phi,t)\left[548\, J_o(pr) - 23.1\,\frac{J_1(pr)}{pr})\vec{i}_r + j(524\, J_o(pr) + 23.1\,\frac{J_1(pr)}{pr})\vec{i}_\phi\right]$$

$$\bar{H} = A(\phi,t)\, J_1(pr)\vec{i}_z$$

$$\bar{J} = A(\phi,t)\left[-j(98.0\, J_o(pr) - 52.9\,\frac{J_1(pr)}{pr})\vec{i}_r + (44.9\, J_o(pr) + 52.9\,\frac{J_1(pr)}{pr})\vec{i}_\phi\right]$$

$$\rho = A(\phi,t)\left[-2.35\times10^{-7}\, J_1(pr)\right]$$

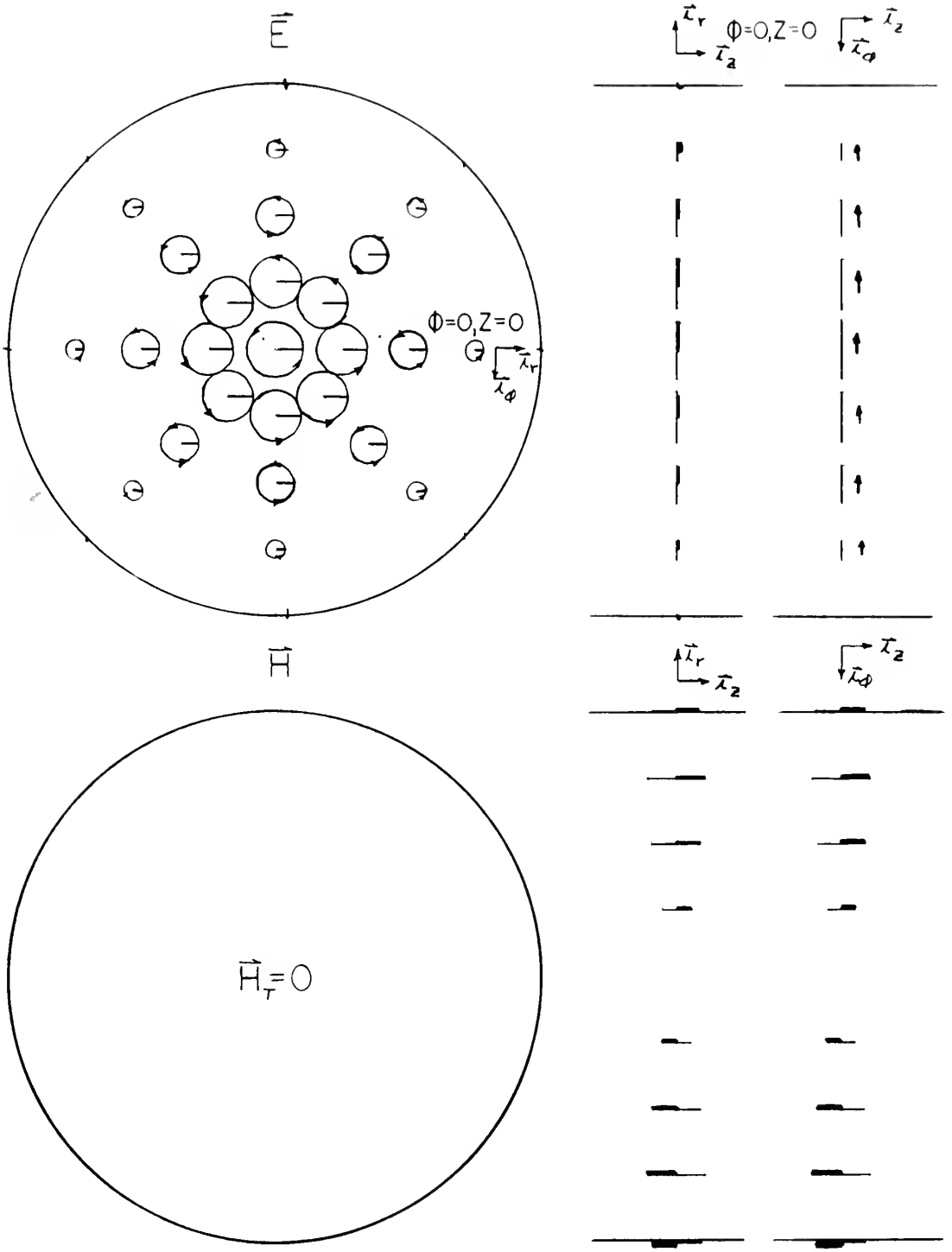
$\vec{E}$
$\Phi=0, Z=0$
$\vec{H}$
$\vec{H}_T=0$

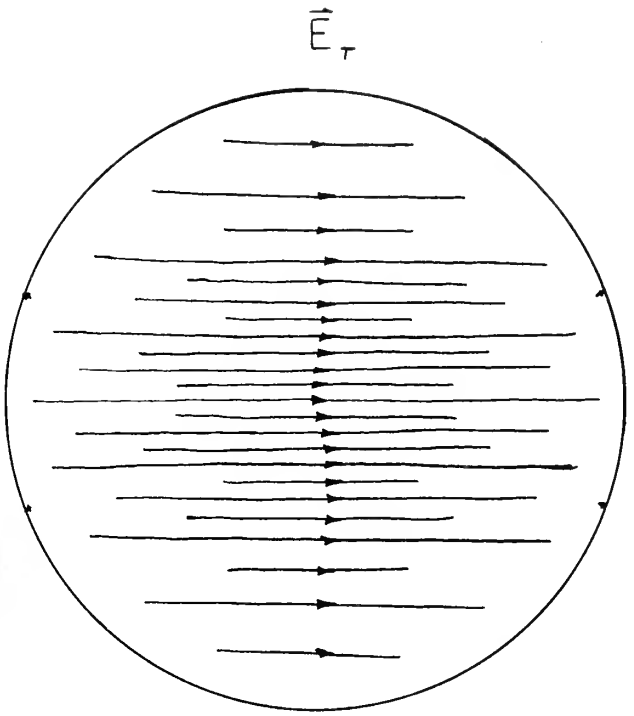
$\vec{E}_T$

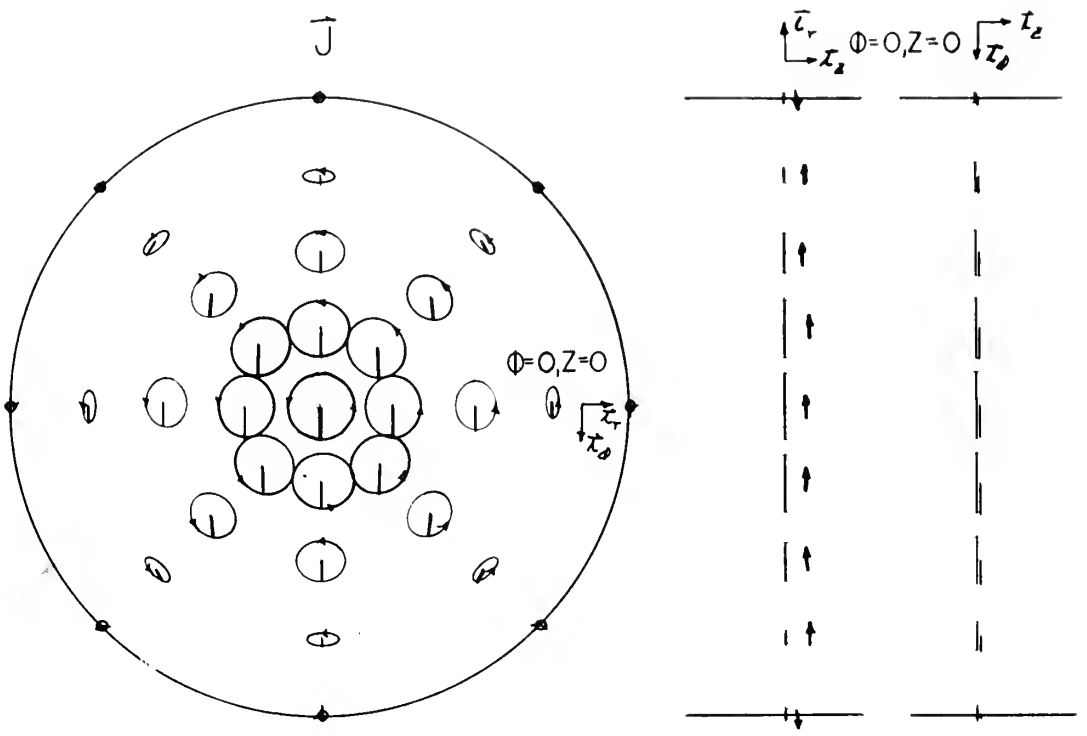

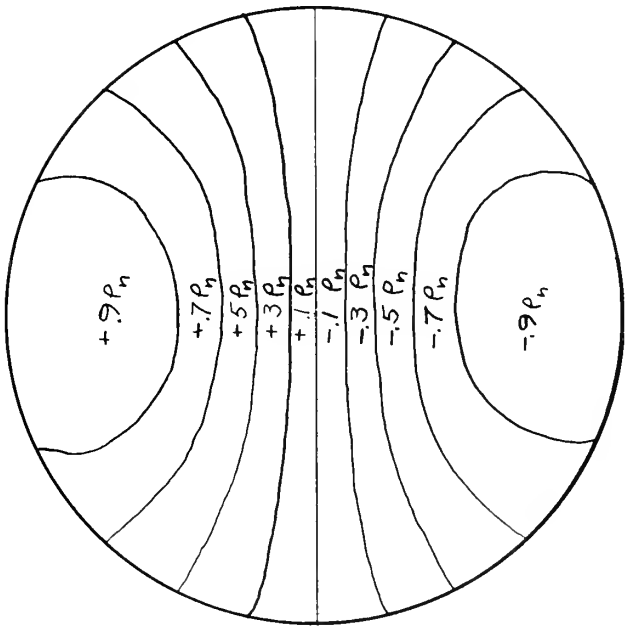

$t = 0$
$\rho_e = \rho_n$
$\rho = \rho_n$

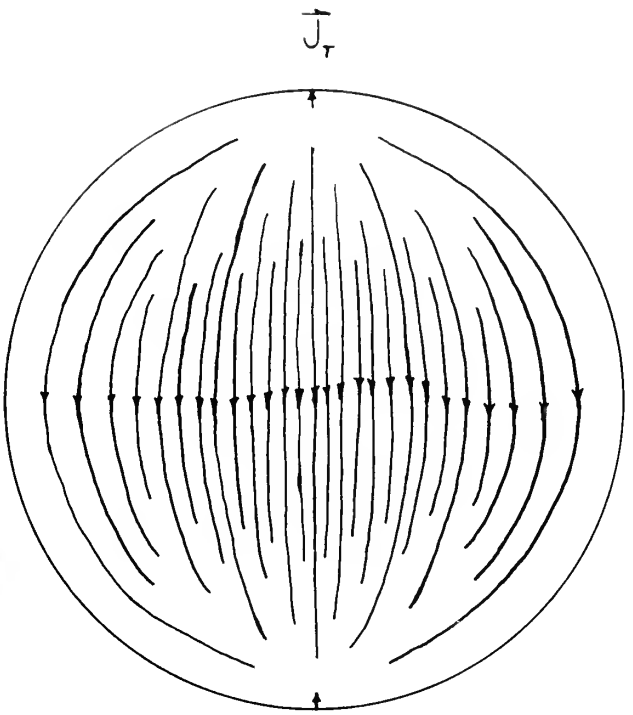
$\vec{J}_T$

CUTOFF FIELDS:

H-Wave

$m = 1$

$u = 5.07$

$p = j \frac{14.00}{a} = j\, q$

$A(\phi,t) = A_1 e^{j5.07\omega_n t}\, e^{j\phi}$

Complex Fields:

$$\overline{E} = A(\phi,t)\left[\left(1.985\times10^{3}\,\frac{I_1(qr)}{qr} - 1.848\times10^{3}\, I_o(qr)\right)\vec{i}_r - j\left(1.985\times10^{3}\,\frac{I_1(qr)}{qr} - 1.366\times10^{2}\, I_o(qr)\right)\vec{i}_\phi\right]$$

$$\overline{H} = A(\phi,t)\, I_1(qr)\,\vec{i}_z$$

$$\rho = A(\phi,t)\left[-4.57\times10^{-6}\, I_1(qr)\right]$$

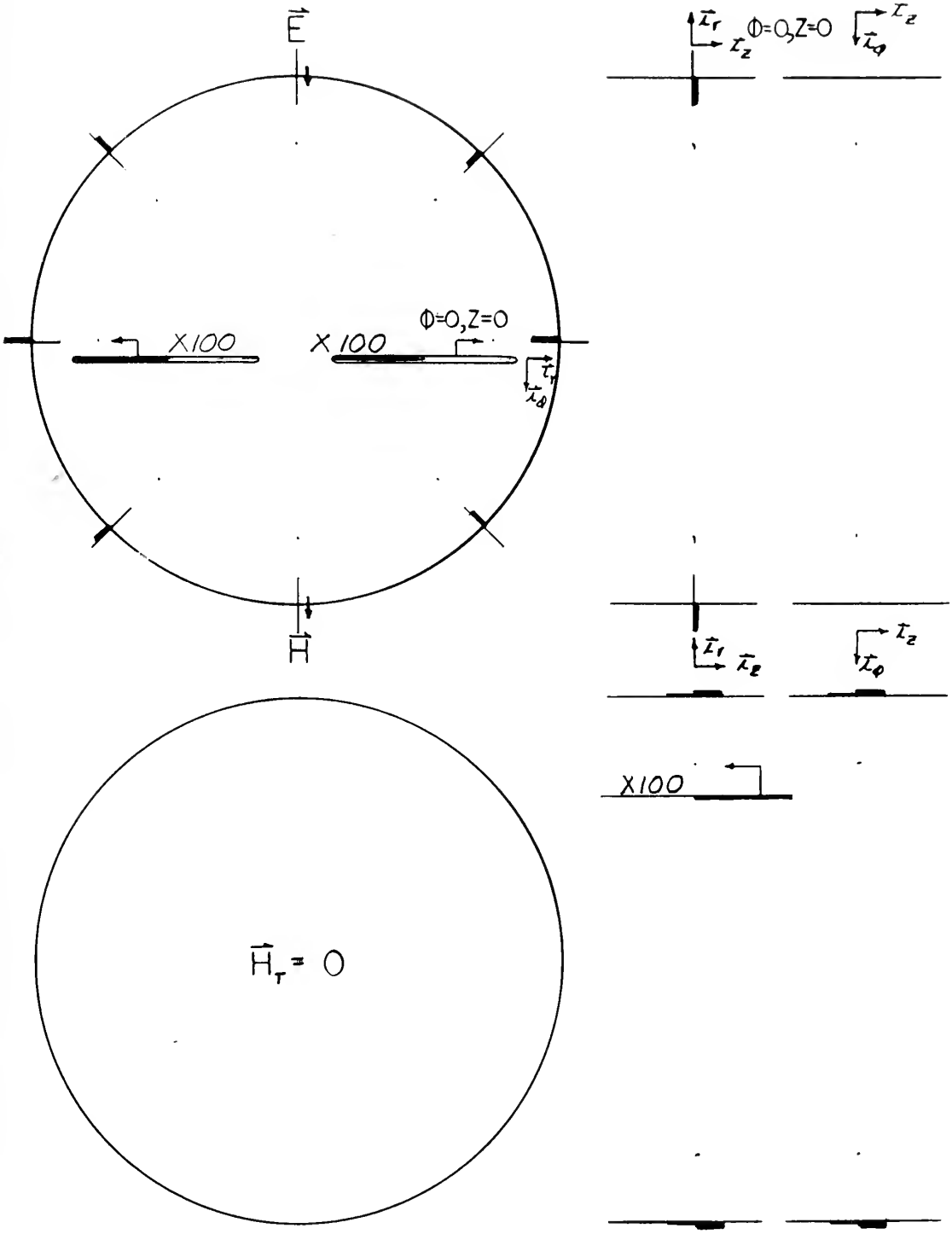
E
H
X100
X100
Φ=0,Z=0
Φ=0,Z=0
X100
$\vec{H}_T = 0$

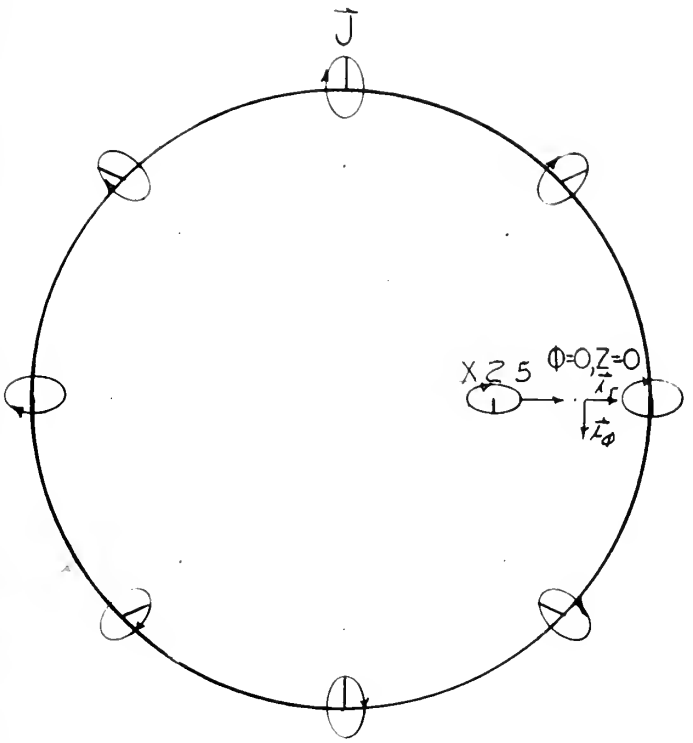

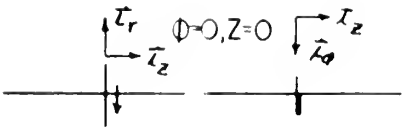

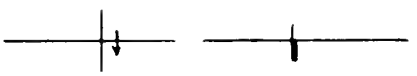

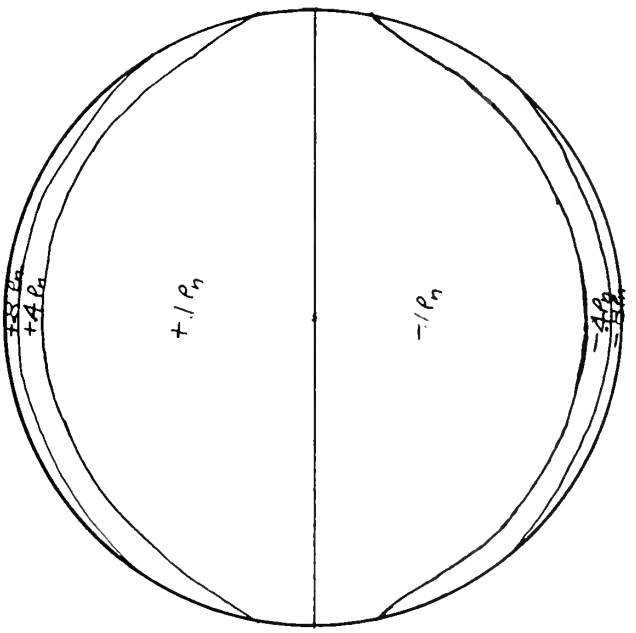

$t = 0$
$\rho = \rho_n$
$\rho_e = \rho_n$

CUTOFF FIELDS:

H-Wave

$m = 1$

$u = 5.77$

$p = j\frac{.01904}{a} = j\,q$

$A(\phi,t) = A_1 e^{j5.77\omega_n t}\, e^{j\phi}$

Complex Fields:

$$\bar{E} = 544\, A(\phi,t)\left[(1 + (\tfrac{r}{a})^2)\vec{1}_r + j(1 - (\tfrac{r}{a})^2)\vec{1}_\phi\right]$$

$$\bar{H} = A(\phi,t)(\tfrac{r}{a})\vec{1}_z$$

$$\bar{J} = 52.8\, A(\phi,t)\left[-j(1 + 3.16(\tfrac{r}{a})^2)\vec{1}_r + (1 - 3.16(\tfrac{r}{a})^2)\vec{1}_\phi\right]$$

$$\rho = 3.85\times10^{-7}\, A(\phi_1 t)(\tfrac{r}{a})$$

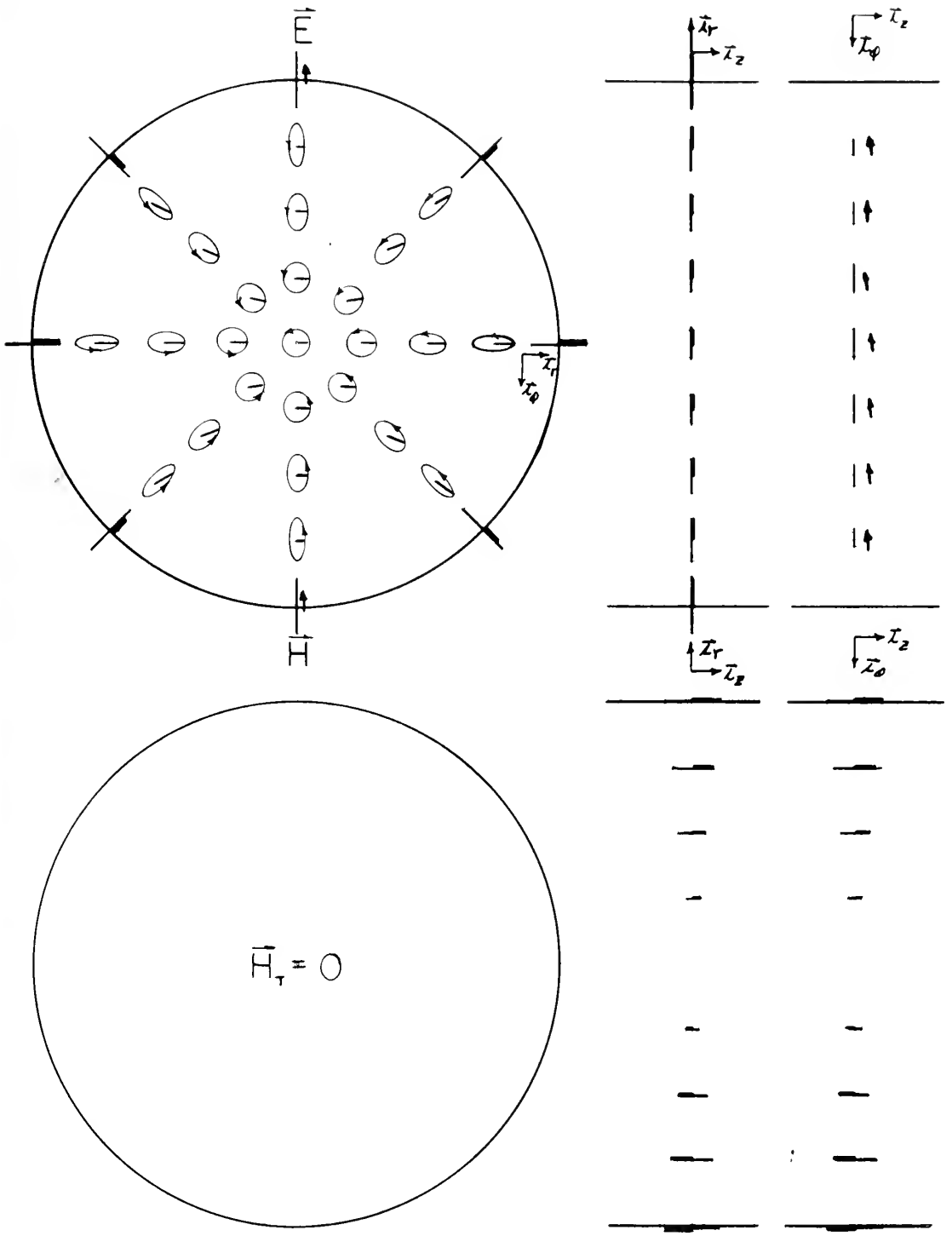
E
H
$\vec{I}_r$
$\vec{I}_z$
$\vec{I}_\varphi$
$\vec{H}_T = 0$

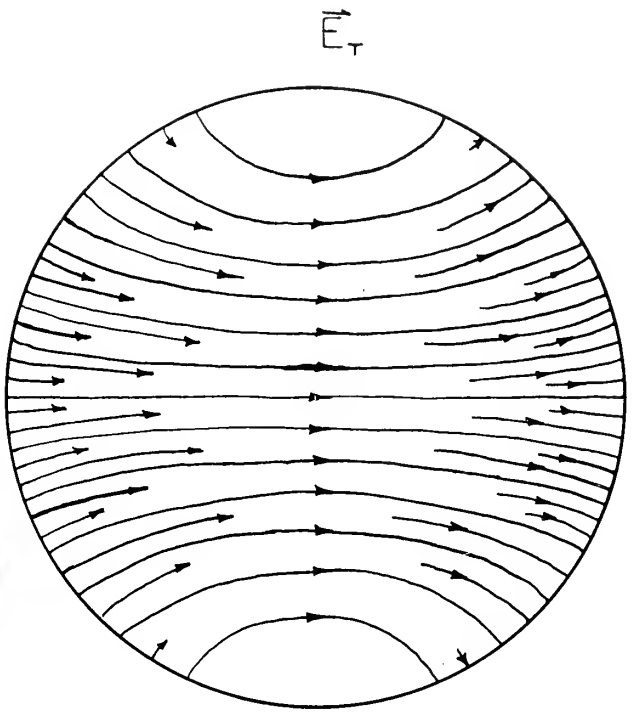
$\vec{E}_T$

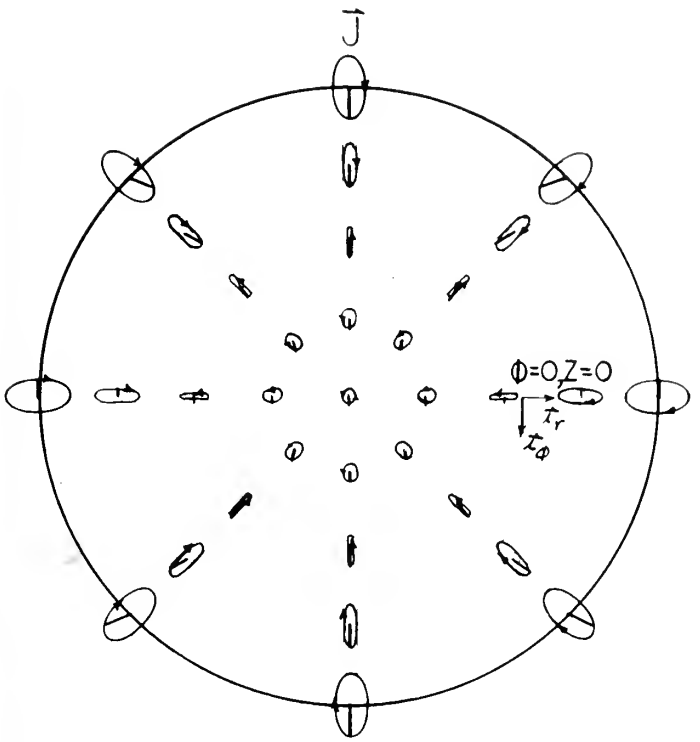

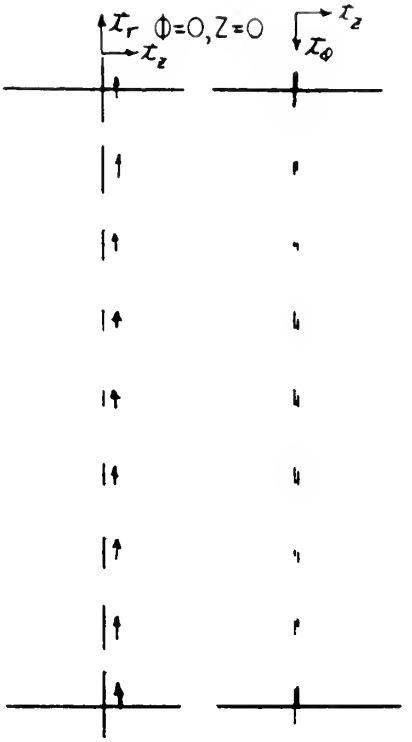

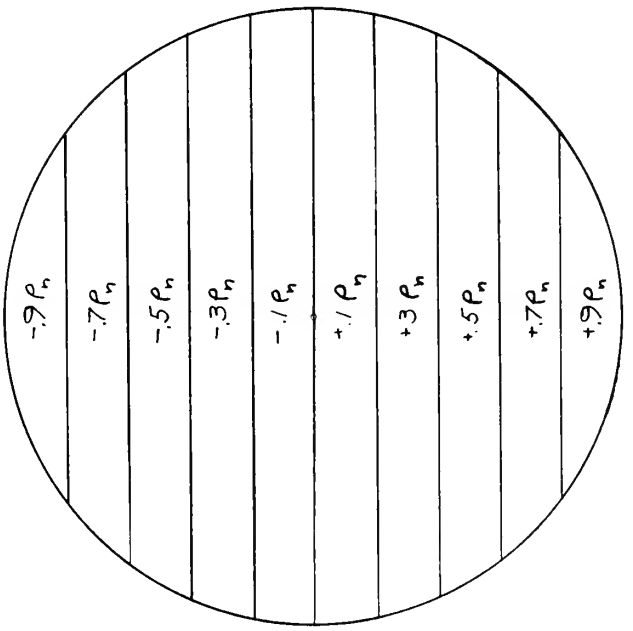

$t = 0$
$\rho = \rho_n$
$\rho_e = \rho_n$

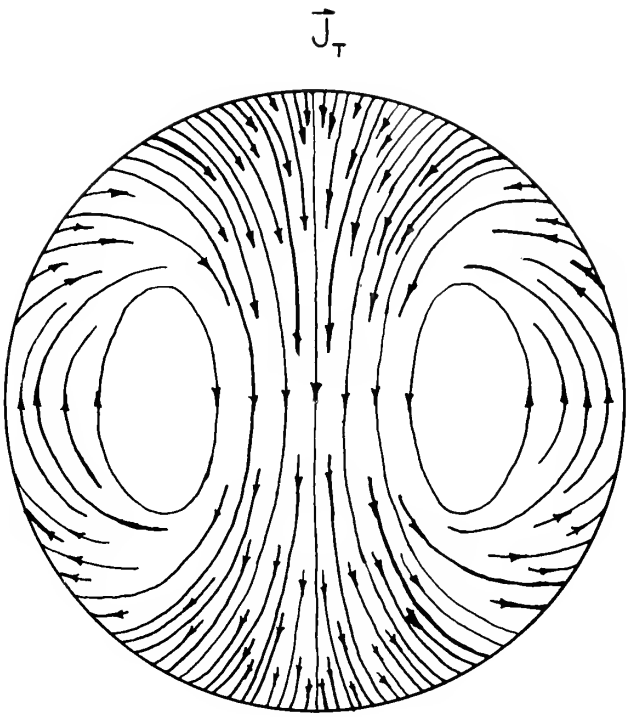
$\vec{J}_T$

Discrete Frequency:

$m = 0$

$u = 1$

$\beta_n = 2.445$

$p_1 = \frac{3.415}{a} e^{j\pi/4}$

$p_2 = \frac{3.415}{a} e^{j\pi/4}$

$A(z,t) = A_1 e^{j(\omega_n t - 2.445 \frac{z}{a})}$

Complex Bessel Function

$J_i(pr) = U_i(pr) + jV_i(pr)$

Complex Fields:

$$\bar{E} = A(z,t)\,[j(-3.55\,U_1(p_1r) + 1.068\,V_1(p_1r))\vec{I}_r - (.957\,U_1(p_1r) + 1.588\,V_1(p_1r))\,\vec{I}_\phi + (1.490\,U_o(p_1r) - .666\,V_o(p_1r))\vec{I}_z]$$

$$\bar{H} = A(z,t)\,[(6.22\times10^{-3}\,U_1(p_1r) + 10.29\times10^{-3}\,V_1(p_1r))\vec{I}_r - (17.77\times10^{-3}\,U_1(p_1r) + 6.83\times10^{-3}\,V_1(p_1r))\vec{I}_\phi - j(16.27\times10^{-3}\,U_o(p_1r) + 3.99\times10^{-3}\,V_o(p_1r))\vec{I}_z]$$

$$\bar{J} = A(z,t)\,[(.679\,U_1(p_1r) + .393\,V_1(p_1r))\vec{I}_r + j(-1.231\,U_1(p_1r) + .1724\,V_1(p_1r))\vec{I}_\phi + j(-1.266\,U_o(p_1r) + .566\,V_o(p_1r))\vec{I}_z]$$

$$\rho = A(z,t)\,[j\times10^{-9}(-1.702\,U_o(p_1r) + 2.26\,V_o(p_1r)]$$

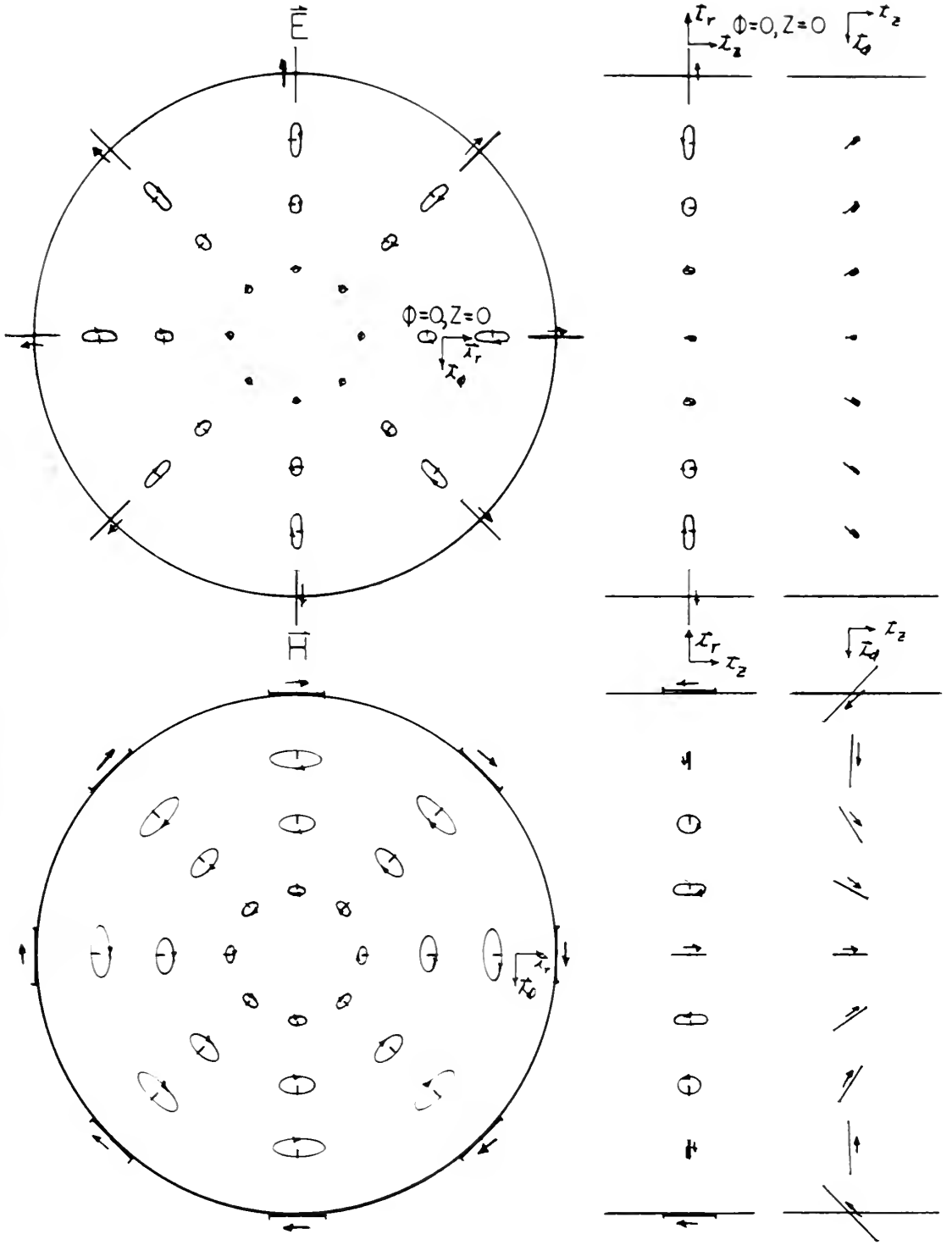
$\vec{E}$
$\vec{H}$
Φ=0, Z=0
Φ=0, Z=0

E_r

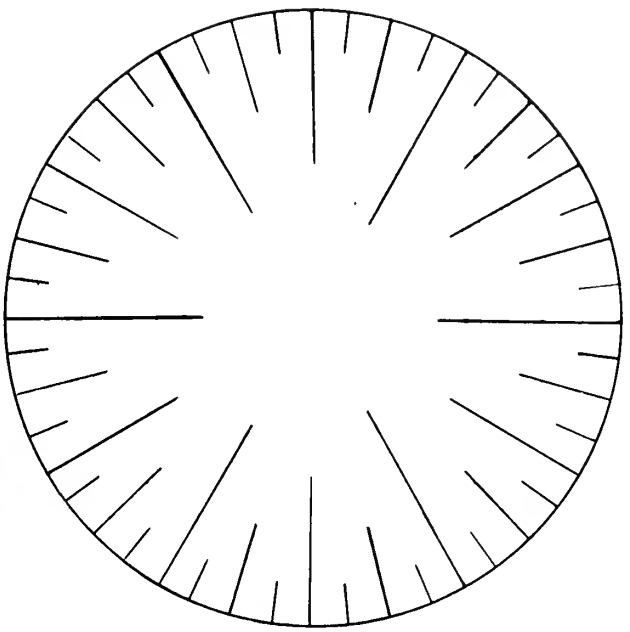

H_r

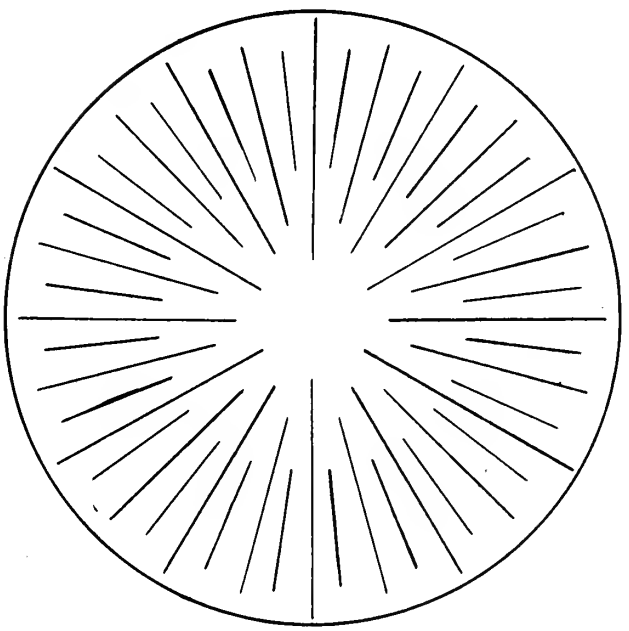

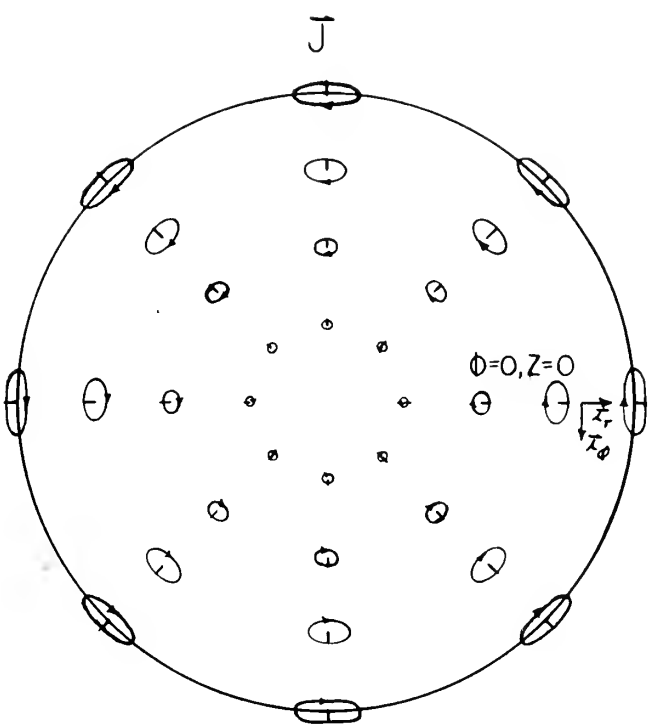

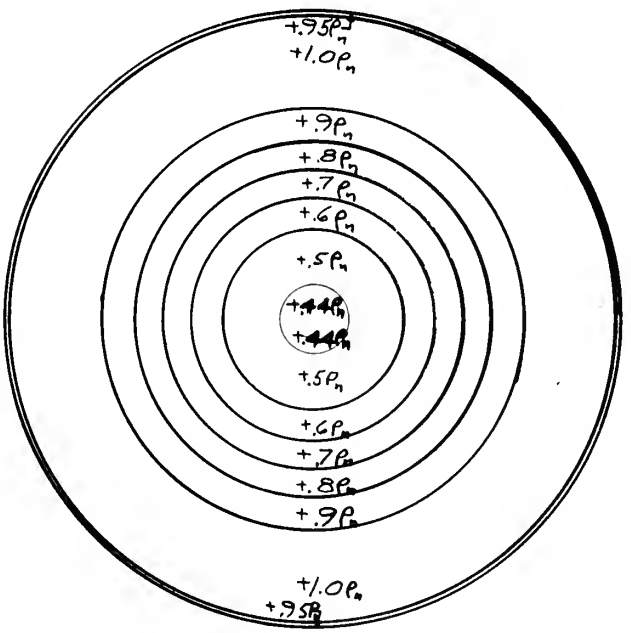

$\omega t = \frac{\pi}{2}$

$\rho = \rho_n$

$\rho_e = \rho_n$

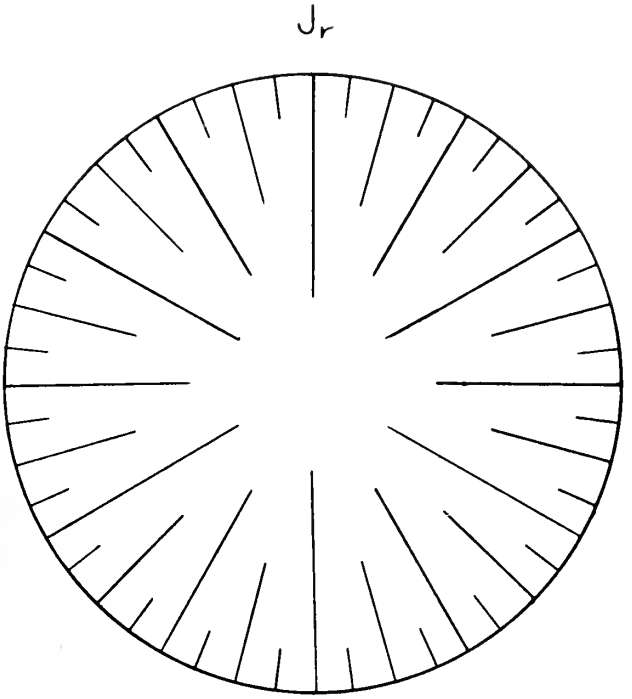
J_r

Discrete Frequency:

$m = 0$

$u = 4.773$

$\beta_n = 1.663$

$p_1 = 2.405/a$

$p_2 = 8.654/a$

$$A(z,t) = A_1 e^{j(4.773\,\omega_n t - 1.663\,\frac{z}{a})}$$

Complex Fields:

$$\bar{E} = A(z,t)\,[j(.248\,J_1(p_1r) - 3.15\,J_1(p_2r))\vec{1}_r + (-.337\,J_1(p_1r) + .643\,J_1(p_2r))\vec{1}_\phi + (J_o(p_1r) + .666\,J_o(p_2r))\vec{1}_z]$$

$$\bar{H} = 10^{-3} x A(z,t)\,[(.312\,J_1(p_1r) - .594\,J_1(p_1r))\vec{1}_r + j(1.568\,J_1(p_1r) + .298\,J_1(p_2r))\vec{1}_\phi + j(-.451\,J_o(p_1r) + 3.19\,J_o(p_2r))\vec{1}_z]$$

$$\bar{J} = A(z,t)\,[(.0096\,J_1(p_1r) - .807\,J_1(p_2r))\vec{1}_r + j(.0533\,J_1(p_1r) + .393\,J_1(p_2r))\vec{1}_\phi - j(.1779\,J_o(p_1r) + .1183\,J_o(p_2r))\vec{1}_z]$$

$$\rho = -j10^{-9}\,A(z,t)\,[.1883\,J_o(p_1r) + 5.01\,J_o(p_2r)]$$

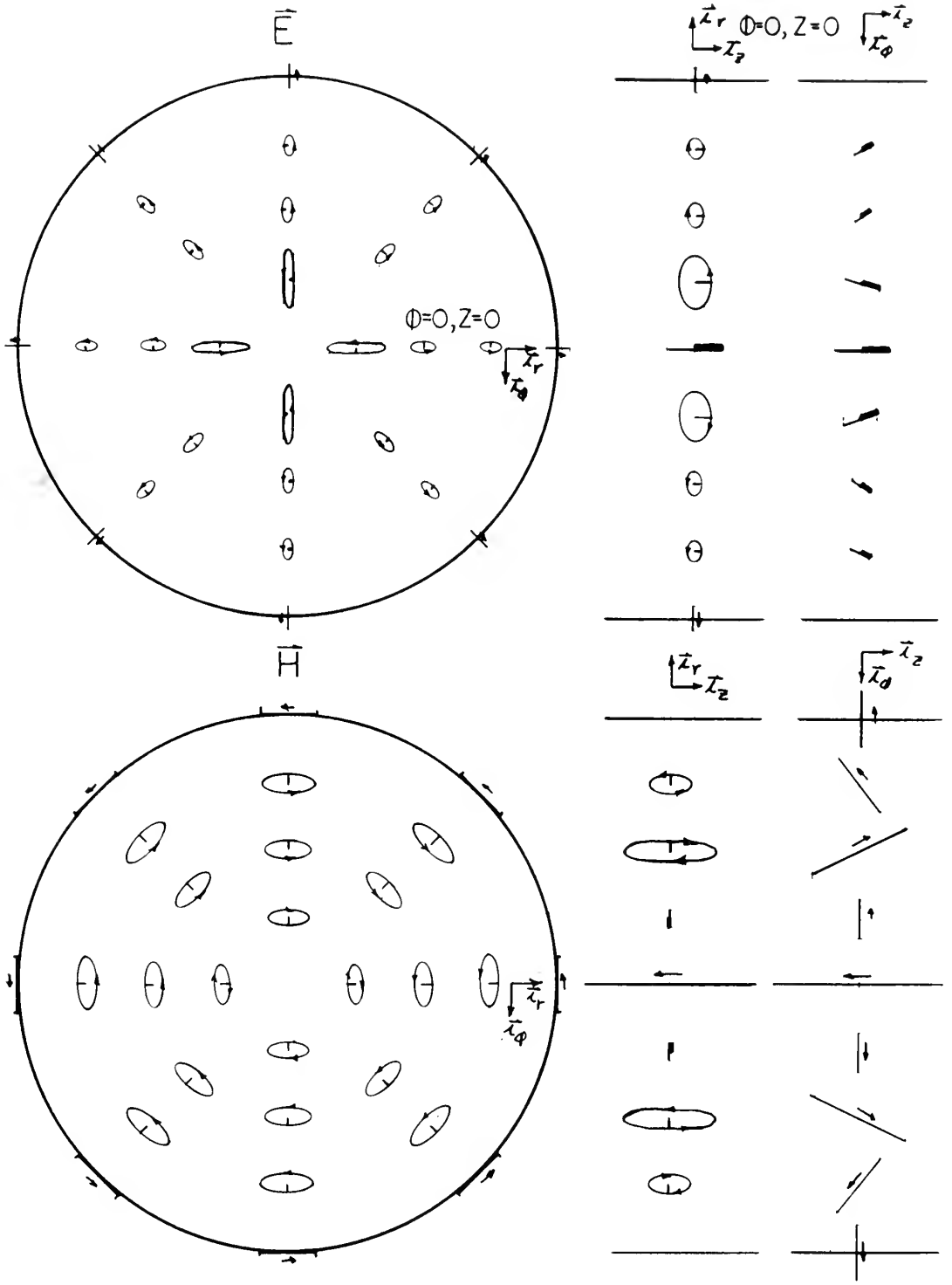
$\vec{E}$
Φ=0, Z=0
$\vec{H}$
Φ=0, Z=0

E_r

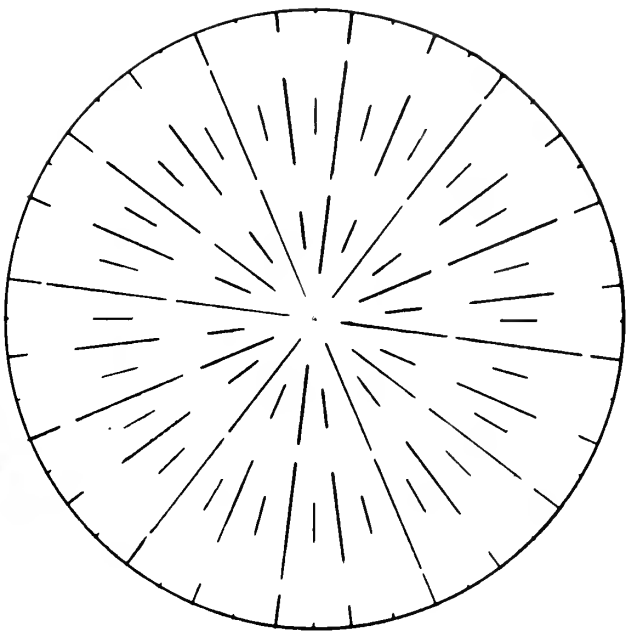

H_r

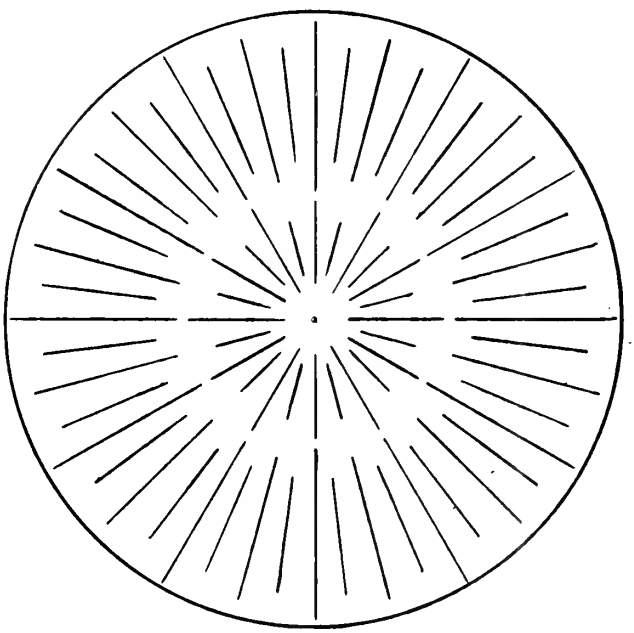

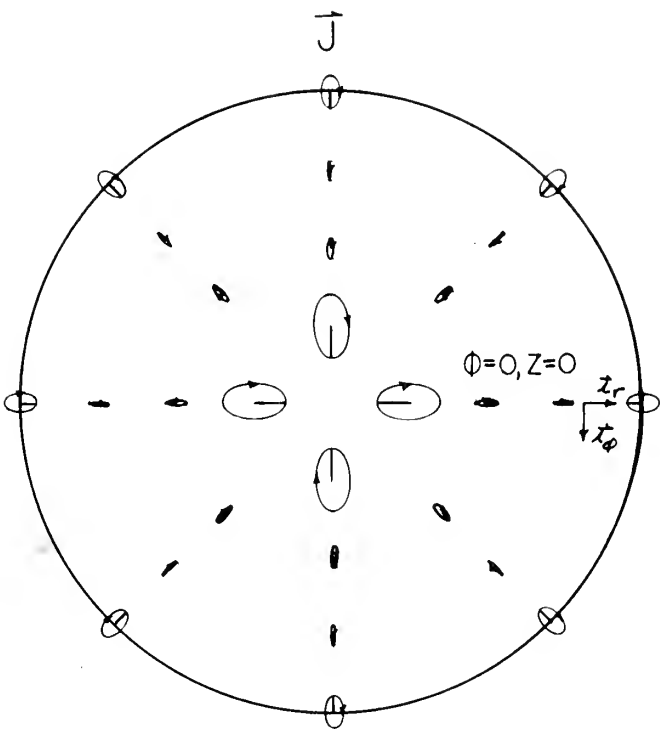

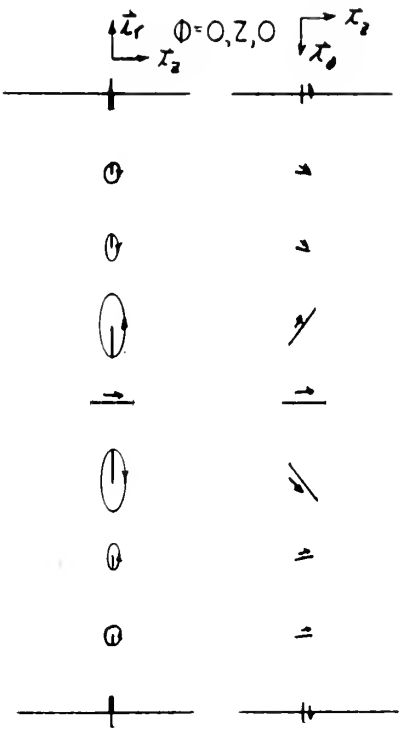

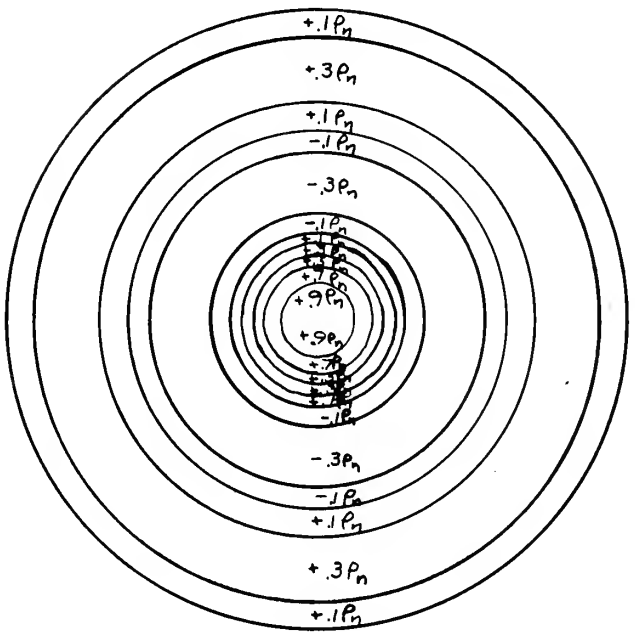

$\omega t = \frac{\pi}{2}$

$\rho = \rho_n$

$\rho_e = \rho_n$

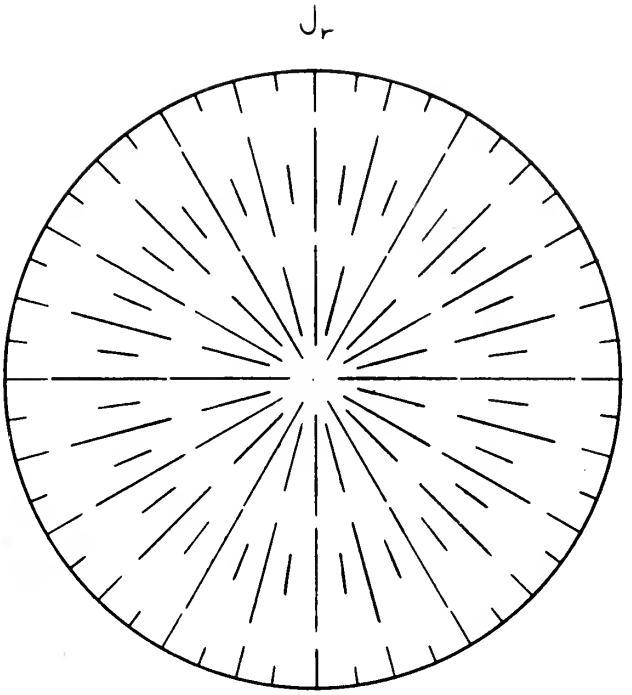
J_r

BIBLIOGRAPHY

1. W. P. Allis, S. J. Bucksbaum, and A. Bers, Waves in Anisotropic Plasma, M. I. T. PRESS, Cambridge, Mass. (1963)

2. V. Bevc and T. E. Everhart, Fast Waves in Plasma Filled Waveguides, Institute of Engineering Research, Series No. 60, Issue No. 362, Research Laboratory, University of California (1961)

3. H. A. Haus, "Microwave Circuits," Course 6.621 Notes, Massachusetts Institute of Technology (1958)

4. M. Camus and J. LeMezec, Propagation des Ondes Dans un Guide Circulaire Rempli de Plasma, en Presence d'un Champ Magnetique. Etude des Modes a Symetric de Revolution, Issy-les-Moulineaux (1962)

5. E. Jahnke and F. Emde, Tables of Functions with Formulae and Curves. 4th Edition, Dover Publication, New York (1945)

6. Table of Bessel Functions $J_0(Z)$ and $J_1(Z)$ for Complex Arguments; Columbia University Press, New York (1943)